Hogentogler & Company, Inc

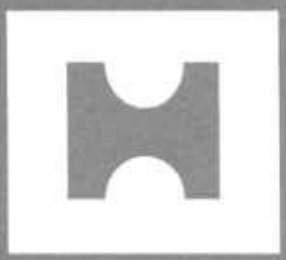

GUIDELINES FOR GEOTECHNICAL DESIGN USING THE CONE PENETROMETER TEST AND CPT WITH PORE PRESSURE MEASUREMENT

by
Dr. P.K. Robertson
University of Alberta
and
Dr. R.G. Campanella
University of British Columbia

Hogentogler & Company, Inc

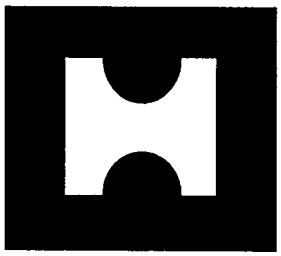

GUIDELINES FOR GEOTECHNICAL DESIGN USING THE CONE PENETROMETER TEST AND CPT WITH PORE PRESSURE MEASUREMENT

by
Dr. P.K. Robertson
University of Alberta
and
Dr. R.G. Campanella
University of British Columbia

Hogentogler & Co., Inc
P.O. Drawer 2219
Columbia, Md. 21045 USA

Phone: (301) 381 - 2390
Cable: CIVILENG
Fax: (301) 381 - 2398
Telex: 898379
Toll Free: (800) 638 - 8582

GUIDELINES FOR GEOTECHNICAL DESIGN USING THE CONE PENETROMETER TEST AND CPT WITH PORE PRESSURE MEASUREMENT

BY

Dr. P. K. Robertson
Civil Engineering Department
University of Alberta
Edmonton, Alberta, Canada T6G 2G7

and

Dr. R. G. Campanella
Civil Engineering Department
University of British Columbia
Vancouver, B. C., Canada V6T 1W5

February 1988
November 1989

Fourth Edition

First Edition January 1984
Second Edition September 1984
Third Edition November 1986

Funding for this manual was provided in part by Hogentogler & Co., Inc., 9515 Gerwig Lane, P.O. Drawer 2219, Columbia, MD 21045, Williams and Associates, 12290 U.S. Hwy. 19-S, Clearwater, FL, 33516, The Natural Sciences and Engineering Research Council of Canada, Pennsylvania Department of Transportation, and The Federal Highway Administration.

GEOTECHNICAL DESIGN USING CPT AND CPTU DATA

Dr. P.K. Robertson and Dr. R.G. Campanella
February 1988
November 1989

TABLE OF CONTENTS

LIST OF SYMBOLS

α	Modulus factor or friction coefficient
a	Net area ratio
A_f	Pore pressure ratio in triaxial test
A_N	Load transfer area behind the cone tip
A_T	Cross-sectional area at base of cone tip
B	Footing or foundation width
B_q	Pore pressure parameter ratio, $\Delta u/(q_c-\sigma_{vo})$
c_h	Coefficient of consolidation in horizontal direction
c_v	Coefficient of consolidation in vertical direction
C_c	Virgin compression index
C_s	Recompression index
Δ	Change in
Δp	Net footing pressure
Δu	$u-u_o$, excess pore pressure
D	Grain size
D_r	Relative density
e	Void ratio, V_v/V_s
E	Young's modulus
E_u	Undrained Young's modulus, $E_u = 3\ G_{max}$ at small strains
E_{25}	Young's modulus at 25% of peak strength
ϕ'	Friction angle in terms of effective stress
f_p	Unit skin friction for pile
f_s	Friction sleeve stress
γ	Unit weight of soil

G	Shear modulus
G_{max}	Maximum shear modulus at small strains
I_R	Soil rigidity index or stiffness ratio = G/S_u
I_z	Strain influence factor
k_c	Bearing capacity factor
k_m	Modulus number
K_o	Lateral earth pressure coefficient at rest
LI	Liquidity index
LL	Liquid limit, %
m_v	Volumetric compressibility, $\Delta v/v/\Delta\sigma'$, in vertical direction
M	Drained constrained modulus = $1/m_v$
$N_{\Delta u}$	Pore pressure factor = $\Delta u/s_u$
M_t	Tangent (constrained) modulus
N	Standard penetration value, blows/ft
N_c	Cone factor without including overburden effect
N_K	Cone factor when using q_c
N_{KT}	Cone factor when using q_T
OCR	Overconsolidation ratio
P_a	Reference stress
PI	Plasticity index, %
PL	Plastic limit, %
q_c	Measured cone bearing stress
q_E	Effective cone bearing = q_c-u (or q_T-u)
q_p	Unit end bearing for pile
q_T	Total cone bearing corrected for pore pressure
R	Radius of cone

R_f	Friction ratio = f_s/q_c x 100% or f_s/q_T x 100%
σ	Total normal stress
σ'	Effective normal stress = σ-u
σ'_{ho}	Effective horizontal stress
σ'_m	Mean effective normal stress
σ'_r	In situ radial effective stress
σ_{vo}	Total overburden stress
σ'_{vo}	Effective overburden stress
s_u	Undrained shear strength
S	Settlement
S_t	Sensitivity (undisturbed strength ÷ remolded strength)
τ	Shear stress
τ_f	Shear stress at failure
T	Time factor
u	Pore water pressure
u_o	Equilibrium pore water pressure, in situ
w	water content, M_w/M_s x 100%

LIST OF FIGURES

LIST OF TABLES

1. INTRODUCTION

1.1. Purpose and Scope

The purpose of this manual is to provide guidance on the use and interpretation of the Cone Penetration Test (CPT) and Cone Penetration Test with pore pressure measurement (CPTU), and their use in geotechnical design. The current ASTM Standard D3441, 1986 for cone penetration testing is reproduced as Appendix A. The authors provide herein their recommended guidelines to interpret a full range of geotechnical parameters from CPT and CPTU data. The use of this data in geotechnical design is complex and often project specific. However, design guidelines have been given (Chapter 5) to assist in their use. Relevant design examples and case histories have been given in a companion volume called "Worked Examples" which illustrates the application of the CPT and CPTU data to geotechnical design.

The practice described is that adopted in North America which closely follows European methods. This manual is applicable to standard electronic cones with a 60 degree apex angle and a diameter of 35.7 mm (10 cm^2 cross-sectional area), although much of the manual is also applicable to mechanical cones of the same dimensions.

Summaries are provided at the end of each chapter on interpretation. These are intended to help the user, and should be used in conjunction with the main text.

To the conscientious reader the manual will appear to have some areas of repetition. This has been done purposely to ensure that readers who only read certain sections are made aware of some important points.

This manual concentrates on the CPT and CPTU. A companion manual was also developed for the Marchetti Dilatometer Test (DMT) as part of this

project.

1.2. General Description of CPT

In the cone penetration test (CPT) a cone (see Fig. 1.1 for terminology) on the end of a series of rods is pushed into the ground at a constant rate and continuous or intermittent measurements are made of the resistance to penetration of the cone. Measurements are also made of either the combined resistance to penetration of the cone and outer surface of a sleeve or the resistance of a surface sleeve.

Probing with rods through weak soils to locate a firmer stratum has been practised since about 1917. It was in the Netherlands in about 1934 that the CPT was introduced in a form recognizable today. The method has been referred to as the Static Penetration Test, Quasi-static Penetration Test, Dutch Sounding Test and Dutch Deep Sounding Test.

The existing CPT systems can be divided into two main groups, mechanical and electronic types. A cone with a 10 cm^2 base area cone tip with an apex angle of 60 degrees is accepted as standard and has been specified in the European and American Standards. The friction sleeve, located above the conical tip, has a standard surface area of 150 cm^2. The mechanical cones require a double-rod system.

In soft soils, cone penetration to depths in excess of 100 meters (330 feet) may be achieved provided verticality is maintained. Gravel layers and boulders, heavily cemented zones and dense sand layers can restrict the penetration severely and deflect and damage cones and rods, especially if overlying soils are very soft and allow rod buckling.

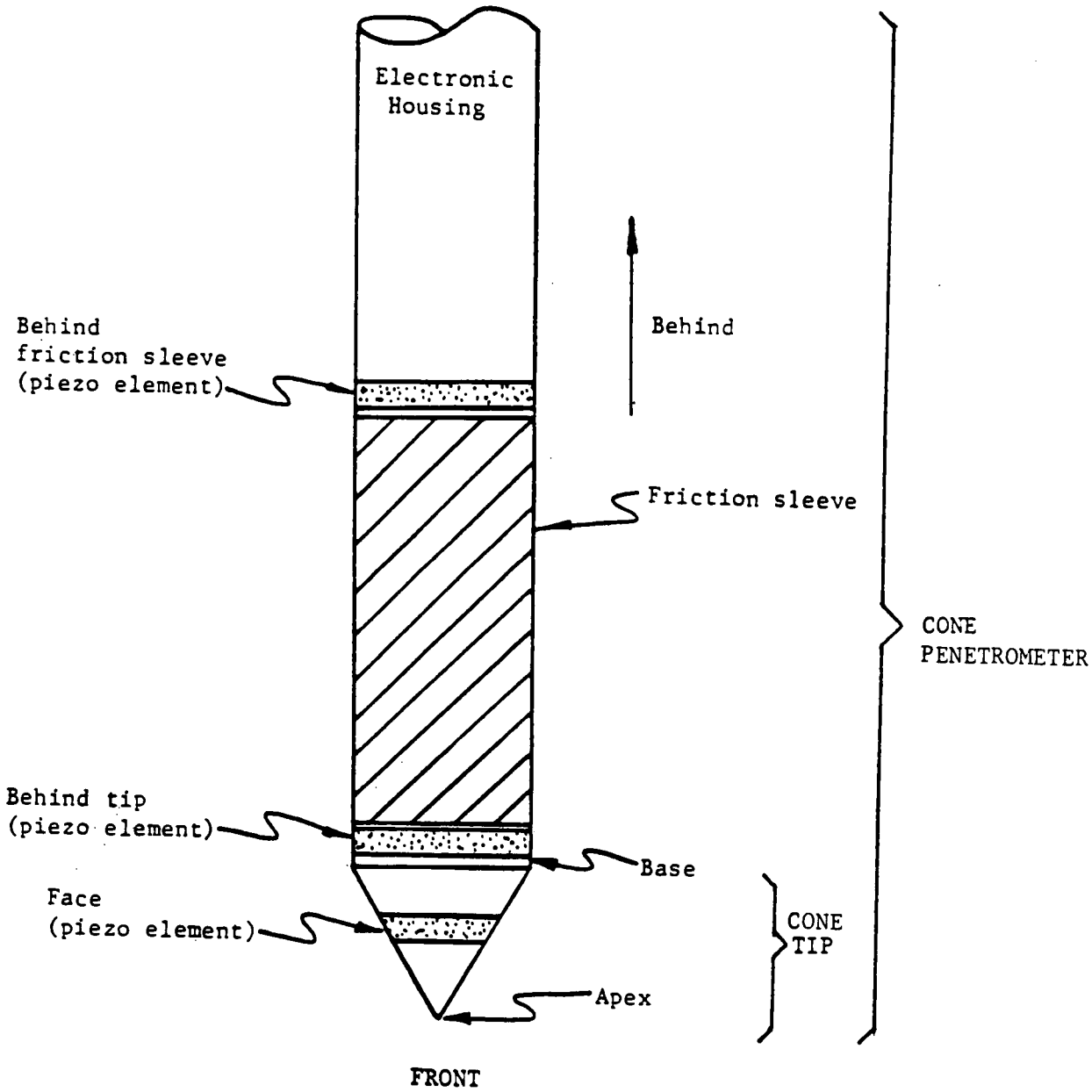

Figure 1.1 Terminology regarding the Cone Penetrometer

The mechanical cone offers the advantage of an initial low cost for equipment and simplicity of operation. However, it does have the disadvantage of a rather slow incremental procedure (usually every 20 cm), ineffectiveness in soft soils, requirement of moving parts, labour intensive data handling and presentation, generally poor accuracy, and shallow depth capability.

The types of mechanical cones generally used are those originally developed in Holland. In rather homogeneous competent soils, without sharp variations in cone resistance, mechanical cone data can be fully adequate, provided the equipment is properly maintained and the operator has the required experience. Nevertheless, the quality of the data remains much more operator dependent than with an electronic penetrometer. In soft soils, the accuracy of the results can sometimes be inadequate for a quantitative analysis of the soil properties. In highly stratified materials even a satisfactory qualitative interpretation may be impossible.

The electronic cone offers obvious advantages, such as a more rapid procedure, continuous recording, higher accuracy and repeatability, potential for automatic data logging, reduction and plotting, and the possibility of incorporating additional sensors in the cone. However, the electronic cones have an initial high cost for equipment and require well skilled operators with a knowledge of electronics. They also require adequate back-up in technical facilities for calibration and maintenance.

The most significant advantage that electronic cones offer is their repeatability and accuracy (Schmertmann, 1975, Schaap and Zuidberg, 1982) and their nearly continuous data. The most significant recent development in the CPT is the addition of pore pressure measurements (CPTU). The

addition of pore pressure measurements has added a new dimension to the interpretation of geotechnical parameters, particularly in loose or soft, saturated deposits.

The main advantages of the CPTU over conventional CPT are:

- ability to distinguish between drained, partially drained and undrained penetration,
- ability to correct measured cone data to account for unbalanced water forces due to unequal end areas in cone design,
- ability to evaluate flow and consolidation characteristics,
- ability to assess equilibrium groundwater conditions,
- improved soil profiling and identification,
- improved evaluation of geotechnical parameters.

The primary purpose of the CPT and CPTU is for stratigraphic logging and preliminary evaluation of geotechnical parameters. Other in-situ test methods or sampling and laboratory testing, may be better suited for use in critical areas that have been defined by the CPT or CPTU. The CPT or CPTU should be used to determine the locations and elevations at which other in-situ tests and/or sampling should be carried out.

Where the geology is uniform and well understood and where predictions based on CPT or CPTU results have been locally verified and correlated with structure performance, the CPT or CPTU can be used alone for design. However, even in these circumstances the CPT or CPTU may be accompanied by boreholes, sampling and testing for one or more of the following reasons:

(1) to clarify identification of soil type

(2) to verify local correlations

(3) to assist where interpretation of CPT or CPTU data is difficult due to partial drainage conditions or problem soils

(4) to assist where the effects of future changes in soil loading are not recorded by the CPT.

2. EQUIPMENT AND PROCEDURES

2.1. CPT and CPTU Equipment

The first electronic cone was introduced in 1948 and later improved in 1971 (de Ruiter, 1971). Since then, numerous designs have been developed. A cone of 10 cm² base area with an apex angle of 60° is generally accepted as standard and has been specified in the European and American Standards (ISSMFE, 1977; ASTM, 1986, see Appendix A). The friction sleeve, located above the conical tip, has a standard area of 150 cm². The friction sleeve on electronic cones has the same diameter as the conical tip and push rods, i.e., 35.7 mm.

Electronic penetrometers have built-in load cells that record end bearing stress, q_c, and friction sleeve stress, f_s. Bonded strain gauges are most commonly used for load cells, because of their simplicity, ruggedness, and zero stability, but inductive and vibrating wire types also exist (Sanglerat, 1972). Load cells have also been developed that incorporate pressure transducers to record load (Torstensson, 1982). In general, however, experience has shown that the use of the strain gauge provides a high precision for load cells. Full details on cone designs are given by Robertson and Campanella (1986).

In general, no single cone design will meet all requirements and needs. Flexibility in cone equipment and designs is important so that various cones can be employed depending on the soil conditions and project requirements. In general, a high capacity cone (tip load cell capacity of 10 tons) should be used to provide the preliminary soil profile and stratigraphy. If a soft layer is encountered within the profile that

requires more careful examination, a dual range cone or lower capacity cone could be used in specific areas, as defined by the high capacity cone. This flexibility in cone use requires careful design of the data acquisition system.

The introduction of pore pressure measurements has significantly improved the use and interpretation of the electronic cone (Wissa, 1975, Torstensson, 1975).

Measuring pore pressures during cone penetration requires careful consideration of probe design, choice and location of the porous element and probe saturation (Campanella and Robertson, 1988). The mechanical design of the cone must ensure that when the cone tip is stressed, no load is transferred to the pore pressure transducer, porous element or fluid volume. This problem can be checked by loading the tip of a fully assembled, saturated cone and observing the pore pressure response. If no mechanical load transfer occurs, no pore pressure response should be observed.

For a high frequency response, (i.e. fast response time), the design must have a small fluid filled cavity, low compressibility and viscosity of fluid, a high permeability of the porous filter and a large area to wall thickness ratio of the filter (Smits, 1982). To measure penetration pore pressures rather than filter compression effects, the filter should be rigid. However, to maintain saturation, the filter should have a high air entry resistance, which requires a finely graded filter and/or high viscosity of the fluid. Clearly, not all of these requirements can be combined.

An essential requirement is to incorporate small fluid cavity, a low compressibility of saturating fluid and a rigid or low compliance pressure transducer. A balance is required between a high permeability of the porous filter to maintain a fast response time and a low permeability to have a high air entry resistance to maintain saturation.

Filter element squeeze can also be important for cones that measure pore pressures at the apex of the tip or on the face of the tip. During penetration into a dense layer with high cone tip resistance, the filter element can become compressed and generate high positive pore pressures. This will occur unless the filter element has a very low compressibility or if filter and soil are of sufficient permeability to rapidly dissipate the pore pressure due to filter element compression. Experience gained at UBC with a relatively compressible porous plastic filter element behind the cone tip has shown no evidence of induced pore pressure due to filter squeeze. This is likely due to the low normal stresses behind the cone tip and the high permeability of the porous plastic element. However, problems may occur with these elements in very stiff soils with permeabilities considerably lower than that of the porous element. In a recent field comparison study between porous polypropylene (a hard plastic) and ceramic filters there were no significant differences in penetration pore pressures. Filter squeeze is mainly critical for pore pressure measurements on the face of the cone tip during initial penetration into dense fine or silty sands and compact glaciated silts and clays.

Figure 2.1 shows the essential elements of the Hogentogler/GMF piezocone tips. The design uses a small pressure transducer mounted within the cone and behind the tip to sense the water pressure. The design also has a

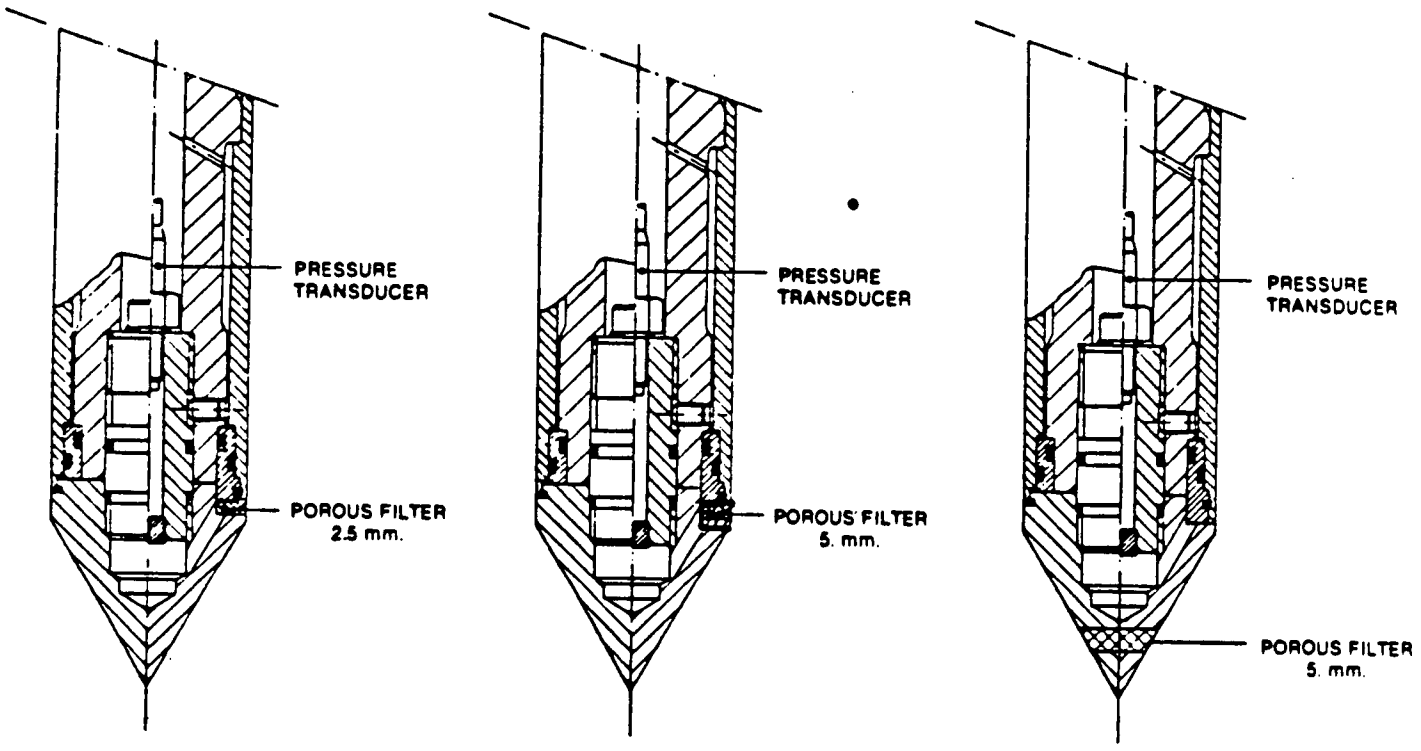

Figure 2.1 Hogentogler Piezometer Cones

minimal volume between the transducer and the external surface of the porous filter. This is important to minimize the response time of the measuring system.

The Hogentogler design enables the filter or porous plastic element to be located either on the face of the conical tip at mid height or immediately behind it. This change in filter location can be made in the field. There are advantages and disadvantages for both filter locations. This will be discussed later in Section 3.1.2.

The filter can be made from the following materials; porous plastic, ceramic, or sintered stainless steel. Its function is to allow rapid movements of the extremely small volumes of water needed to activate the pressure sensor while preventing soil ingress or blockage. Both machining and abrasion through dense sand tends to close off the openings into a stainless filter. A ceramic filter does not usually survive penetration through dense sands. Porous polypropylene, a tough hard plastic, survives nicely in dense sands and gravelly soils showing only minor wear.

2.2. Pushing Equipment

2.2.1. On Land

The rigs used for pushing the penetrometer consist basically of a hydraulic jacking system. They are usually specially built for this purpose, but sometimes the push-down of an anchored drill rig is used. The thrust capacity needed for cone testing commonly varies between 10 and 20 tons (100 and 200 kN). 5 and 2 tons capacity (50 kN and 20 kN) is also common for use in soft soils. 20 tons (200 kN) is about the maximum allowable thrust on the 35.7 mm diameter high tensile steel push rods.

Exceeding that load often results in damage and/or buckling of the test rods, either in the rig or in softer upper layers of the soil. Experience shows that as long as the pushing thrust is below 10 tons (100 kN), it is rare that any damage occurs to the rods or cone. A thrust capacity of 10 tons (100 kN) will likely handle more than 95% of cone penetration testing to 100 feet (30 m) depth in most uncemented normally consolidated soils that do not contain large gravels and boulders.

Land based rigs are often mounted in heavy duty trucks that are ballasted to a total deadweight of around 15 tons (150 kN). Screw anchors are used to develop the extra reaction required for a thrust of 20 tons (200 kN). The power for the hydraulic rig is usually supplied from the truck engine. A detailed description of a modern cone penetration testing vehicle is given by Davidson and Bloomquist (1986). With a double rear axle and both rear and front wheel drive, the trucks can operate off the road in most terrain conditions. Sometimes all-terrain vehicles are used for work in marshy areas or soft fields.

The load of the hydraulic ram is transferred either by a thrust head on top of the test rods or by a clamping system that works by friction on the outside of the upper rod or by a notch cut into the rods. An automatic mechanical clamp saves time in the operation as the next rod can be screwed on, while the rig is pushing down the previous one. The clamping system was first developed for offshore rigs, where it is indispensable. The standard cone rods have special tapered threads and are 1 meter (approximately 3.3 feet) in length. Rods are connected hand-tight and wrenches are rarely needed during disassembly. The enclosure of a truck provides ideal space for the installation of all electronic equipment for depth recording

and read out. In hot humid climates the truck should be air conditioned for the comfort of personnel and preservation of electronics.

The penetrometer rig can also be placed on a light trailer equipped with earth anchors. A high production truck mounted rig can produce up to 800 feet (250 meters) of penetration testing in one day, as compared to about 400 feet (120 meters) for a trailer mounted rig, both under favourable site conditions. The most time consuming part of the trailer mounted operation is the setting of screw anchors which are usually required to provide additional reaction because of the lack of deadweight. An intermediate solution is to mount the rig on a heavy trailer or heavy duty pick-up truck frame which can be ballasted. CPT can also be performed using standard drill rigs, as is currently being done by PennDOT, but pushing capacity is often limited to about 5 tons without anchors. Use of a drill rig has the added advantage of improved cost and flexibility. Hogentogler & Co. can supply all types of pushing equipment including those mounted on heavy trucks and lighter pick-up trucks, drill rig conversions and portable equipment.

A friction reducer or expanded coupling is used at distances from 1 foot to 3 feet (30 cm to 100 cm) behind the cone tip. The purpose of the friction reducer is to expand the diameter of the hole to reduce soil contact against the cone rods and thus reduce rod friction behind the friction reducer at the expense of increased bearing and friction forces locally around the reducer. Also, experience suggests that the further back the friction reducer is from the tip, the better are chances of maintaining a vertically aligned hole but this is at the expense of increased friction force in front of the friction reducer.

It has been found that a 2 inch (50 mm) long, high strength steel tube of 1.75 inch O.D. slipped over the cone rod with ends welded and machined to a 30° chamfer works well in most soils.

Many cone operators prefer to use four steel blocks about 5 to 10 mm square welded and evenly spaced around the standard cone rod. This technique tends to break up and slightly push the soil to reduce subsequent friction on the rod, but it does not appear to be as effective as a complete sleeve.

A 20 ton (200 kN) thrust will normally result in penetration depths of 150 to 200 feet (50 to 60 meters) in dense to medium dense sands and stiff clays. In weaker soils penetration to depths in excess of 100 meters may be achieved provided verticality is maintained. Gravel layers and boulders or heavily cemented zones can of course restrict the penetrations severely and deflect and damage cones and rods.

To reduce the pushing force required for cone penetration, a system has been developed (Jefferies and Funegard, 1983) where a natural or polymer drilling mud is pumped down the inside of the cone rods and is injected into the soil at a steady flowrate of about 0.2 gallons/min. (1 litre/min.) from several injection ports located approximately 5 feet (1.5 m) behind the tip and immediately behind the friction reducer. The mud holds the soil off the cone rods thus minimizing friction. Trials have shown that the pushing force can be reduced by up to 50%. This has enabled CPT work to be performed using a standard drill rig with about 5 ton (50 kN) effective thrust. Hogentogler & Co. have provided mud pumping systems for standard electronic cone systems to reduce pushing force requirements.

Standard Dutch Type cone rods of 20 ton capacity (high strength steel) are recommended for all cone soundings unless special requirements exist. The standard cone rods are the same diameter as the base of the tip and sleeve, measure 1 meter in length, have tapered threads and are assembled and dismantled by hand. Some operators prefer to use the locally available drill rods in longer lengths. Although it is more convenient and economical to use these, they do not have the capacity and buckling resistance. However, with reduced pushing forces of 5 - 10 tons as with drill rigs, the use of local drill rods can work well.

2.2.2. Over Water

Modification of the standard techniques on land is necessary for cone testing over water and/or offshore. CPT work offshore can be divided into two main groups:

a) Shallow water (Depth < 100 feet (30 m) approx.)

b) Deep water (Depth > 100 feet (30 m) approx.)

For shallow-water CPT work, where the water depth is less than about 100 feet (30 m), equipment and procedures are similar to onshore CPT work. A ship or barge is often used as a platform and a dual casing used for lateral support of the cone rods. An anchored barge must have a heave compensation system to prevent cyclic loading during swells and wave action. If the water depth is shallow, a free-standing platform or jack-up barge resting on the seabed is very desirable and free of wave action.

A combination free standing platform (large heavy casing with inner cone rod casing founded on the seabed) and floating barge often provide the most economical solution in shallow waters. The free standing casing

protrudes through the anchored barge with penetrometer mounted on the "stable" casing.

For deeper offshore CPT work special equipment is needed which can be divided into two categories:

1) Seabed bottom rigs and

2) Downhole penetrometers.

Full details of these can be found in Zuidberg (1975) and Semple and Johnson (1979).

2.3. Test Procedures

2.3.1. General Comments

Efficient field operations with electronic cone testing requires well-skilled operators and adequate technical back-up facilities for calibration and maintainance of the equipment. The cones and the data acquisition systems including cables and connections need to be regularly checked or recalibrated. In the field simple check calibrations and procedures are essential after connecting the equipment to ensure that all is functioning properly. These checks include measuring the variation of the output of the strain gauge load cells over their full operational range to check the calibration curve and the non return at zero load. Checks and inspections of the equipment are also needed between each sounding or series of soundings. Full details of the procedures for the Hogentogler equipment is given in the operator's manual (Hogentogler).

The standard penetration speed for CPT and CPTU testing is 2 cm/sec ±.5 cm/sec (see ASTM standard). It is important to obtain measurements of this speed to check that the speed control systems are functioning

correctly. The use of a solid steel "dummy cone" of 15 cm^2 area (1.75 in. O.D. by 60° apex angle cone tip) is recommended to be pushed first in the upper zone (0 to 3 ft) especially if gravel or random fill is suspected.

2.3.2. Saturation of CPTU

There are no major differences in field test operations between standard CPT testing and CPTU soundings, except those required for the preparation of the piezo-element. This preparation usually consists of the following operations:

1) Deairing of porous filter elements.
2) Deairing of cone, especially with respect to the pressure chamber immediately adjacent to the pressure transducer.
3) Assembling of cone and filter.
4) Protection of system during handling, if required.

In the early days of piezocone sounding, it was normal practice to deair the filter elements and the cone by boiling the complete system, but this proved to affect seriously the life of the cone, and is no longer done.

General preferred practice today is to carefully saturate the filter elements in the laboratory by placing them under a high vacuum with saturating fluid for approximately 5 to 24 hours. The practice at UBC has been to submerge the porous filter elements in warmed (90 to 130°F) glycerin in a small ultra-sonic bath under a high vacuum (Use a two stage vacuum pump with a water trap). After several hours vibration, the glycerin increases in temperature which reduces its viscosity, boils under vacuum and improves saturation. The filter elements are then placed in a

small glycerin filled container ready for transportation into the field. Note that glycerin boils at over 200°C (392°F) at atmospheric pressure which will damage porous plastic and is dangerously hot to handle.

The voids in the cone itself should be deaired by flushing with a suitable fluid from a plastic syringe and hypodermic needle. It is suggested that all piezometer cone designs should be made such that flushing the void within the cone tip can be performed with a hypodermic. The cone can be held with tip pointing upward and fitted with a cut-off large plastic funnel sealing around the friction sleeve. The entire tip is submerged in the saturating fluid during piezometer and tip assembly. Good results have been obtained when glycerine is used to fill the void space.

The next step after cone preparation and assembly is the lowering of the string of cone rods. A thin protective rubber sleeve is sometimes placed over the cone. To avoid premature rupture of the rubber sleeve, a small hole is pushed with a "dummy cone" of a larger diameter (approx. 44 mm O.D.) than the piezocone. Sometimes a hand dug or a predrilled hole is made depending on circumstances and soil-stratigraphy. Predrilling is not always necessary if the filter element and saturating fluid develop a high air entry value to prevent loss of saturation. However, in some clay soils suctions can be very large and predrilling may be necessary. The entire saturation procedure should be repeated after each sounding, including a change of the filter element. If undamaged, the filter elements can be reused after being resaturated in the ultrasonic vacuum bath.

2.3.3. CPTU Dissipation Test Procedures

During a pause in the penetration any excess pore pressures measured on the cone will start to dissipate. The rate of dissipation depends upon the coefficient of consolidation which, in turn, depends on the compressibility and permeability of the soil.

A dissipation test can be performed easily at any depth. In the dissipation test the rate of dissipation of excess pore pressure to a certain percentage of the equilibrium pore pressure is measured. At the depth at which a dissipation test is needed the penetration is stopped.

If the cone rods are clamped when penetration is stopped that theoretically stops the movement of the cone rods instantaneously. However, in practice the cone will continue to move very slightly as the elastic strain energy in the rods causes the soil in front of the cone and around the rods to be displaced. The longer the cone rods or the deeper the penetration, the greater the tendency for the soil to creep, and the more significant this movement may be. This movement alters the total stresses in the soil around the conical tip and can influence the measured decay of pore pressure with time. It has been shown (Campanella et al, 1983) that this effect is only significant with the piezo element on the face of the cone tip. With the piezo element behind the tip (as in the current PennDOT equipment) it is not necessary to clamp the rods and it is standard procedure to completely release the load on the rod during pore pressure dissipation measurements.

Sometimes a fixed period of dissipation for all soil layers is used and sometimes dissipation is continued to a predetermined percentage of the hydrostatic or equilibrium pore pressure; for example, 50%.

The pore pressure is recorded in a time base mode and the measurement of equilibrium pressures provides important hydro-geologic information.

2.4. Data Acquisition and Processing

The electronic penetrometer produces continuous data that requires relatively complex data collection and processing. The signals are usually transmitted via a cable prethreaded down the standard push rods.

Modern systems have evolved to include analog to digital (A/D) converters so that the analog signals can be directly converted to digital form for data logging (de Ruiter, 1982). The digital data is incremental in nature, typically recording all channels every 5 cm in depth. Data is stored on magnetic tape, bubble or floppy diskette for future transfer of data to an office computer and plotter. Printers and plotters can also be used in the field with microprocessors to calculate, print and plot data, such as friction ratio, immediately after completion of or during a cone sounding. A modern system such as described above is currently in use by PennDOT.

Recent advances in data acquisition systems have been made possible because of rapid advances in silicon chip technology. It is now possible to condition and amplify the signals in the cone before transmission. This provides a larger signal for transmission which is less susceptible to interference. The decreased cost of electronic components has also made it possible to digitize the data in the cone and thus transmit a clear digitized signal. This enables considerably more channels to be recorded with a minimum number of wires within the cable.

Clearly the future designs of cones and data acquisition systems will make more use of electronic components to amplify and digitize the signals

within the cone before transmission to the ground surface. This will enable considerably more channels to be recorded with a high degree of resolution.

With increasing numbers of channels required for other measurements, such as pore pressure and inclination, the data processing and presentation becomes more complex. The field or office computers require flexibility in software to enable a variety of calculations to be performed to produce profiles that correlate various parameters, such as pore pressure and cone bearing.

2.5. Calibration

All calibrations should be done using reference type load cells (superior zero stability and linearity with little hysteresis) and a dead weight tester or pressure reference transducer. Calibrations should be done with all O-rings and dirt seals in place in the cone as they would be during penetration.

After all transducers have been loaded to capacity approximately 20 times the calibration procedure should be set up to measure and record all channels (i.e., cross-talk effects). For example, when the tip is loaded to reference values to establish the calibration curve of output versus load, each of the other measurement channels should be read and recorded at each tip load. By so doing mechanical load transfer error, which should be a minimum, can be evaluated for each channel.

The pore pressure calibration should be done with a pressure chamber which completely encloses the cone and is sealed at a point above the friction sleeve. Measurement of the tip stress and friction sleeve stress

at applied pore pressures will allow direct determination of unequal end area effects and their correction factors as discussed in Section 3.1.1.

The calibration should evaluate repeatability, non-linearity and hysteresis effects to determine the best straight line fit for the data as indicated in Section 3.1.4. However, the accuracy can be improved by using a 4-point calibration curve of three best fit straight segments for low, medium and high range. For example, a 1000 t/ft² (bar) full scale tip load cell might have calibration points at 10, 100 and 1000 t/ft² as well as zero. This 3- segment calibration curve technique is easily handled by a computer based acquisition and data reduction system and reduces the error due to non- linearity. Zero load error is variable and is determined for each sounding by determining the zero load output **before** and **after** for each sounding. The zero load error during calibration should be negligible (less than .05% F.S.).

For completeness, the effect of temperature on zero load output and on calibration factors should be determined by performing calibrations over a range in temperature which might correspond to field conditions. The effect of temperature variations can be minimized in the field by pushing the cone into the ground about 1 m and leaving it for about 1/2 hr. or more while setting up the data system. When the test is started, the cone is withdrawn to ground surface, zero outputs or baselines are recorded and the sounding is started. In this way the cone is brought to ground temperature before starting the test. However, it might be easier to plunge the cone into a bucket of water which is near ground temperature for about 15-30 minutes immediately before a sounding.

2.6. Maintenance

The cone and friction sleeve should be checked for no obvious damage or wear at the start of each sounding. Frequent checks should be made to ensure that the cone dimensions do not exceed the tolerances set out in the ASTM standard (Appendix 1).

Before each test, the seals between different elements should be cleaned and inspected to ensure their integrity. After each sounding, it is good procedure to clean and inspect the cone and seals. Soil should be removed from all seals and the cone cleaned before and after each sounding.

Electric cones provide more accurate and repeatable results than mechanical tips, but they are subject to zero-load errors and calibration errors, both of which tend to change during testing. The zero load error should be checked by observing the zero-load output (or baselines) **before** and **after** each test, and recording the values on the data output.

The load measurement systems should be calibrated at intervals not exceeding three months, and more frequently when the equipment is in use continuously, and after every overhaul or repair. Details of calibration procedures are given in Section 2.5.

To avoid disturbed ground, a CPT sounding should not be performed within a distance from a borehole less than 25 times the borehole diameter, nor within one meter (3 feet) of a previously performed CPT.

3. DATA REDUCTION

3.1. Factors Affecting CPT and CPTU Measurements

Because of the wide variety in cone designs, it is not possible within the scope of this manual to discuss in detail all the factors that affect the measured results. However, several significant aspects that pertain to almost all cone designs will be discussed. The reader is encouraged to investigate the details of the particular cone design being used before performing detailed interpretation of the data.

3.1.1. Unequal Area Effects

Water pressures can act on the exposed surfaces behind the cone tip and on the ends of the friction sleeve (see Fig. 3.1). These water forces result in measured tip resistance (q_c) and sleeve friction (f_s) values that do not represent true total stress resistances of the soil. This error introduced in the measurement can be overcome by correcting the measured q_c for unequal pore pressure effects using the following relationship (Baligh et al, 1981; Campanella et al, 1982):

$$q_T = q_c + u\ (1 - a) \qquad (3.1)$$

where:

q_T = corrected total tip resistance

u = pore pressure generated immediately behind the cone tip

a = net area ratio = A_N/A_T (see Fig. 3.1)

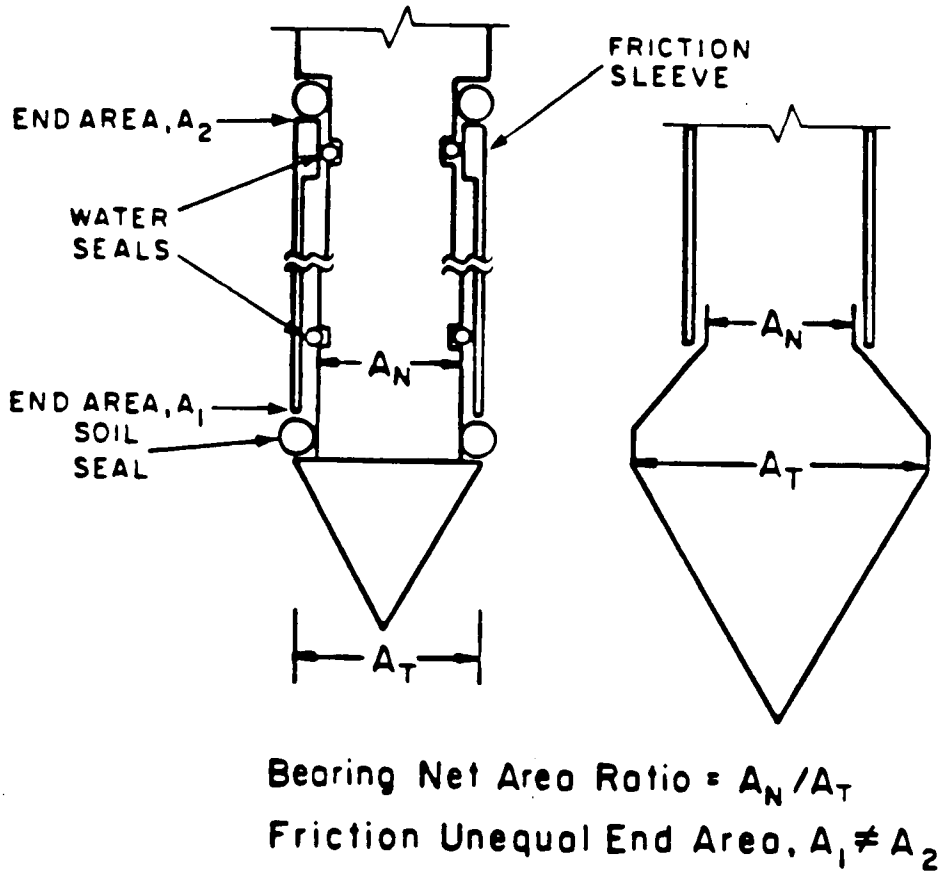

Figure 3.1 Influence of Unequal End Areas
(After Campanella et al, 1982)

An example of the determination of the net area ratio using a simple calibration vessel is shown in Fig. 3.2. The calibration vessel is designed to contain the cone and to apply an all around air or water pressure. Many cones have values of net area ratio ranging from 0.90 to 0.60, but sometimes this ratio may be as slow as 0.38 (see Fig. 3.2). This correction for bearing area cannot be eliminated except with a unitized, jointless cone design.

The importance of this correction is especially significant in soft clays, where high values of pore pressure and low cone resistance may lead to the physically incorrect situation of $u > q_c$.

Also, previous correlations developed to obtain soil properties, such as undrained shear strength (s_u), from q_c measurements incorporate systematic errors, depending on cone design.

A similar correction is required for sleeve friction data. However, information is required of the pore pressures at both ends of the friction sleeve. The importance of the sleeve friction correction can be significantly reduced using a cone design with an equal end area friction sleeve.

Several cone operators and researchers who use cones that record the pore pressure on the face of the cone tip have suggested correction factors to convert the measured pore pressures on the face to those that are assumed to exist immediately behind the tip. The assumed ratio of the pore pressure on the face to the pore pressure behind the tip is generally taken to be about 1.2 (i.e., the pore pressure on the face is assumed to be 20% larger than that immediately behind the tip). Measurements (Campanella et al, 1985; Jamiolkowski et al, 1985; Lunne et al, 1986) have shown that the

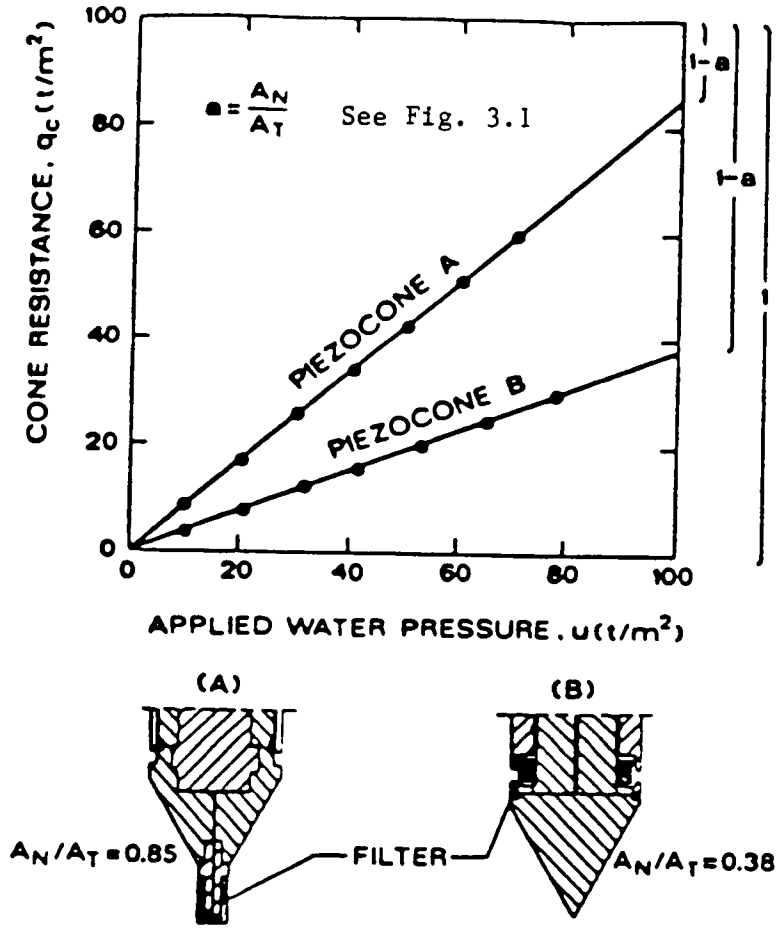

Figure 3.2 Determination of A_N/A_T for Two Types of CPTU Probes (After Battaglio and Maniscalco, 1983)

ratio of 1.2 is generally only true for soft, normally consolidated clays. In stiff, overconsolidated, cemented or sensitive clays, the pore pressure on the face of the tip can be many times larger than that immediately behind the tip. Therefore, to correct the cone bearing to q_T, the pore pressure must be measured behind the tip.

Soil ingress may change the net area ratios somewhat during field testing. Also, the distribution of pore pressure around the cone varies such that a simple net area ratio is not always correct, especially for a bulbous cone. But these problems tend to be rather minor since the corrections are usually most important in soft cohesive soils where the variation in pore pressures around the cone are generally small. The potential error due to these problems are significantly less than the error if no correction is applied.

A detailed discussion regarding cone design is given by Schaap and Zuidberg (1982).

3.1.2. Piezometer Location, Size and Saturation

The measured pore pressures during piezometer cone testing (CPTU) depends very much on the piezometer element location, Tavenas et al (1981), Campanella et al (1982). In normally consolidated soft clays and silts pore pressures measured on the face of the tip are generally 10-20 percent larger than those measured immediately behind the tip. In over-consolidated clays and silts, and fine sands pore pressures on the face of the tip tend to be large and positive whereas pore pressures measured immediately behind the tip may be considerably smaller and possibly negative.

The choice of pore pressure element location is very important with regard to data interpretation. The two main areas at present for measuring pore pressures are either,

i) on the cone face,

or ii) immediately behind the cone tip.

Data collected at several different sites with the pore pressure element located behind the tip and on the face of the tip is shown on Fig. 3.3. In normally consolidated insensitive clays and silts, pore pressures measured on the face are often approximately three times larger than the equilibrium pore pressure (u_o) and about 20% larger than pore pressures measured immediately behind the tip. As the overconsolidation ratio increases in clays and silts, the pore pressure on the face increases. This is due to the increased cone end bearing which causes larger normal stresses on the face in overconsolidated soils.

No single location can provide information for all applications of pore pressure interpretation. However, a convincing argument can be made to standardize the location behind the tip to provide a wide range of applications but yet maintain a practical location for saturation and protection.

The following is a list of advantages of having the pore pressure element located immediately behind the cone tip:

1) Porous element is much less subject to damage and abrasion;

2) Measurements are less influenced by element compressibility;

3) Position is appropriate for correction due to unequal end areas;

4) Good stratigraphic detail is still possible.

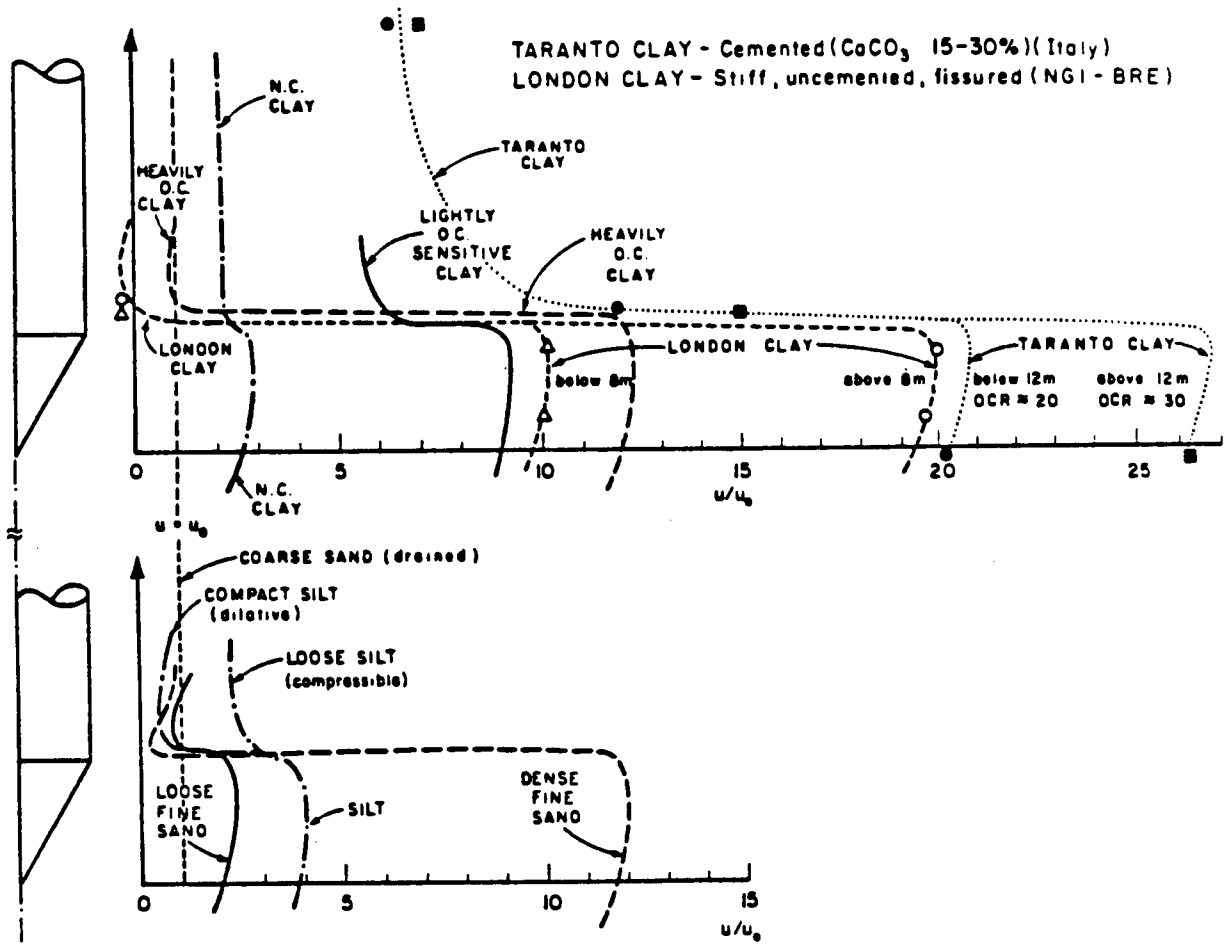

Figure 3.3 Conceptual Pore Pressure Distribution in Saturated Soil During CPT Based on Field Measurements (After Robertson et al, 1986)

In general, no single location can provide information for all applications of pore pressure interpretation. It is recommended that the overall cone design should be such that the porous element location can be changed in the field to allow soundings to be carried out to obtain specific pore pressure data. Alternatively, a cone could be used with piezometer elements both in the tip and behind the friction sleeve. However, saturation of the piezometer element behind the tip can become difficult unless the cone is designed carefully. All pore pressure measurements from cone testing must clearly identify the location and size of the sensing element.

The size of the porous element also influences the measured pore pressures, although little data is available to quantify the importance of this factor. If a porous element is located immediately at the shoulder of the cone tip, it is prone to damage and wear and is in an area of large stress gradients.

It has been observed that for thin pore pressure elements located immediately behind the tip, very small pore pressures (less than u_o) have been recorded. These pore pressures have sometimes been smaller than those recorded with thicker elements located in the same position. It is believed that thin pore pressure elements can sometimes measure low pore pressures due to a shadow effect from a cone tip slightly larger in diameter. Thus, the O.D. of the cone tip should be identical or less than the O.D. of the porous element and friction sleeve by about 0.25 mm.

Complete saturation of the piezometer element in CPTU is essential. Pore pressure response can be inaccurate and sluggish for poorly saturated piezocone systems. Both maximum pore pressures and dissipation times can

be seriously affected by air entrapment. Response to penetration pore pressures can be significantly affected by entrapped air within the sensing element, especially in soft, low permeability soils.

Saturation of the piezometer element and cavity are especially important for shallow onshore soundings where equilibrium water pressure is small. Once significant penetration below the water table has been achieved, the resulting equilibrium water pressure is often sufficient to ensure saturation.

3.1.3. Temperature Effects

The load cells and pressure transducers within the cone are often temperature dependent and are almost always calibrated at room or air temperature. However, soil and groundwater are often considerably cooler than the calibration temperature and a shift in the zero can occur for both load cells and pressure transducer during penetration. For cone testing in dry sand, considerable heat can be generated during penetration. These changes in temperature have little consequence for cone testing in sand where measurements are usually large. However, the zero shift can be significant in very soft or loose soils. A temperature zero shift can make friction measurements very unreliable especially with subtraction type cones where the zero shift may be different for each load cell. Good temperature compensation can limit the variation to about 0.05% of full scale output over the normal expected temperature range.

Cones that use amplifiers within the cone can also suffer temperature shifts if the amplifiers are not temperature compensated. If the temperature of the cones is continuously monitored and temperature zero shift calibrations obtained, it is possible to correct all data as a function of

temperature. These corrections are easily accommodated in a computer based acquisition system.

If temperature is not monitored, an alternate procedure is to allow the cone to reach equilibrium with the groundwater temperature before taking the initial zero readings (before penetration). Zero load readings should also be taken immediately after penetration.

3.1.4. Accuracy of Measurements

A detailed discussion on accuracy, calibration and performance of electronic cones is given by Schaap and Zuidberg (1982).

Electronic cones provide significantly better accuracy and repeatability than the mechanical cones. However, there are some aspects concerning electronic cone design that influence the accuracy of the measurements. The two main errors related to the design of the load cells are:

i) Calibration error

ii) Zero load error

An illustration of these terms is given in Fig. 3.4, which is a graph of loading and unloading for a load cell.

Studies have shown that the major factor that contributes to changes in calibration error is soil ingress along the joints in the cone. However, this can be significantly reduced by regular inspections and maintenance. Also, the time between calibrations should be kept to a minimum. To assist in this latter part, a simple calibration loading device should be included in the field equipment to allow frequent field calibration checks.

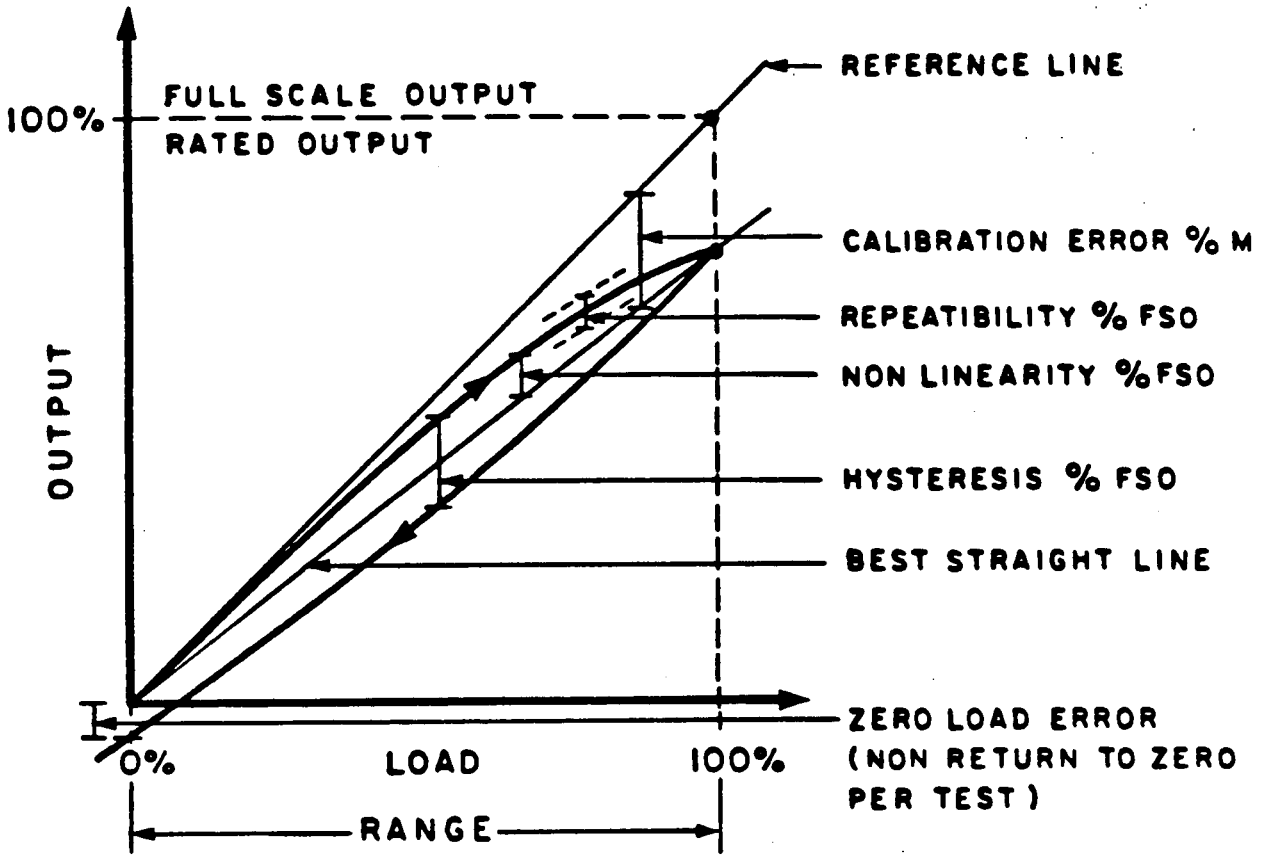

Figure 3.4 Definition of Terms Related to Calibration
(After Schaap and Zuidberg, 1982)

To reduce the hysteresis in the calibration curve, the cone should be loaded at least 20 times to its full capacity before performing the calibration.

The non-linearity of the calibration curve can become very important when testing in very soft soils. In some cases, a different calibration line should be used for different load levels.

If the output at zero load is measured before and after a test, the zero load error can be measured. In general, the zero load error is a reliable indication of the quality of a test and is the sum of a number of possible effects:

i) Output stability

ii) Temperature induced apparent load

iii) Soil ingress

iv) Internal O-Ring friction (threshold)

v) Moisture ingress

vi) Very short duration overload often causes a zero offset error

vii) Deflection resulting in bending and local yielding.

Except for item (i) the zero error can be reduced if proper care is taken in the field testing by means of testing and maintenance.

The zero load conditions should always be displayed on the recorded data to enable the engineer to check its variation. The zero load error should, in general, not exceed 1/2% to 1% of the full scale output. For measurements in soft soils, the error should be considerably less than 1/2% of full scale.

Load cells within penetrometers are generally compensated for temperature variations. With good temperature compensation, the output variation

can be limited to about 0.05% of full scale output. However, procedures to reduce temperature variation should be used (as discussed in Section 3.1.3).

Unfortunately, little data is published concerning the accuracy of other cone designs. In general, however, strain gauge load cells have proven to provide better precision than vibrating wire and pressure transducer load cells. With careful design and maintenance strain gauge load cells can have calibration errors less than 0.4% of full scale output.

A recent study at NGI (Lunne et al, 1986) has shown that high capacity load cell cones can give as repeatable and as accurate results as cones with lower load ranges provided the load cells are of a high quality and are carefully calibrated in various operation ranges and that attention is given to thermal zero shifts. The study at NGI also showed that the friction sleeve measurement was the least reliable for cones of different design.

Other factors that affect the accuracy of the measurements are related to the methods of calibration, data acquisition and processing. These were discussed more fully in Chapter 2.

The tolerance in machining the standard friction cone is such that the difference in diameter between the tip and the sleeve can be up to 0.010 inches (0.25 mm). This combined with wear during usage often results in significant differences in diameter between the tip and sleeve. It has been found that variations in diameters between the tip and sleeve can result in significant differences in measured friction values. This variation can be reduced by careful machining during construction and regular tolerance checks during the life of the cone. The O.D. of the cone tip

should be identical or less than the O.D. of the friction sleeve by about 0.010 inches (0.25 mm). ASTM D3441 allows up to 0.024 in. (0.5 mm) less.

3.1.4.1. Negative Friction Sleeve Measurements

Since it is physically not possible for the friction sleeve stress to be negative, measurements of negative friction are due to inaccuracies or errors caused by one or more of the following:

1. Negative zero load offset resulting from a temperature change
2. Side loading against the friction sleeve
3. Unequal end area of friction sleeve in soils with very high porewater pressure
4. Lack of accuracy of the load cell at very small readings (less than .05%).

Negative zero load offset due to a temperature change is most often the cause of negative frictions. Such temperature effects are dominant because of the very small value of friction but can be corrected if the temperature is monitored and the procedures given in Section 3.1.3 are followed.

Side loading against the friction sleeve can cause negative readings and this effect can be reduced with eight strain gauges placed symmetrically around the load cell to cancel out or reduce side load effects as is done in Hogentogler's current designs.

Unequal end area effects can be reduced and essentially eliminated with the modern designs which have equal end area friction sleeves like those made by Hogentogler & Co.

Lack of accuracy is always a problem since a very small reading can either be plus or negative and these are often accompanied by very small

bearing values. This gives rise to rather large 'negative' values of friction ratio which would go unnoticed if they were positive.

When negative friction values appear it is important to isolate the cause and adjust your procedures. Negative frictions are rarely associated with tests in sands but often occur in very low bearing clays which generate high pore pressures. Data files containing negative frictions should be edited and adjusted after the cause is identified. There is little engineering difference between a very small negative or very small positive friction except that the negative value is very evident especially when plotted. The essential feature to realize is not the "negative" value but the "very small value" of friction which is often less than the accuracy of the instrument. Modern cone designs and test procedures can virtually eliminate the occurrence of apparent negative friction sleeve measurements.

3.1.5. Inclination

Most electronic cones today have simple slope sensors incorporated in the design to enable a measure of the non-verticality of the sounding (de Ruiter, 1982). This is particularly useful for very deep soundings where eventual tip inclinations in excess of 45° are not uncommon especially in stratified soil. The maximum depth for which a slope sensor can be omitted depends on the acceptable error in recorded depth provided obstructions do not exist. However, for most CPT work the maximum depth without a slope sensor, for which negligible error in recorded depth can be assumed, is about 15 m (Van de Graaf and Jekel, 1982). All Hogentogler and Co. electronic cones contain slope sensors,

Experience suggests that once a cone tip is deflected, it continues along a path with a relatively consistent radius of curvature. The standard equipment tends to accept about 1° of deflection per meter length without noticeable damage. A sudden deflection in excess of 5° over one meter or less may cause damage to the cone and rods from bending, which is not apparent to the operator, and penetration should be ceased.

3.1.6. Friction-Bearing Offset

The center of the friction sleeve is approximately 4 inches (10 cm) behind the cone tip. To calculate the friction ratio (R_f), the average friction resistance (f_s) and bearing resistance (q_c) are compared at the same depth. This usually involves an offset of the friction resistance by the physical distance of 4 inches (10 cm). However, the bearing resistance is affected by the soil ahead of the tip, whereas, the friction is only affected by the soil in direct contact with the friction sleeve. Thus, the standard offset distance of 4 inches (10 cm) may not always produce realistic friction ratio plots, especially in heavily interbedded soils and in relatively stiff soils where the offset can be considerably more than 10 cm. In general, however, the standard practice of 10 cm friction-bearing offset usually provides adequate friction ratio plots.

3.1.7. Checks and Recalibration

Table 3.1 presents a suggested summary of maintenance requirements (checks and recalibrations) for CPT and CPTU soundings. This summary can be used as a basis for setting up an ongoing maintenance program and checklist of procedures which should be established in conjunction with the

Item	Ref. to Section	FREQUENCY			
		At Start of CPT Program*	At Start of CPT Sounding	At End of CPT Sounding	At 3-monthly Intervals
Verticality of thrust machine	3.1.5		•		
Straightness of push rods	3.1.5		•		
Precision of measurements	2.3.1	•			•
Zero load error (taking baselines)	2.3.1 2.5 2.6 3.1.4		•	•	
Wear:					
- dimensions of cone, friction sleeve	2.6	•			•
- roughness	3.1.4	•			•
Seals:					
- presence of soil particles	2.3.1	•	•		
- quality	2.6	•	•		
Calibration					
- load cells and pressure transducers	2.5 3.1.4	•			•
- unequal end area	3.1.1				•
- temperature	2.5 3.1.3				•
- pressure gauge (Mech. CPT)	3.1.4	•			•

* And regularly during a long testing program.

TABLE 3.1: Summary of Checks and Recalibrations for CPT and CPTU Soundings

manufacturer's operator's manual in order to maintain a high quality of cone data.

3.2. Presentation of Data

The recommended graphical presentation of CPT data should include the following:

i) measured cone resistance, q_c vs. depth
(where q_c = bearing force divided by bearing area of 10 sq. cm)
measured sleeve frictional stress, f_s vs. depth
(where f_s = friction sleeve force divided by surface area of sleeve, usually 150 sq. cm.)
measured pore pressure, u vs. depth

ii) corrected total cone resistance, q_T vs. depth
measured sleeve friction, f_s vs. depth
measured pore pressure, u vs. depth
(including equilibrium water pressures, u_o).

Details and definitions of the above terms are given in later sections.

A range of recomended parameters may also be included in (ii) above as follows,

a) Friction ratio, $f_s/q_c \times 100\%$ or $f_s/q_T \times 100\%$ vs. depth.

b) Differential pore pressure ratio, $\frac{\Delta u}{q_c}$ or $\frac{\Delta u}{q_T}$ and $\Delta u/(q_c - \sigma_{vo})$ or $\Delta u/(q_T - \sigma_{vo})$ vs. depth where σ_{vo} = vertical total stress = $\Sigma\gamma h$, and $\Delta u = u - u_o$.

or c) Differential pore pressure ratio, $\Delta u/(q_T - u_o)$ vs. depth.

d) Corrected total cone resistance, q_T vs. σ'_{vo} (in-situ vertical effective stress).

Any parameter using σ_{vo} or σ'_{vo} requires additional input data, e.g., soil unit weight, (γ), or a profile of unit weight with depth.

3.3. Evaluation of CPT and CPTU Data

In stiff soils CPT data is generally very reliable. However, in soft soils (q_c <20 t/ft^2) the cone resistance may be somewhat less reliable due to various factors (see Section 3.1). To evaluate the performance in soft soils, the zero load readings (baselines) before and after each sounding should be reviewed. The CPT data should be corrected based on the change in zero load readings. This can be important in very soft deposits where temperature variations can cause zero load readings to change significally in relation to the measured values.

If CPTU data is to be evaluated, the pore pressure data should be reviewed to identify; a rapid response and detailed stratigraphy. The pore pressure data can be used to further correct the measured q_c values in soft soils (see Section 3.1).

If dissipation tests have been performed, the response time and equilibrium pore pressures should be reviewed to assess the level of saturation of the piezocone system.

4. INTERPRETATION OF CPT AND CPTU DATA

4.1. Factors Affecting Interpretation

Before analyzing any electric cone data, it is important to realize and account for the potential errors that each element of data may contain. Significant aspects that pertain to cone designs will be discussed. The reader is encouraged to investigate the details of the particular cone design before performing detailed interpretation of the data.

The reader should also be aware of the significant factors regarding soil conditions and how these influence the measured cone data and thus the interpretation.

4.1.1. Equipment Design

Section 3.1 outlined the significant factors regarding cone design that influence the measured parameters and therefore the subsequent interpretation. The three major areas of cone design that influence interpretation are:

1) Unequal Area effects
2) Piezometer location, size and saturation
3) Accuracy of measurements

It is strongly recommended that bearing cones be calibrated for all around pressure effects and when possible correct q_c to q_T. The errors associated with equipment design are usually only significant for penetration in soft, normally consolidated, fine grained soils. Test results in sand are little influenced by the above factors, except possibly variations in friction sleeve stress, f_s.

4.1.2. In-situ Stress

Theoretical models and chamber test studies have shown that the in situ radial stress, σ'_r, has a dominant effect on the cone resistance, q_T, and the friction sleeve stress. Therefore, the soils stress (geologic) history is of great importance in CPT interpretation. Unfortunately, there is often only qualitative data concerning geologic history and the techniques for measuring in-situ radial stresses are not very reliable, especially for sands.

We know that excavation will reduce σ'_r in horizontally adjacent soils. Even an open borehole, if closer than about 25 hole diameters may significantly reduce σ'_r. Both static and vibratory roller compaction or the use of compaction (or displacement) piles can greatly increase σ'_r. Vibroflotation and dynamic compaction can also significantly increase σ'_r, but sometimes in the case of fine sands when using a fine sand vibro- flotation backfill, a decrease in σ'_r may occur. The engineer must consider, at least qualitatively, such effects when evaluating CPT data for design. For example, an increase in friction ratio is often measured after in situ densification due to increased in σ'_r.

Subsequent sections will show that the relative density correlations for sand are significantly influenced by changes in horizontal stresses. However, the correlations of friction angle, (ϕ), appear to be much less influenced by changes in σ'_r.

4.1.3. Compressibility, Cementation and Particle Size

The compressibility of a sand can significantly influence q_c and f_s. Highly compressible carbonate sands tend to have low q_c and high friction

ratios values. Some carbonate sands have friction ratios as high as 3%, whereas, typical incompressible quartz sands have friction ratios of about 0.5%. The compressibility of sand during cone penetration is also influenced by grain crushing.

Subsequent sections will show that variations of sand compressibility have a significant influence on correlations with relative density but a smaller influence on correlations with friction angle.

Cementation between particles reduces compressibility and thereby increases q_c. Cementation is always a possibility in-situ and is more likely in older soil deposits. When the particle size of a soil penetrated becomes a significant fraction of the cone diameter, then q_c can increase abruptly because of the decreased compressibility due to having to displace these particles as rigid units. This effect tends to produce sharp peaks in the q_c profile when encountering gravel sized particles. Intersecting very large particles can abruptly stop penetration or cause a sudden deflection. Penetration through gravelly soils often produces a distinct sound up the cone rods.

4.1.4. Stratigraphy

Theoretical cavity expansion models and chamber test studies have shown that the cone penetration resistance, q_c, is influenced by an interface ahead and behind the tip. The distance over which the cone tip senses an interface increases with increasing soil stiffness. Thus, the cone tip can respond fully (i.e., q_c to reach full value within the layer) in thin soft layers better than in thin stiff layers. Therefore, care should be taken when interpreting cone bearing in a thin sand layer located

within a soft clay deposit. Further discussion of layering effects will be given in Section 4.3.

This effect of layering can also cause scale affects when using cones of a larger diameter (i.e., 15 cm² cone area). The natural variability of many sand deposits produces q_c profiles with many sharp peaks and troughs. A comparison of CPT data in sands from 10 cm² and 15 cm² cones shows that the 15 cm² data will not reproduce the stiff peaks but will reproduce the soft troughs. Since the relative layer thickness for full response of q_c is smaller for softer layers, the average q_c profile tends to be slightly lower for the 15 cm² cone in sands. Generally speaking, however, in moderately uniform soil the results of a 15 cm² cone are essentially the same as those for the standard 10 cm² cone.

4.1.5. Rate of Penetration

Rate effects are generally due to pore pressure effects. However, rate effects can also be caused to some extent by creep and particle crushing. In general, however, the pore pressure effects predominate and are of most interest, especially when using the piezometer cone.

The recommended constant rate of penetration for an electronic static cone sounding is 2 cm/sec. The ASTM D3441 Standard allows a penetration rate of 2-4 ft/min (10-20 mm/s) ±25%. Traditionally cone penetration in sands has been considered to be drained and penetration in clays undrained. However, for mixed soils such as silts and clayey silts, the drainage condition during penetration is not well defined. The drainage condition can be approximated from the soil classification chart (Fig. 4.2 in next section) or by measuring the rate of dissipation of excess pore pressure in a CPTU test.

4.2. Soil Classification

The most comprehensive work on soil classification using electric cone penetrometer data was presented by Douglas and Olsen (1981). A copy of their proposed soil-behaviour type classification chart is shown in Fig. 4.1. The chart shows how cone penetration test data has been correlated with other soil type indices, such as those provided by the Unified Soil Classification System. The correlation was based on extensive data collected from areas in California, Oklahoma, Utah, Arizona and Nevada (USGS Open-file Report No. 81-284, 1980).

The complexities of the chart by Douglas and Olsen (1981) make it difficult to use. For this reason, Robertson (1985) adapted the chart based on the original data plus the UBC experience to produce the simpler but somewhat less comprehensive classification chart shown in Fig. 4.2.

The usual progression of site investigation using the cone penetration test (CPT) is to perform the CPT soundings, develop detailed site profiles with the soil behaviour type charts (Fig. 4.2), and then selectively sample and test to provide any additional information regarding ambiguous classifications. With local experience this latter step is often not necessary.

Fig. 4.1 shows how increasing K_o (i.e. increasing OCR) will increase both the cone resistance and friction ratio. For fine grained soils, an increase in liquidity index (LI) will produce a decrease in both q_c and R_f. Thus, sensitive soils tend to have low friction ratios. Increasing compressibility produces a decrease in cone resistance with an increase in friction ratio. Thus, carbonate sands or sands with a high mica content tend to have high friction ratios, and may fall in the sandy silts region.

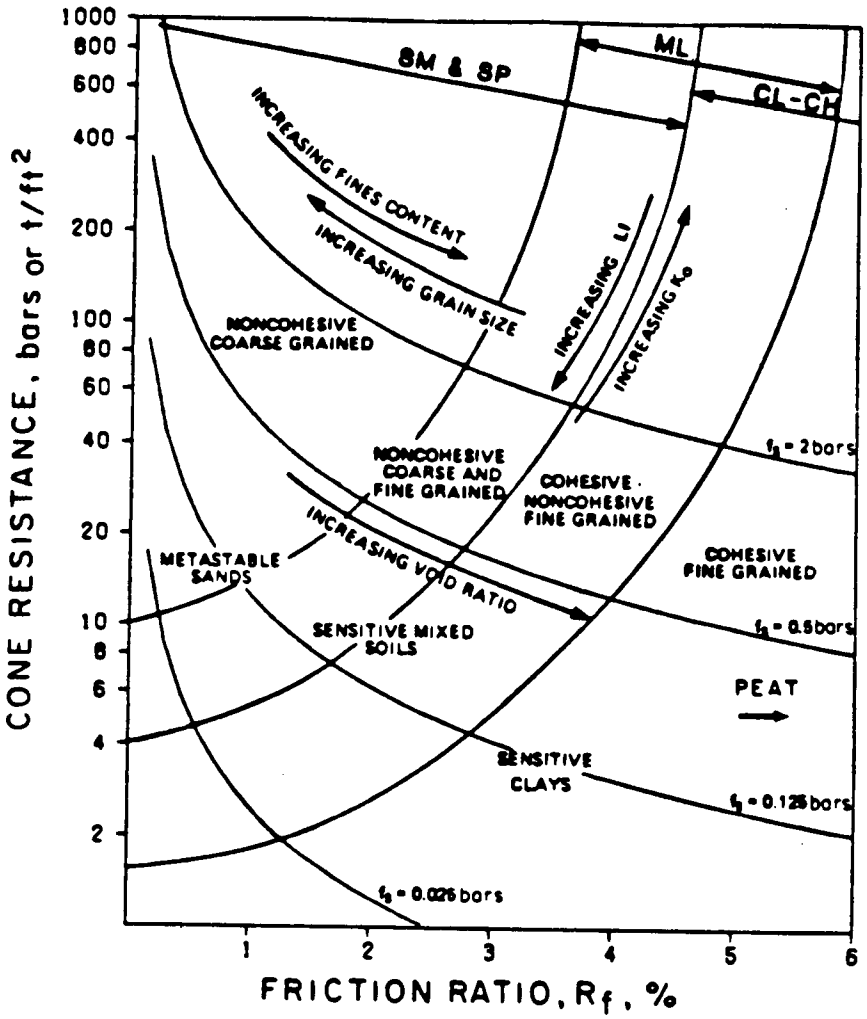

1 bar = 100 kPa ≈ 1 kg/cm²

Figure 4.1 Soil Classification Chart for Standard Electronic Friction Cone (Adapted from Douglas and Olsen, 1981)

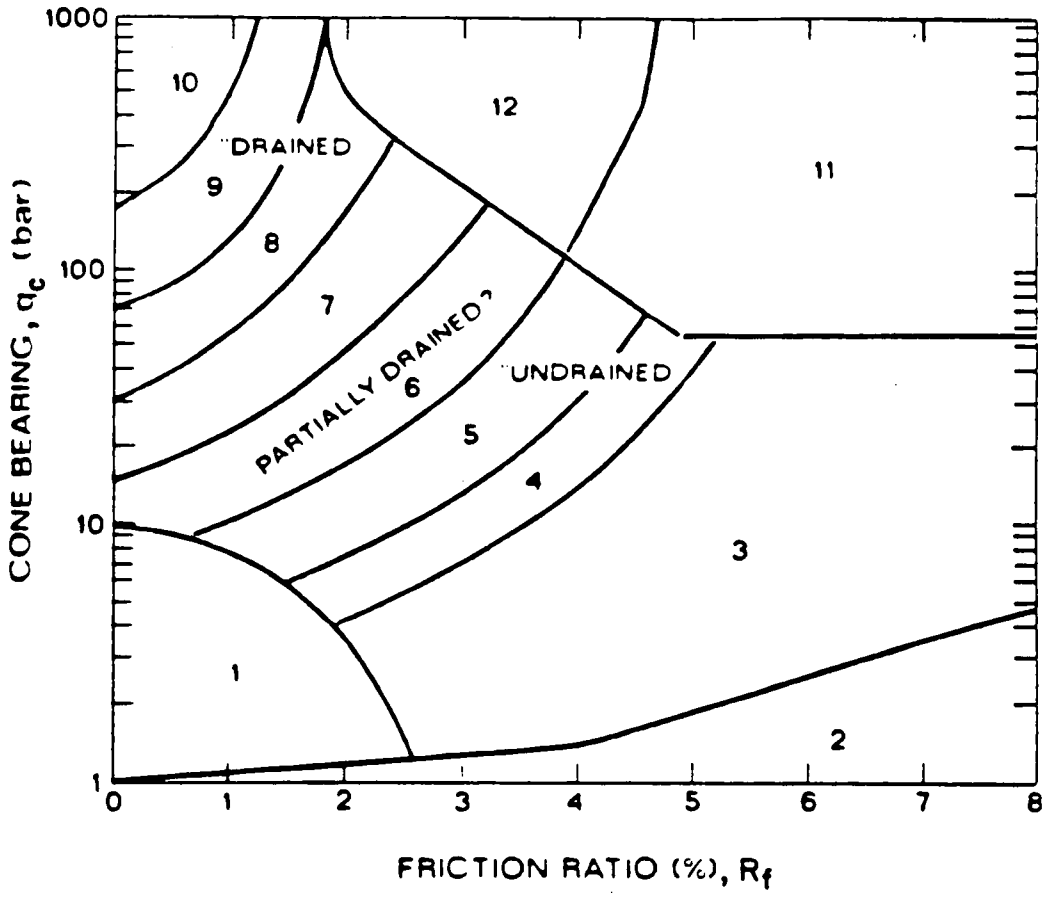

Zone	q_c/N	Soil Behaviour Type
1)	2	sensitive fine grained
2)	1	organic material
3)	1	clay
4)	1.5	silty clay to clay
5)	2	clayey silt to silty clay
6)	2.5	sandy silt to clayey silt
7)	3	silty sand to sandy silt
8)	4	sand to silty sand
9)	5	sand
10)	6	gravelly sand to sand
11)	1	very stiff fine grained (*)
12)	2	sand to clayey sand (*)

(*) overconsolidated or cemented

Figure 4.2 Simplified Soil Classification Chart for Standard Electronic Friction Cone (Robertson et al, 1986)

Recent research has illustrated the importance of cone design and the effect that water pressures have on the measured bearing and friction due to unequal end areas. Thus cones of slightly different designs will give different bearing, friction and friction ratios. With proper calibration and measurement, the effects of unequal end areas can be corrected. A detailed discussion concerning cone design is also given by Schaap and Zuidberg (1982). The data used to compile the classification charts (Figs. 4.1 and 4.2) used bearing and friction values that had generally not been corrected for pore pressure effects, since, in general, pore pressure measurements were not made. Recent data indicates that there is little difference between corrected and uncorrected friction ratios for most soil types except for those soils that classify in the lower portion of the charts (Fig. 4.1). These soils usually generate large positive pore pressures during penetration and have very low measured bearing (q_c<10 t/ft^2) and small friction values where corrections become very significant. These soils also tend to have high liquidity index values, as noted by Douglas and Olsen (1981). Most standard electronic cone data (CPT) does not include pore pressure measurements and the measured bearing and friction values are therefore not corrected for pore pressure effects. For this type of data the charts in Figs. 4.1 and 4.2 can be used directly to provide a reasonable estimate of soil type. If pore pressure measurements are included and the necessary corrections applied to the data, Figs. 4.1 and 4.2 should be used with caution, especially for soft saturated soils, and should <u>always be adjusted to reflect local experience</u>.

The measurement of sleeve friction is sometimes less accurate and reliable than the tip resistance. Also cones of different designs will

often produce variable friction sleeve measurements. This can be caused by variations in mechanical and electrical design features of the friction sleeve as well as unequal end areas.

To overcome the problems associated with sleeve friction measurements, several classification charts have been proposed based on q_T and pore pressures (Jones and Rust, 1982; Baligh et al, 1980; Senneset and Janbu, 1984). The chart by Senneset and Janbu (1984) uses the pore pressure parameter ratio, B_q, defined as;

$$B_q = \frac{\Delta u}{q_T - \sigma_{vo}} \tag{4.1}$$

where Δu = excess pore pressure, measured behind the tip,

q_T = cone resistance corrected for pore pressure effects,

σ_{vo} = total overburden stress.

The original chart by Senneset and Janbu (1984) uses q_c. However, it is generally agreed that the chart and B_q should use the corrected cone bearing, q_T. The correction is usually only significant in soft, fine grained soils where q_c can be small and Δu can be very large.

The authors have found from their experience that it is not always possible to clearly identify a soil type based solely on the q_T and Δu data. Sometimes changes in the friction ratio have been able to more clearly define changes in soil type. Therefore, the authors recommend and use all three pieces of data (q_T, u, f_s) in the form of q_T, B_q and R_f to

define soil behaviour type. A first attempt at defining such a system is shown in Fig. 4.3. Note that the pore pressure is measured immediately behind the cone tip.

The charts in Figs. 4.1, 4.2 and 4.3 are global in nature and should only be used as a guide to define soil behaviour type based on CPTU data. Factors such as changes in, stress history, sensitivity, stiffness and void ratio will influence the classification using either the R_f or the B_q chart. Occasionally soils will fall within different zones on each chart, in these cases judgement is required to correctly classify the soil behaviour type. Often the rate and manner in which the excess pore pressures dissipate during a pause in the cone penetration will aid in the classification. For example, a soil may have the following CPTU parameters; q_T = 10 t/ft², R_f= 4%, B_q = 0.1. It would classify as a clay on the R_f chart and as a clayey silt to silty clay on the B_q chart. However, if the rate of pore pressure dissipation were very slow this would add confidence to the classification of a clay. If the dissipation were rapid (t_{50} < 60 secs) the soil may be more like a clayey silt or possibly a clayey sand. The manner of the dissipation can also be important. In stiff, overconsolidated clay soils, the pore pressure behind the tip can be very low in comparison to the high pore pressures on the face. When penetration is stopped, pore pressures recorded immediately behind the tip may initially rise before dropping to the equilibrium pressure. The rise can be caused by local equilization of the high pore pressures on the nearby cone face, although poor saturation can also cause a similar response.

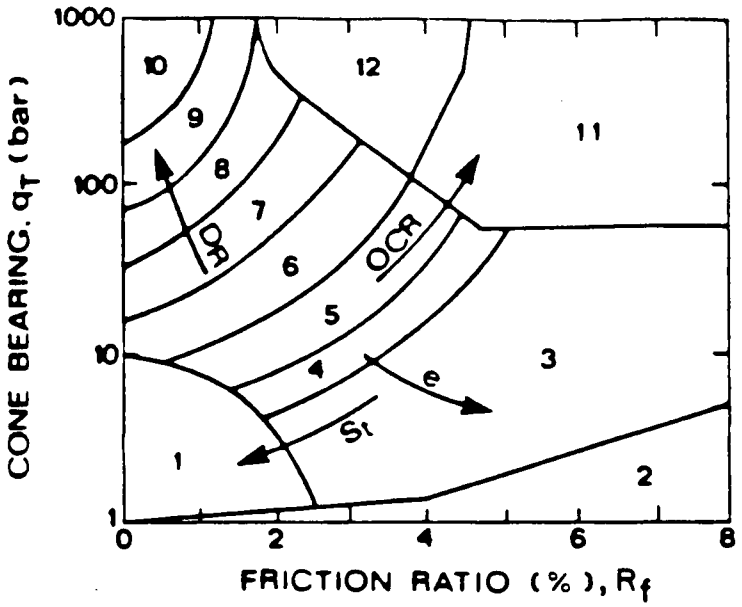

Notes:

1. Expect some overlap in zones
2. Local correlations preferable
3. Based mainly on data obtained from depth <30 m
4. Review available dissipations of u to guide overlap in charts.

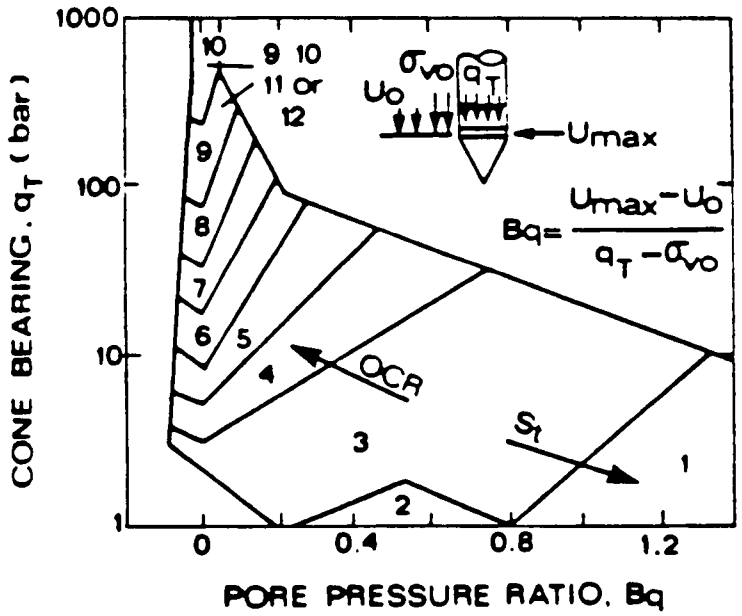

Zone	q_T/N	Soil Behaviour Type
1)	2	sensitive fine grained
2)	1	organic material
3)	1	clay
4)	1.5	silty clay to clay
5)	2	clayey silt to silty clay
6)	2.5	sandy silt to clayey silt
7)	3	silty sand to sandy silt
8)	4	sand to silty sand
9)	5	sand
10)	6	gravelly sand to sand
11)	1	very stiff fine grained (*)
12)	2	sand to clayey sand (*)

(*) overconsolidated or cemented

Figure 4.3 Proposed Soil Behavior Type Classification System from CPTU Data (After Campanella and Robertson, 1988)

A further problem associated with existing CPT classification charts is that soils can gradually change in their apparent classification as cone penetration increases in depth. This is due to the fact that q_T, u and f_s all tend to increase with increasing overburden pressure. For example, in a thick deposit of normally consolidated clay, the cone bearing will increase linearly with depth resulting in an apparent change in CPT classification. Existing classification charts are based predominantly on data obtained from CPT profiles extending to a depth of less than 100 ft (30 m). Therefore, for CPT data obtained at depths significantly greater than 30 m some error can be expected when using the standard global CPT classification charts.

Attempts have been made to account for this by normalizing the cone data with the effective overburden stress, σ'_{vo} (Robertson and Campanella, 1985; Olsen, 1984; Douglas et al, 1985). However, it is not clear how CPT data in general should be normalized. Olsen and Farr (1986) use different normalization methods for different soil types, but this produces a somewhat complex iterative interpretation that requires a computer program.

In theory, any normalization to account for increasing stress should also account for changes in horizontal stresses. This could be achieved by using a parameter such as the mean or octahedral stress, $\sigma'_m = \frac{1}{3}(\sigma'_1+\sigma'_2+\sigma'_3)$,

where
$$\sigma'_m = \frac{1}{3}\sigma'_{vo}(1 + 2K_o) \qquad (4.2)$$

However, at present, this has little practical benefit without a prior knowledge of the in-situ horizontal stresses (K_o). Even normalization

using only vertical effective stress requires some input of soil unit weights and ground water conditions.

Normalization of the CPT data would avoid some of the problems associated with variations in q_T with soil strength. At present, a very loose clean sand may be classified as a sandy silt to silty sand because of the low q_T.

Until a consistent method for normalization is adopted, the authors use and recommend the charts shown in Figs. 4.2 and 4.3. However, some caution is suggested if the cone data extends beyond a depth of about 100 ft (30 m) below existing ground surface.

It is often important to realize that the classification charts are generalized global charts that provide a guide to soil behaviour type. The charts cannot be expected to provide accurate prediction of soil type for all soil conditions. However, in specific geological areas, the charts can be adjusted for local experience to provide excellent local correlations.

4.3. Stratigraphic Logging

The cone penetration tip resistance is influenced by the soil properties ahead and behind the tip. Chamber studies (Schmertmann, 1978a, Treadwell, 1975) show that the tip senses an interface between 5 to 10 cone diameters ahead and behind. The distance over which the cone tip senses an interface increases with increasing soil stiffness. For interbedded deposits, the thinnest stiff layer the cone bearing can respond fully (i.e. q_c to reach full value within the layer) is about 10 to 20 diameters. For the standard 10 cm² electric cone, the minimum stiff layer thickness to ensure full tip resistance is therefore between 14 inches to 28 inches

(36 cm to 72 cm). The tip will however, respond fully for soft layers considerably thinner than 14 inches (36 cm) in thickness. Since the cone tip is advanced continuously, the tip resistance will sense much thinner stiff layers, but not fully. This has significant implications when interpreting cone bearing, for example, for relative density determination in sand. If a sand layer is less than about 28 inches (70 cm) thick and located between, say, two soft clay deposits, the cone penetration resistance may not reach its full value within the sand because of the close proximity of the adjacent interfaces. Thus, the relative density in the sand may be severely underestimated.

The continuous monitoring of pore pressures during cone penetration can significantly improve the identification of soil stratigraphy (Campanella et al, 1983). The pore pressure develops in response to the soil type being penetrated in the immediate area of the pore pressure sensing element. To aid in the identification of very thin silt or sand layers within clay deposits, some researchers (Torstensson, 1982) have proposed and successfully used thin (2.5 mm) pore pressure elements located immediately behind the cone tip. For a pore pressure sensing element behind the tip, sands give very low or negative pore pressures while clays are very high. Dilative silts also give low or negative pore pressures while contractive silts give high positive pore pressures.

The frequency response of a fully saturated piezometer cone is usually fast enough to observe changes in pore pressure with a period of 0.25 seconds or less. This corresponds to layer thickness of about 0.2 inches (5 mm) or less at the standard penetration rate of 2 cm/sec. Whether or not such thin layers are observed in practice depends on the response of the soil to the advancing cone and the depth interval of data recording.

For thin sand layers within a body of clay the drainage characteristics of the sand become very important.

4.4. Drained Soil

4.4.1. Relative Density (D_r)

For cohesionless soils the density, or more commonly the relative density, is often used as an intermediate soil parameter. Recent research has shown that the stress-strain and strength behaviour of cohesionless soils is too complex to be represented solely by the relative density of the soil. Several papers in ASTM (1973) have discussed difficulties associated with determination of maximum, minimum and in-situ densities as well as problems in correlating relative density with measured soil properties. However, because many engineers continue to use relative density as a guide in design some discussion is given here on recent work relating cone penetration resistance to soil relative density.

Recent work in large calibration chambers (Veismanis, 1974, Chapman and Donald, 1981, Baldi et al, 1981, Parkin et al, 1980 and Villet and Mitchell, 1981) has provided numerous correlations of cone resistance (q_c) with soil relative density (D_r). Most of these works have also shown that no single unique relationship exists between relative density, in-situ effective stress and cone resistance for all sands.

It is not surprising that no unique relationship exists between cone resistance, in-situ effective stress and relative density since other factors such as soil compressibility also influence cone resistance.

A review of the numerous calibration chamber tests performed on a variety of different sands shows a significant range of D_r versus q_c relationships. However, all the chamber test results show that the curves

are all similar in shape and most show that the cone resistance can be more uniquely related to relative density, for any given sand, if correlated with the in-situ initial horizontal effective stress (σ'_{ho}). If the horizontal effective stress is used the relationship can be expected to apply to both normally and overconsolidated sand. Fig. 4.4 shows a comparison between the curves proposed by Schmertmann (1978b), Villet and Mitchell, (1981) and Baldi et al (1981) for two levels of relative density. All the curves have been corrected for chamber size. Details of the sands used in the calibration chamber studies are given in Table 4.1.

The calibration test data (Fig. 4.4) shows the importance of sand compressibility. The curves by Schmertmann (1978b) represent the results of tests on Hilton Mines sand, which is a relatively compressible quartz, feldspar, mica mixture with angular grains. The curves by Villet and Mitchell (1981) represent results on Monterey Sand which is a relatively incompressible quartz sand with subrounded particles. Schmertmann (1978b) also performed tests on Ottawa sand, which is also an incompressible quartz sand with rounded particles, and obtained curves almost identical to those of Villet and Mitchell (1981). Thus, it appears that sands with a low compressibility have a D_r- q_c relationship similar to that shown by Villet and Mitchell (1981) and sands with a high compressibility have a relationship similar to that shown by Schmertmann (1978b). The sand used by Baldi et al (1981) (Ticino Sand) was a quartz, feldspar, mica mixture with subangular particles. The Ticino Sand appears to have a moderate compressibility somewhere between the two extremes of Hilton Mines and Monterey Sand. Figure 4.5 illustrates the range of D_r- q_c relationships for most of the sands tested in calibration chambers. (Note: D_R is used in some of the figures in place of D_r.)

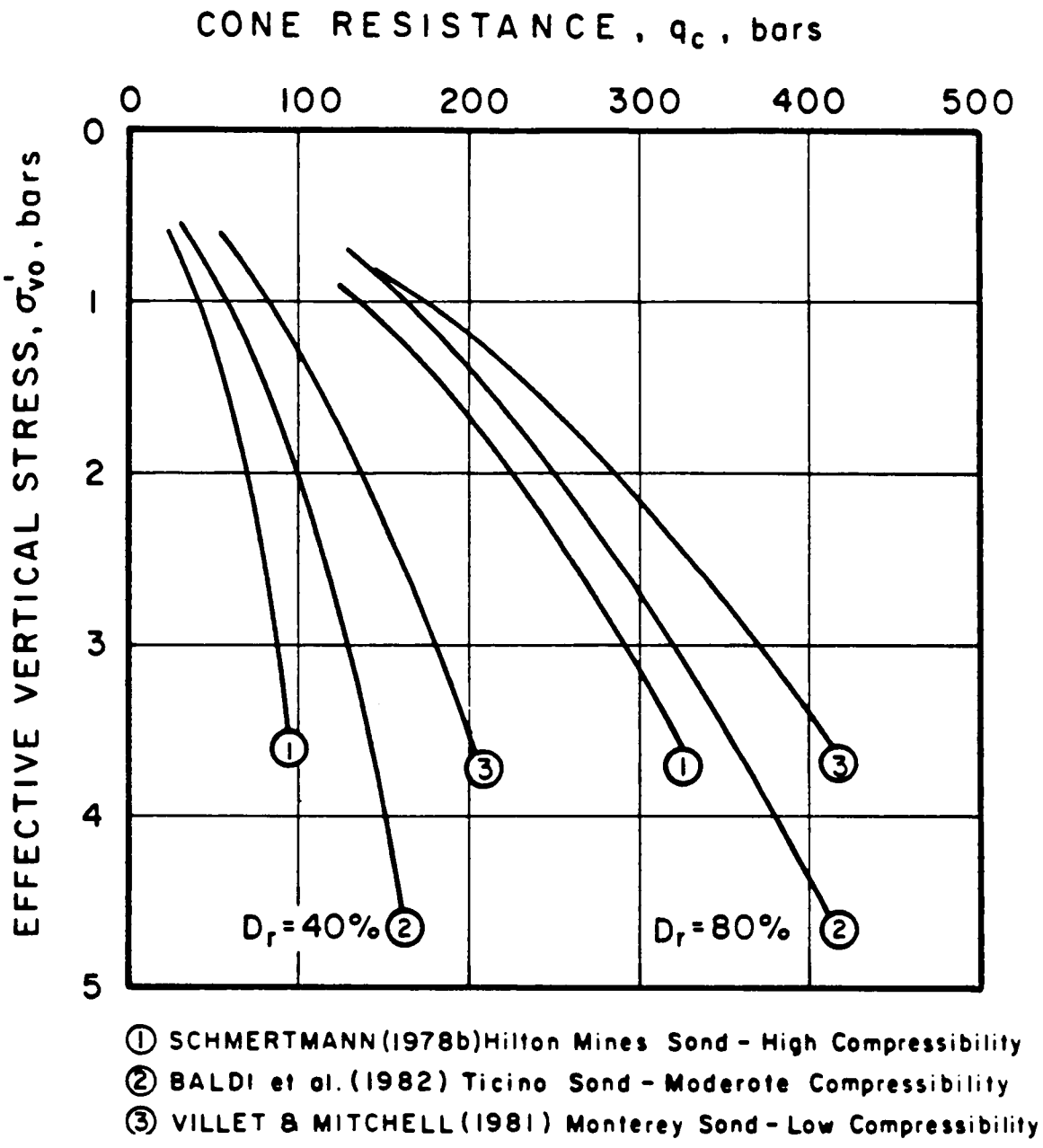

Figure 4.4 Comparison of Different Relative Density Relationships (After Robertson and Campanella, 1983a)

Reference	Sand Name	Mineralogy	Shape	Gradation (mm)		Porosity	
				D_{60}	D_{10}	n_{max}	n_{min}
Baldi et al., (1981, 1982)	Ticino	Mainly quartz 5%* mica	Subangular to angular	0.65	0.40	0.50	0.41
Villet & Mitchell (1981)	Monterey	Mainly quartz some feldspar	Subrounded to subangular	0.40	0.25	0.45	0.36
Schmertmann (1978b)	Ottawa #90	quartz	Rounded	0.24	0.13	0.44	0.33
——— " ———	Hilton mines	quartz + mica + feldspar	Angular	0.30	0.15	0.44	0.30
Parkin et al (1980)	Hokksund	35% quartz 45% feldspar 10%* mica	Rounded to subangular	0.5	0.27	0.48	0.36
Veismanis (1974)	Edgar	Mainly quartz	Subangular	0.5	0.29	0.48	0.35
——— " ———	Ottawa	Quartz	Subangular	0.54	0.45	0.42	0.32
Holden (1971)	South Oakleigh	Quartz	Subangular	0.19	0.12	0.47	0.35
——— " ———	——— " ———	Quartz	Subangular	0.37	0.17	0.43	0.29
Chapman & Donald (1981)	Frankston	Mainly Quartz	Rounded to Subangular	0.37	0.18	----	----

* Percent mica by volume

TABLE 4.1: Properties of Sand Tested in Calibration Chamber Studies (After Robertson and Campanella, 1983a)

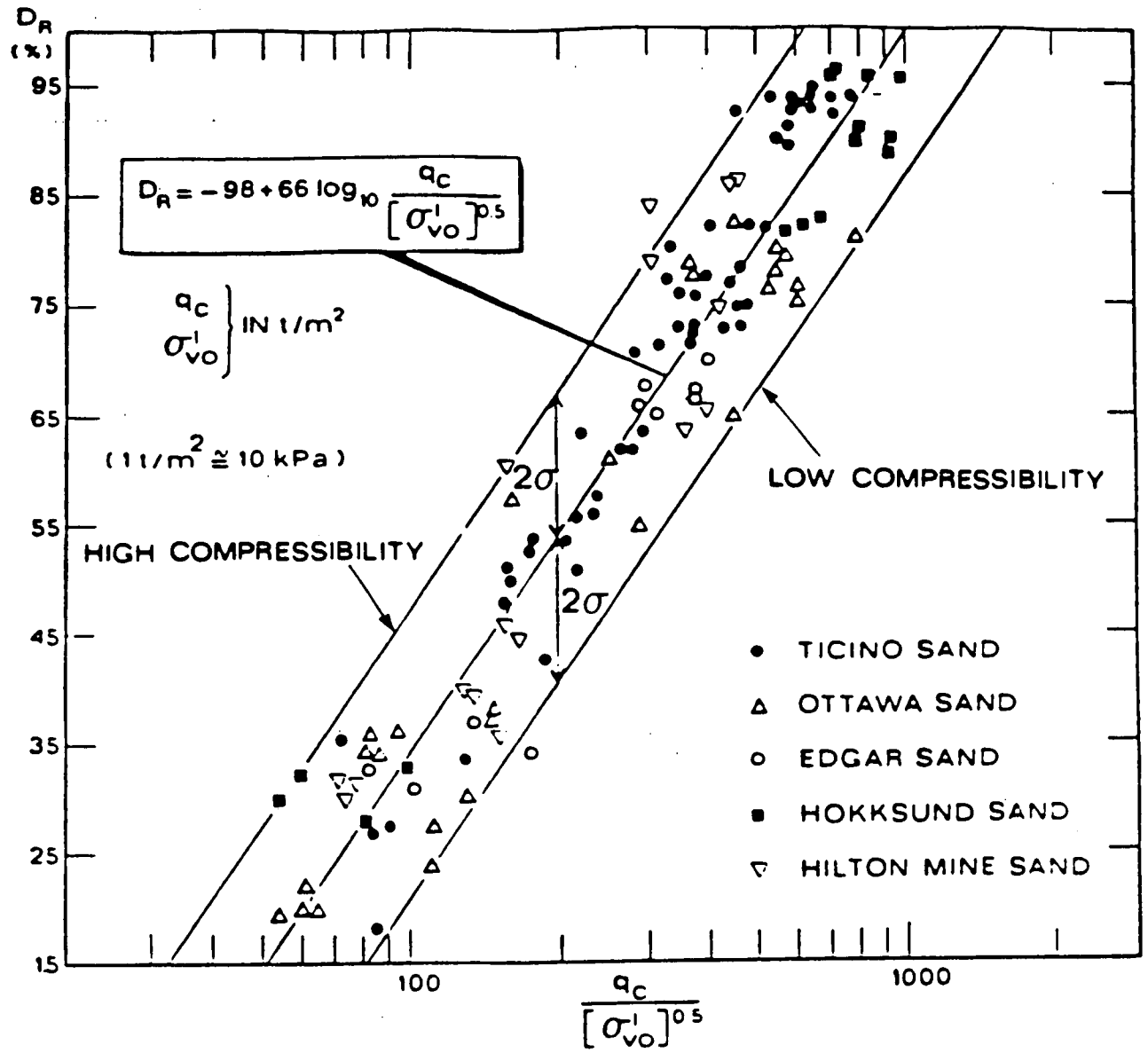

Figure 4.5 Influence of Compressibility on N.C. Uncemented, Unaged, Predominantly Quartz Sands
(After Jamiolkowski et al, 1985)

A large portion of CPT work is often carried out in sands where the grain minerals are predominately quartz and feldspar. These are sands similar to those tested in most of the calibration chamber work. Research has shown that there is relatively little variation in the compressibility for most quartz sands, although this depends on the angularity of the grains (Joustra and de Gijt, 1982). Angular quartz sands tend to be more compressible than rounded quartz sands. If an estimate of relative density is required for a predominantly quartz sand of moderate compressibity, the writers recommend that the relation given by Baldi et al (1986) be used.

Fig. 4.6 shows Baldi's relationship between relative density (D_r) vertical effective stress (σ'_{vo}) and cone resistance (q_c). The relationship is for normally consolidated, where K_o = 0.45, uncemented and unaged sands. The relationships shown in Fig. 4.6 are practically identical to those recommended by Schmertmann (1978b). If overconsolidated or aged sands are encountered, the horizontal effective stress (σ'_{ho}) should be used instead of σ'_{vo}. However, the application of this relationship to overconsolidated sands appears, at present, very difficult because of the inherent difficulties in measuring or choosing an appropriate σ'_{ho} in-situ and assessing the stress history of natural sand deposits.

It is suggested that Fig. 4.6 should be used only as a guide to in-situ relative density, but can be expected to provide reasonable estimates for clean normally consolidated moderately compressible quartz sands. Some engineers have suggested that the D_r values obtained from charts like 4.6 should be referred to as **"Equivalent"** D_r values when applied to natural

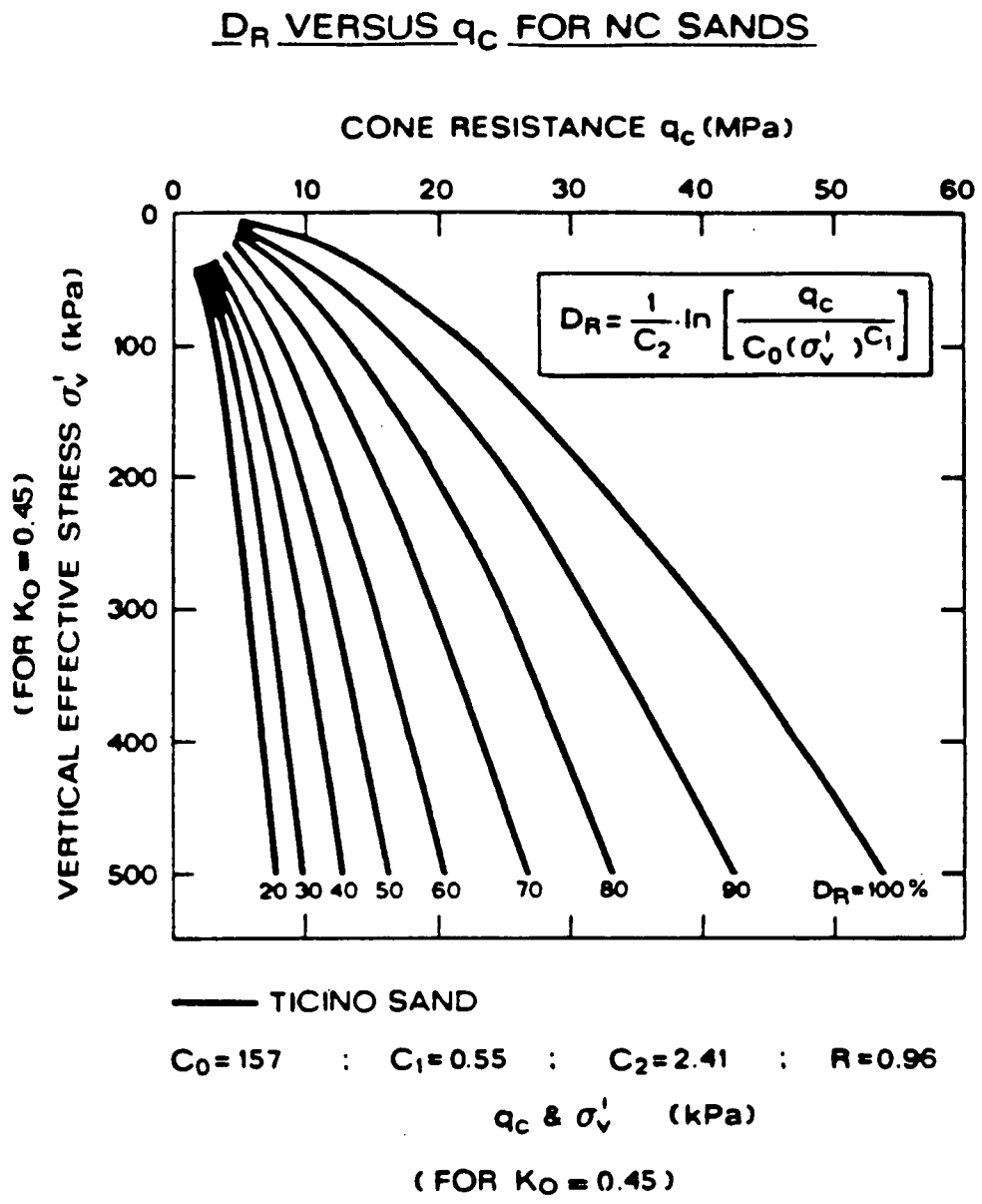

Figure 4.6 Relative Density Relationship for N.C., Moderately Compressible, Uncemented, Unaged Quartz Sands (After Baldi et al, 1986)

sands. Figure 4.5 can be used as a guide to adjust the correlations for sands that may be more or less compressible. A visual classification of the grain characteristics would significantly improve the choice of relative density correlation. The compressibility of sands tends to increase with increasing uniformity in grading, with increasing angularity of grains, with increasing mica content and with increasing carbonate content. Care should be exercised in interbedded deposits where the cone resistance may not have reached the full value within a layer.

4.4.2. Friction Angle (ϕ)

Many theories and empirical or semi-empirical correlations for the interpretation of drained shear strength of sand from cone resistance have been published. The theories can be divided into two categories; namely those based on bearing capacity theory (Janbu and Senneset, 1974, Durgunoglu and Mitchell, 1975) and those based on cavity expansion theory (Vesic, 1972).

Work by Vesic (1963) has shown that no unique relationship exists between friction angle for sands and cone resistance, since soil compressibility influences the cone resistance. The curvature of the Mohr-Coulomb failure envelope for granular soils has been observed repeatedly by numerous investigators and is presently recognized as a typical material behaviour. Most of the available bearing capacity theories on deep penetration neglect both the curvature of the shear strength envelope and the compressibiity of the soil. The increasing influence of these two factors tend to reduce the tip resistance.

Based on cavity expansion concepts, Vesic (1972) developed a theory for tip resistance taking account of soil compressibility and volume change characteristics. Baligh (1976) developed this further to incorporate the curvature of the strength envelope. The comprehensive calibration chamber test work by Baldi et al (1986) and recent work by Mitchell and Keaveny (1986) show that the cavity expansion theory appeared to model the measured response extremely well. The cavity expansion analysis, however, is complex and requires considerable input data regarding compressibility and shear strength. Calibration chamber results illustrate the complex nature of cone penetration in sands and show that simple closed form solutions to derive the shear strength for all sands are not possible. In addition, chamber tests provide valuable insight into the relative importance of the various factors that influence cone penetration in sands. In general, it would be expected that the bearing capacity theories, which cannot take account of soil compressibility, could not provide reliable predictions of friction angle. The work by Mitchell and Keaveny (1986) showed that the bearing capacity theory developed by Durgunoglu and Mitchell (1975) provided reasonable predictions for a variety of sands but poor prediction for highly compressible sands.

Bearing capacity theories will give conservatively low estimates of friction angle for more compressible sands (i.e. carbonate sands).

A review of the calibration chamber test results was carried out by Robertson and Campanella (1983a) to compare the measured cone penetration resistance to measured peak friction angle from drained triaxial tests. The peak friction angle values were obtained from triaxial tests performed at confining stresses approximately equal to the horizontal effective

stress in the calibration chamber before cone penetration (i.e., in-situ σ'_{ho}). The results of the comparison are shown on Fig. 4.7. Details of the sands used in the studies are given in Table 4.1. The scatter in the results illustrate the limited influence of soil compressibility. Also shown in Fig. 4.7 are the theoretical relationships proposed by Janbu and Senneset (1974) and Durgunoglu and Mitchell (1975). The Durgunoglu and Mitchell method includes the effect of in-situ horizontal stresses. The difference between the normally consolidated state, where $K_o = 1-\sin\phi$, and the overconsolidated state (OCR ≈ 6), where $K_o = 1.0$, is less than 2 degrees, as shown on Fig. 4.7.

Since the solution by Janbu and Senneset (1974), for $\beta = 0$, (see Fig. 4.7) tends to slightly over-estimate ϕ and Durgunoglu and Mitchell tends to under-estimate ϕ, an average empirical relationship was proposed by Robertson and Campanella (1983a), as shown on Figs. 4.7 and 4.8. The proposed chart in Fig. 4.8 can be expected to provide reasonable estimates of peak friction angle for normally consolidated, uncemented, moderately incompressible, predominantly quartz sands, similar to those used in the chamber studies. For highly compressible sands, the chart would tend to predict conservatively low friction angles (see Fig. 4.7). Durgunoglu and Mitchell's theory shows that there is little change in predicted friction angle for relatively large changes in stress history. It is important to note that the friction angle predicted from Fig. 4.8 is related to the in-situ initial horizontal stress level before cone penetration.

The friction ratio for sands increases with increasing compressibility. Many compressible carbonate sands have friction ratios as high as 3 percent (Jonstra and de Gijt, 1982) whereas, typical incompressible quartz

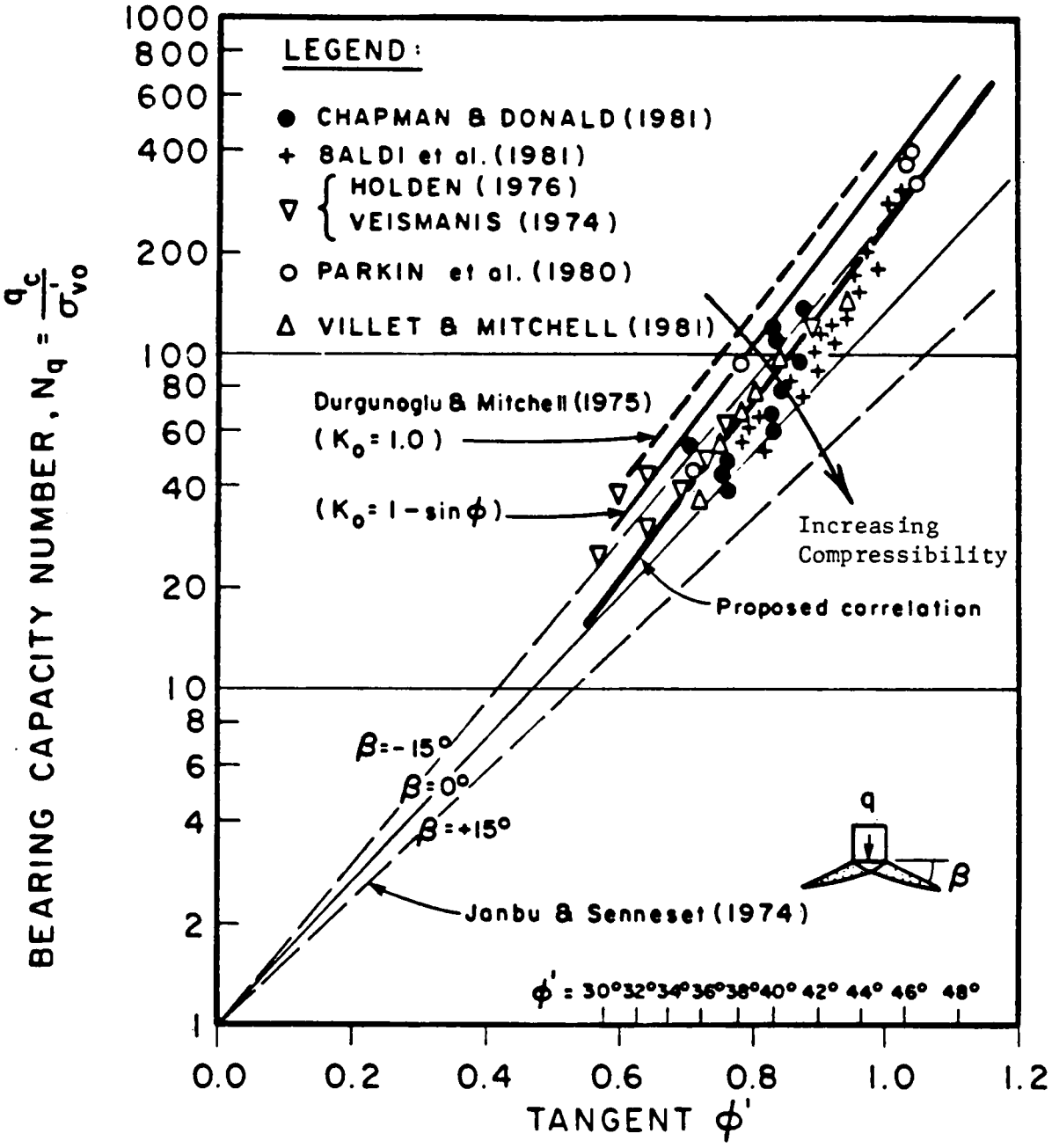

Figure 4.7 Relationship between Bearing Capacity Number and Friction Angle from Large Calibration Chamber Tests (After Robertson and Campanella, 1983a)

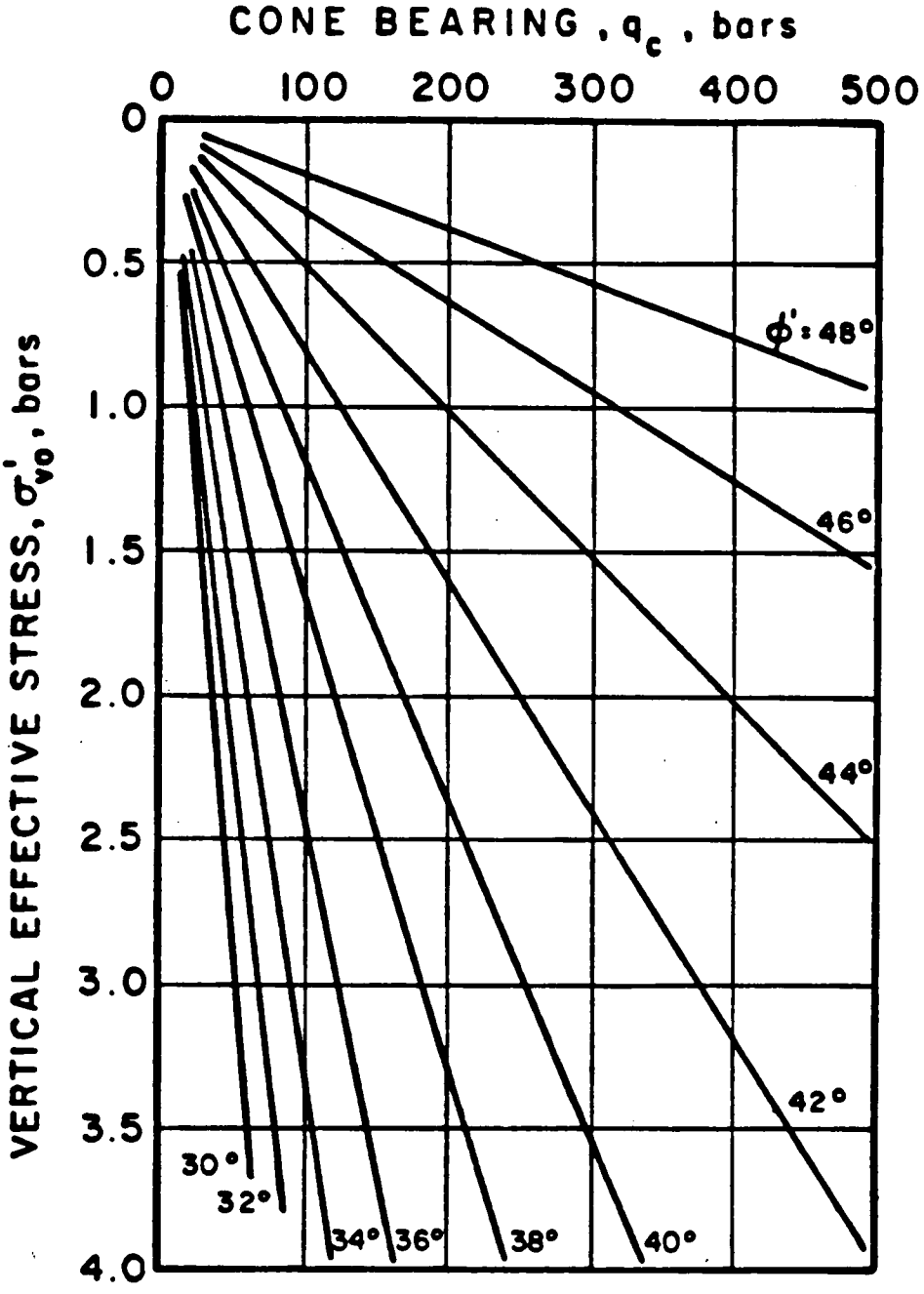

Figure 4.8 Proposed Correlation Between Cone Bearing and Peak Friction Angle for Uncemented Quartz Sands (After Robertson and Campanella, 1983a)

sands have friction ratios of about 0.5 percent. Thus, the presence of compressible sands may be identified using the friction ratio.

It is recommended that, for sands that fall within zones 7, 8, 9 and 10 in Fig. 4.2, the peak friction angle can be estimated using Fig. 4.8. In overconsolidated sands, Fig. 4.8 may slightly overestimate the friction angle by up to about +2° (see Fig. 4.7). Care should be exercised in interbedded deposits where the cone resistance may not have reached the full value within a layer.

A recent approach to the interpretation of CPT data in sands has been proposed (Been et al, 1985) that uses a State Parameter approach. This method incorporates the determination of the Steady State Line (SSL) on disturbed samples of sand and the measurement of the in situ horizontal stress (σ'_{ho}). The incorporation of the slope of the SSL attempts to account for variations in sand compressibility. For sands with dominant silica content the state parameter approach gives similar answers to that using Fig. 4.8.

4.4.3. Modulus and Compressibility

As already discussed, the cone penetration resistance in sand is a complex function of both strength and deformation properties. Hence, no generally applicable analytical solution for cone resistance as a function of deformation modulus is available. Instead, many empirical correlations between cone resistance and deformation modulus have been established.

The empirical correlations for the DMT are generally more reliable for estimating modulus in silica sands, especially since the DMT provides an estimate of OCR.

4.4.3.1. Constrained Modulus

Mitchell and Gardner (1975) made a comprehensive review of the existing correlations for sand. The correlations generally take the form

$$\frac{1}{m_v} = M = \alpha q_c \qquad (4.3)$$

where M is the drained constrained modulus (equal to $1/m_v$ from oedometer tests). The factor α is generally recommended in the range of 1.5 to 4.0.

Considerable confusion appears to exist as to whether or not α should remain constant with depth. Vesic (1970) proposed $\alpha = 2(1+D_r^2)$, where D_r = relative density. Dahlberg (1974) found α to increase with q_c based on M values obtained from screw plate tests for precompressed sand. Other references by Mitchell and Gardner use decreased α values when q_c exceeds a certain limit.

Review of calibration chamber tests (Lunne and Kleven, 1981) are shown in Table 4.2. Results indicate that $\alpha = 3$ should provide the most conservative estimates of one-dimensional settlement. The choice of α value depends on judgement and local experience.

Considerable insight into the relationship between one dimensional deformation modulus and cone resistance can be obtained from a careful review of calibration chamber tests. Baldi et al (1981) report tangent moduli corresponding to the last load increment for normally consolidated samples, and apply them to the empirical formula proposed by Janbu (1963):

$$M_t = k_m \, Pa \left(\frac{\sigma'_{vo}}{Pa}\right)^n \qquad (4.4)$$

Reference	N.C. Sand		O.C. Sand	
	No. sands	α	No. sands	α
Veismanis (1974)	2	3 - 11	3	5 - 30
Parkin et al, (1980)	1	3 - 11	1	5 - 30
Chapman & Donald (1981)	1	3 - 4 3 absolute lower limit	1	8 - 15 (12 = average)
Baldi et al, (1982)	1	>3	1	3 - 9

TABLE 4.2: Summary of Calibration Chamber Results for Constrained Modulus Factor α (After Lunne and Kleven, 1981)

where M_t = tangent constrained modulus

k_m = modulus number, which varies with relative density

n = modulus exponent, which may be approximately 0.4

σ'_{vo} = vertical effective stress

Pa = reference stress, usually taken as 1 t/ft² (1 bar or 100 kPa).

The test results by Baldi et al (1981) on Ticino sand show a relationship between the modulus number, k_m and relative density, D_r as follows:

Medium dense, D_r = 46% k_m = 575

Dense , D_r = 70% k_m = 753

Very dense , D_r = 90% k_m = 815

Similar values were reported by Parkin and Arnold (1977) and Byrne and Eldridge (1982).

If the relationship between relative density and modulus number is used in conjunction with the correlation developed by Baldi et al (1981), shown in Fig. 4.5, a series of curves relating tangent constrained modulus, M_t, to cone resistance, q_c, for different levels of vertical effective stress, σ'_{vo} can be developed, as shown on Fig. 4.9.

Review of Fig. 4.9 illustrates the apparent reason for the wide range in α values reported in Table 4.2.

The recommended method for estimating modulus is to estimate the average effective overburden stress (σ'_{vo}) and the average cone bearing, then enter Fig. 4.9 to obtain M_t and calculate the average α value applicable for the deposit or layer. Say the average cone bearing for a sand deposit is in the range of 100 to 200 t/ft² (bars) at an average σ'_{vo} = 1 t/ft² (bar), from Fig. 4.9 the average constrained modulus, M_t, would

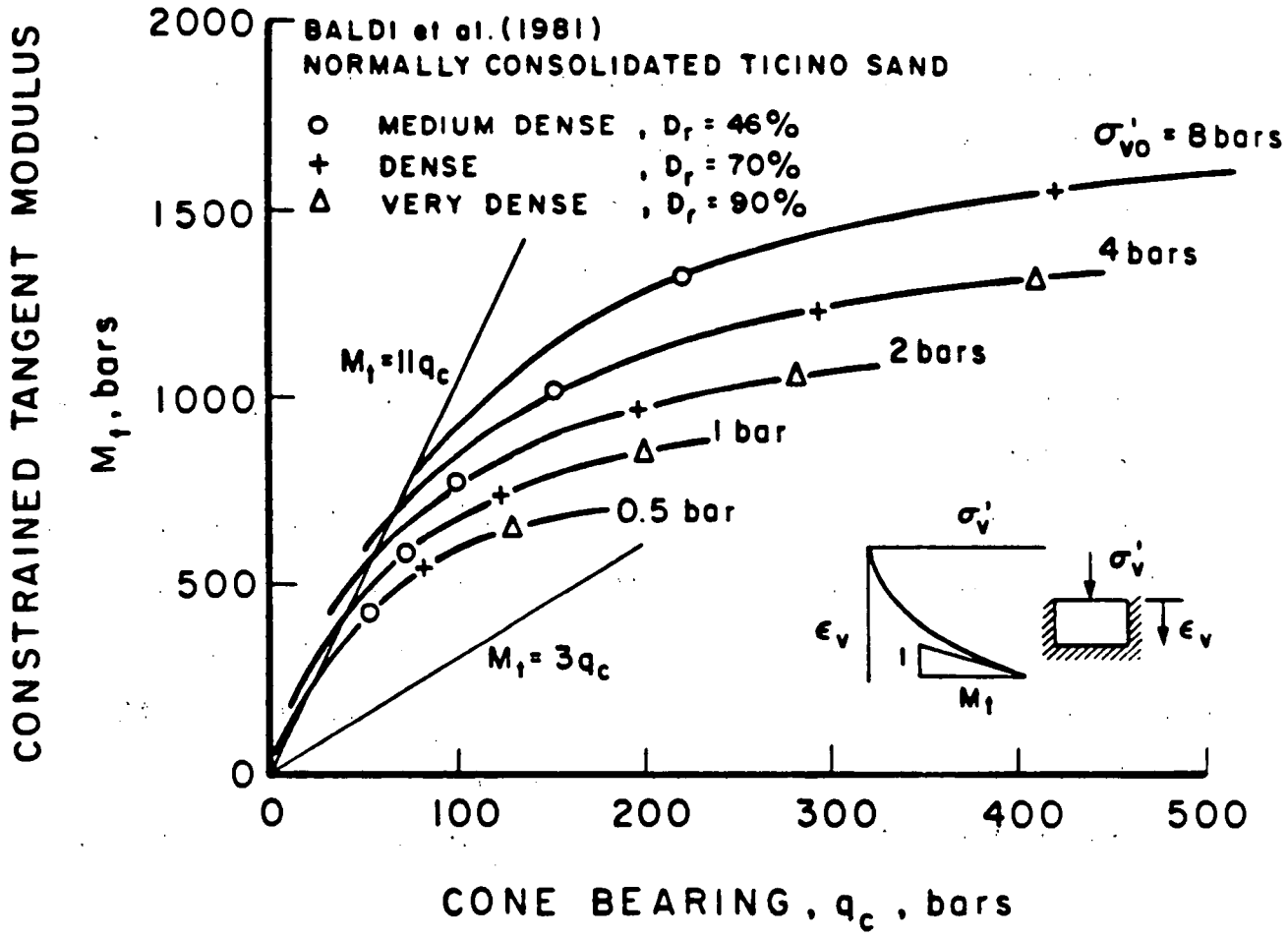

Figure 4.9 Relationship between Cone Bearing and Constrained Modulus for Normally Consolidated, Uncemented Quartz Sands (Based on Data from Baldi et al, 1981) (After Robertson and Campanella, 1983a)

be about 750 t/ft² (bars) at a cone bearing of 150 t/ft² and the average α value about 5.

For overconsolidated sands the α value increases with OCR (Baldi et al, 1986), as shown in Table 4.2 and Fig. 4.10. However, caution is required because of the difficulty in estimating OCR.

Some of the confusion concerning the use of CPT for interpretation of deformation modulus can be overcome if the following points are considered.

a) Soil is not linear elastic and modulus varies with both stress and strain level.

b) Modulus is often derived from or applied to non one-dimensional loading conditions.

c) Different theoretical methods were applied when obtaining correlations.

The simple fact that soil is not a linear elastic material makes the assumption of a constant modulus unrealistic. This is further complicated by the fact that many of the correlations where derived from non one-dimensional loading conditions for which "elastic" solutions were applied to back-figure a modulus. Thus, reasonable agreement can be expected only if the required problem involves similar boundary conditions and the same theoretical method is reapplied. Schmertmann's (1970) CPT method for predicting settlements in sand under spread foundations is a typical example. Schmertmann applied his strain influence elastic theory to analyze the results of screw plate tests. An equivalent Young's modulus (E_s) was calculated using a secant slope over the 1 bar - 3 bars (1 tsf - 3 tsf) increment of plate loading. This interval was chosen principally because real footing pressures commonly fall within this interval. Thus,

M_o VERSUS q_c CORRELATION FOR N.C. AND O.C. TICINO SAND

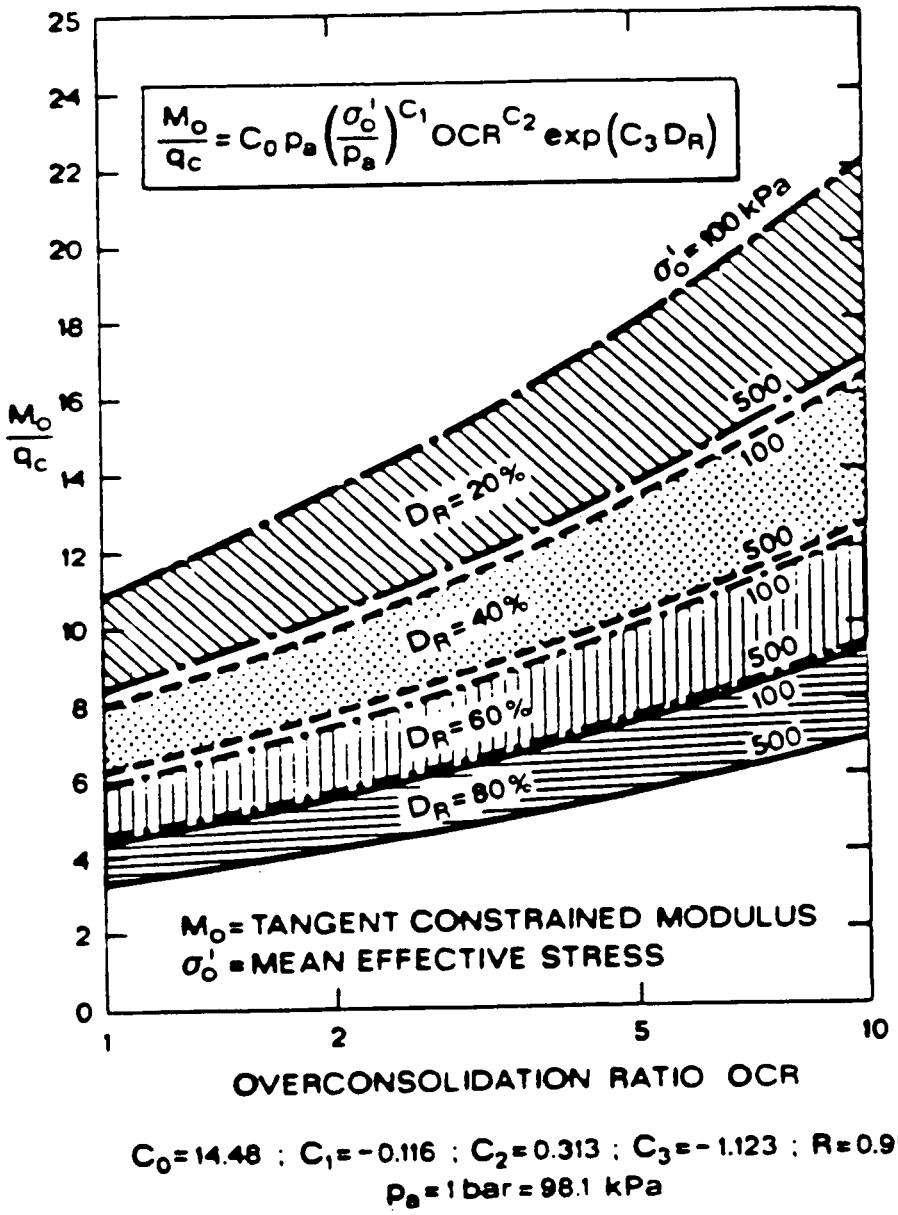

$C_0 = 14.48$; $C_1 = -0.116$; $C_2 = 0.313$; $C_3 = -1.123$; $R = 0.95$

$p_a = 1\ bar = 98.1\ kPa$

Figure 4.10 Relationship between Cone Bearing and Constrained Modulus for N.C. and O.C., Uncemented, Unaged Quartz Sands (After Baldi et al, 1986)

Schmertmann's design method, where $E_s = 2\ q_c$ can be expected to produce good results if the proposed design problem has similar loading conditions to the screw plate (i.e. circular spread footing loaded from 1-3 bars) and the same strain influence theory is reapplied.

4.4.3.2. Young's Modulus

A common problem, in geotechnical engineering, appears to be the use of the one-dimensional constrained modulus (M_t) applied to non one-dimensional loading conditions. For non one-dimensional cases an equivalent Young's modulus, as suggested by Schmertmann (1970), would appear to be a more logical parameter. A review, performed by the writers, of the calibration chamber results (Baldi et al 1981) provides a relationship between the drained secant Young's modulus at the 50 and 25 percent or 1/4 failure stresses, E_{50} and E_{25}, respectively, and cone resistance, q_c, for different levels of vertical effective stress (Fig. 4.11). Since the overall safety factor against bearing capacity failure is usually around 4 for foundations on sand, the designer is usually interested in a Young's modulus for an average mobilized stress level around 25 percent of the failure stress.

Thus, the calibration chamber results on <u>normally consolidated</u> sand give values of E_{25}/q_c or α varying between 1.5 and 3.0 which are in good agreement with the recommended value of 2 by Schmertmann (1970) for computation of settlements of circular shallow foundations on sand. Schmertmann (1978a) has changed the value to 2.5 and 3.0 to allow for the variation of shape factors for square and strip footings, respectively.

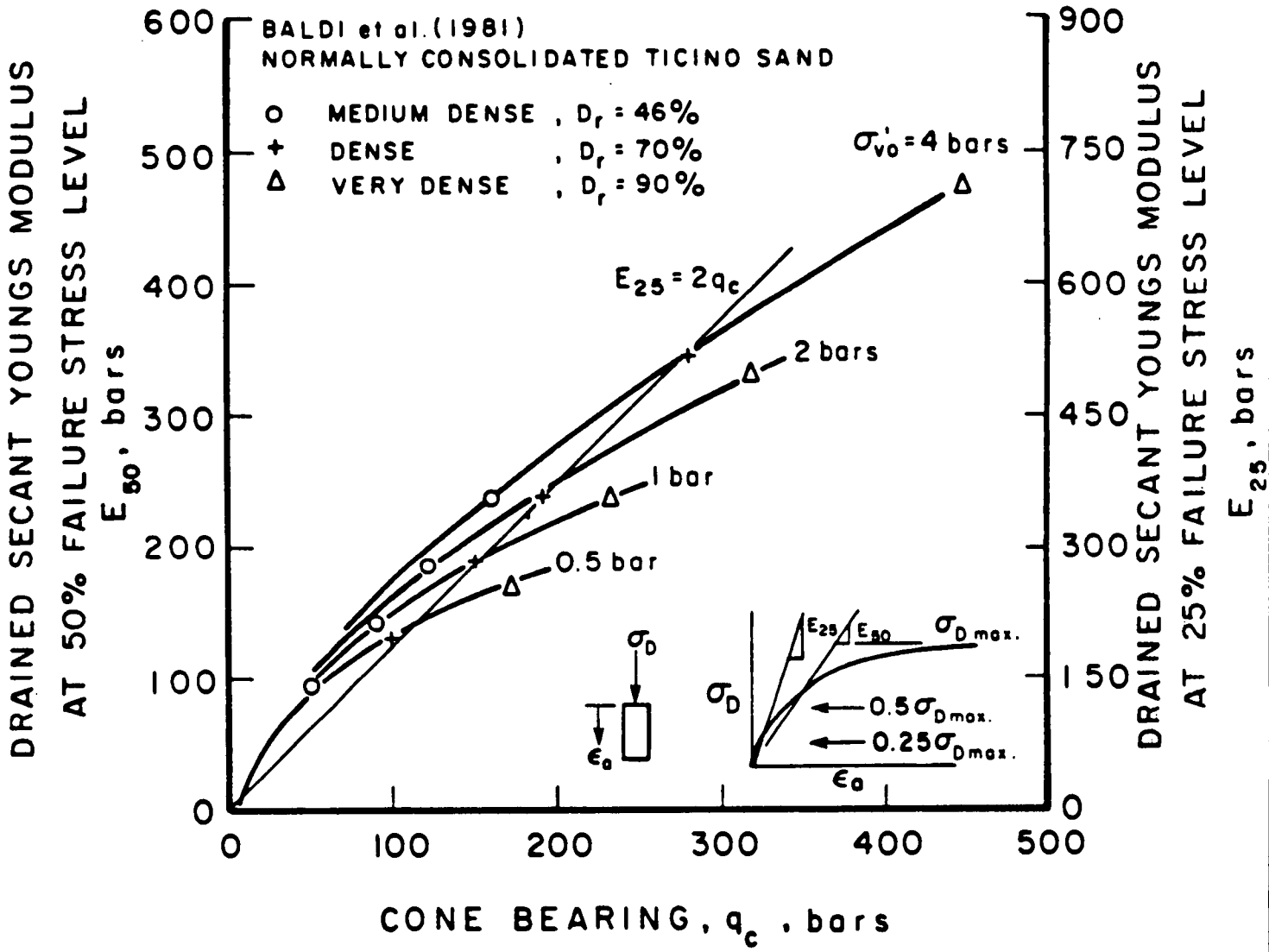

Figure 4.11 Relationship between Cone Bearing and Drained Young's Modulus for Normally Consolidated, Uncemented Quartz Sands (Based on Data from Baldi et al, 1981) (After Robertson and Campanella, 1983a)

Results from chamber tests suggest the ratio of E_{25}/q_c for <u>over-consolidated</u> sands is in the range of 3 to 6 times larger than those for normally consolidated sands (i.e. $6 \leq \alpha \leq 18$) (see Fig. 4.12). However, the application of these larger factors to overconsolidated sands should be used with caution, since the increase is dependent on degree of overconsolidation and density (Baldi et al 1986).

The use of Fig. 4.11 may underestimate the in-situ Young's Modulus because it is based on laboratory measured moduli using unaged and re-constituted samples. Many in-situ aged sand deposits (age >3000 years) have had some past stress or strain history that can cause a significant increase in soil stiffness.

4.4.3.3. Shear Modulus (G)

A similar approach has been applied to develop a correlation between cone resistance and shear modulus, G, for sands. Extensive laboratory work has been conducted by several researchers (Seed and Idriss, 1970, Handin and Drnevich, 1972) to relate dynamic shear modulus, G_{max} to soil index properties. Based on this work, Robertson (1982) proposed an empirical relationship between G_{max} and q_c for uncemented, predominantly quartz sands, as shown in Fig. 4.13. The major advantage of the correlation between G_{max} and q_c is the fact that it is little influenced by stress history (Jamiolkowski et al, 1986). Therefore, considerable confidence can be placed on the estimate of G_{max} from q_c.

Once a correlation has been developed for the dynamic shear modulus it should be possible to estimate the shear modulus at any strain level by using the reduction curves suggested by Seed and Idriss (1970).

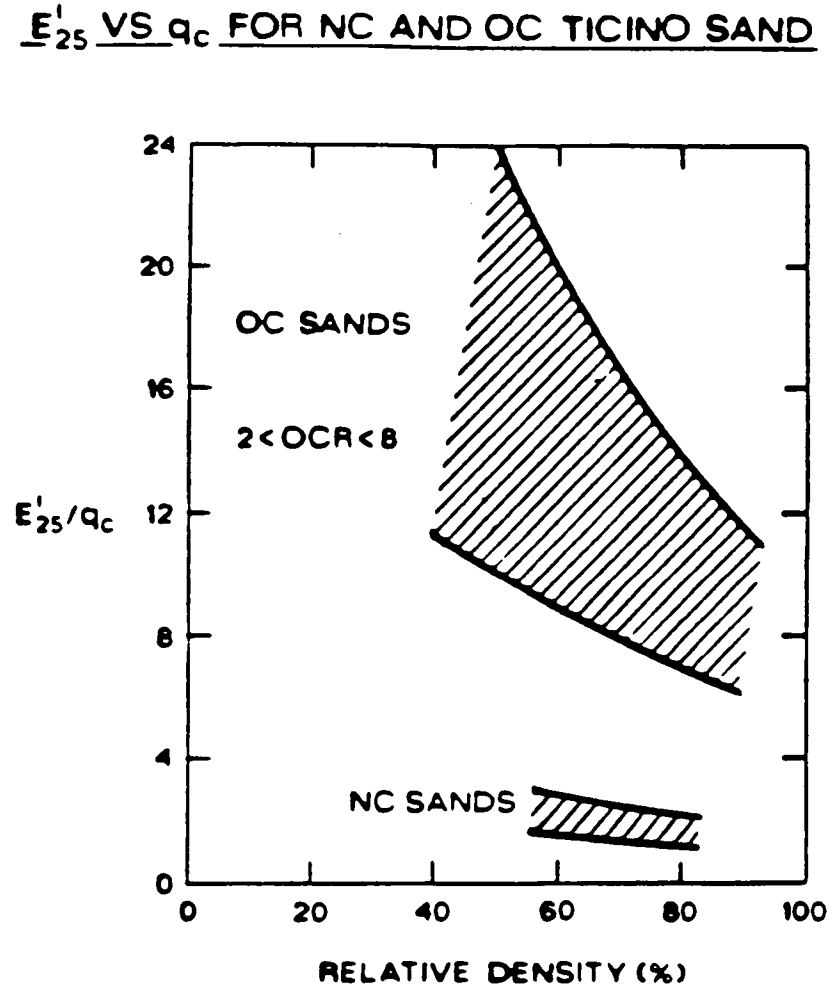

Figure 4.12 Relationship between Cone Bearing and Drained Young's Modulus (E'_{25}) for N.C. and O.C., Unaged, Uncemented Sands (After Baldi et al, 1986)

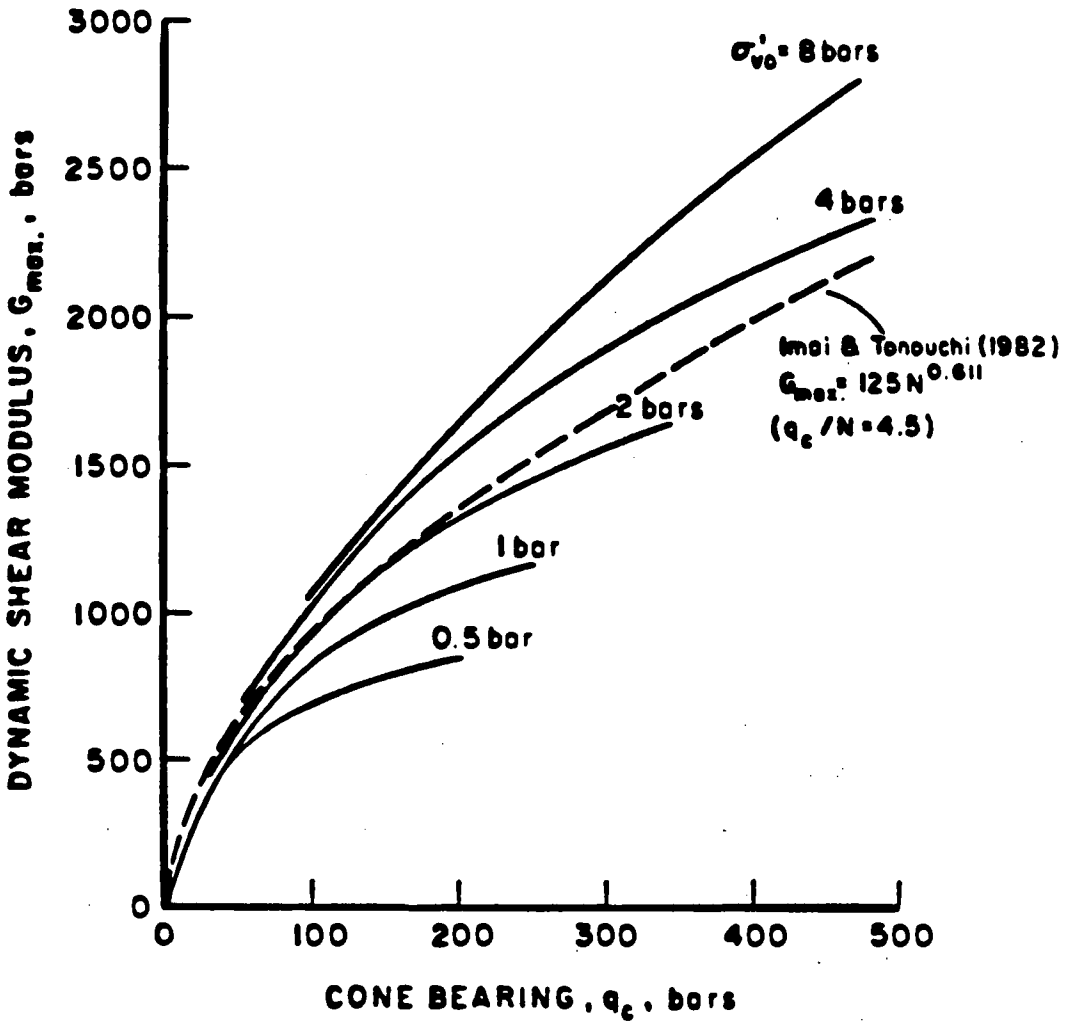

Figure 4.13 Relationship between Cone Bearing and Dynamic Shear Modulus for Normally Consolidated, Uncemented Quartz Sands (After Robertson and Campanella, 1983a)

Also shown on Fig. 4.13 is the relationship developed in Japan (Imai and Tonouchi, 1982) between dynamic shear modulus and SPT N value for sands. The SPT N value has been converted to cone bearing, q_c, using the relationship for sands (Robertson et al, 1983),

$$\frac{q_c}{N} = 4.5 \; . \qquad (4.5)$$

4.4.4. Stress History

Unfortunately, it is not possible to distinguish the stress history from cone penetration data during drained penetration. Sometimes, an indication of high horizontal stresses, i.e. high OCR, can be obtained from the relative density correlation (Fig. 4.6). If Fig. 4.6 is used with the vertical effective stress, σ'_{vo}, it is possible to predict relative densities in excess of 100% ($D_r >> 100\%$). This, is usually a sign of high horizontal stresses or cementation.

Sometimes the presence of high horizontal stresses can produce high friction sleeve values, f_s. However, to quantify the stress level, it is necessary to know the friction sleeve value of the same sand under normally consolidated conditions. Thus, it is impossible to distinguish between a dense normally consolidated sand and a loose overconsolidated sand.

Marchetti (1985) developed a chart to determine K_o in sands using the combined data from the DMT and the CPT. A modified version of Marchetti's method is given in Fig. 4.14. The combination of CPT and DMT data can be very useful for interpretation in sands. Some of the correlations for CPT in sands are sensitive to the in-situ stress condition (K_o). Therfore, a

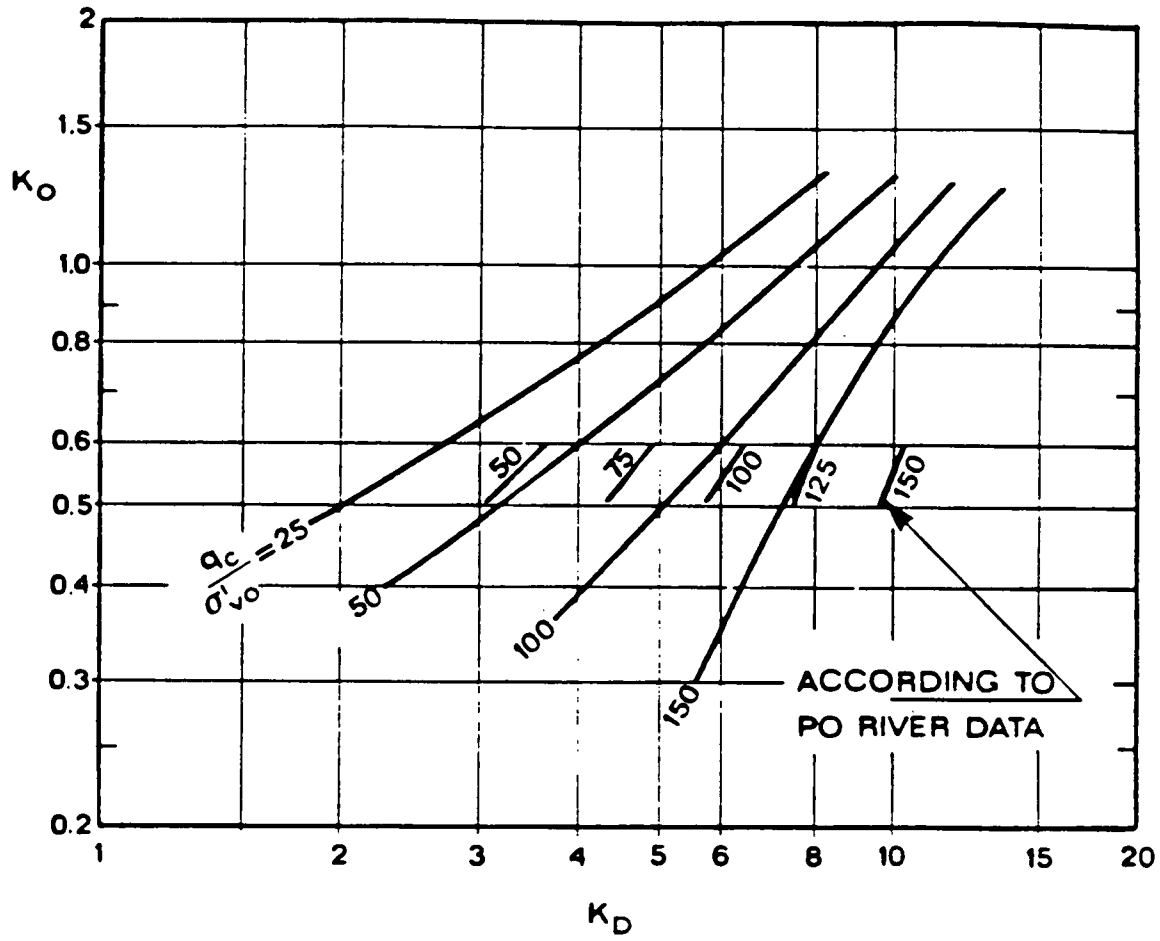

Figure 4.14 Modified Chart for Interpreting K_o from K_D (DMT) and q_c (CPT) Using Robertson and Campanella (1983) q_c-ϕ Relationship and Showing Po River Data and Calibration Chamber Data (After Marchetti, 1985)

knowledge, or some estimate, of K_o can significantly improve the correlations. This is especially true for the CPT correlation for moduli. If the combined DMT and CPT data are used to estimate K_o, an estimate of OCR can be made using the following relationship:

$$K_{o(OC)} = K_{o(NC)}(OCR)^{0.42} \qquad (4.6)$$

where $K_{o(NC)} = 1 - \text{Sin } \phi'$.

Robertson (1986) discussed how a similar approach could be taken using the friction sleeve stress as a measure of the horizontal stress. However, the resulting approach showed that the friction sleeve stress combined with the cone bearing are insensitive parameters to changes in K_o. This is especially true if the variation in friction sleeve stress is evaluated for cones of different design.

A discussion of how the piezometer cone can be used to estimate stress history is given in Section 4.5.5. Unfortunately, in sandy soils the pore pressures tend to dissipate almost as fast as they are generated resulting in a measured pore pressure close to the in-situ equilibrium water pressure.

4.5. Undrained Soil

4.5.1 Undrained Shear Strength

One of the earliest applications of the cone penetration test was in the evaluation of undrained shear strength (s_u) of clays. Comprehensive

reviews of s_u evaluation from CPT data have been presented by Baligh et al (1980), Jamiolkowski et al (1982), Lunne and Kleven (1981), and Robertson et al (1986). Note that the undrained shear strength of clay is not a unique parameter and depends significantly on the type of test used, the rate of strain and the orientation of the failure planes.

Using bearing stress to estimate s_u - Estimates of s_u from CPT using cone bearing results usually employ an equation of the following form:

$$s_u = \frac{q_c - \sigma_o}{N_k} \qquad (4.7)$$

where σ_o is the in-situ total overburden pressure

N_k is the cone factor.

The contribution of the total overburden pressure (σ_o) has been interpreted as either the in-situ vertical stress (σ_{vo}), or the in-situ horizontal stress (σ_{ho}), or the in-situ mean stress ($\sigma_m = \frac{1}{3}(\sigma_{vo} + 2\sigma_{ho})$). Theoretical solutions for N_k have been based on bearing capacity theories (eg., Meyerhof, 1961) and more recently by use of cavity expansion theories (eg., Ladanyi, 1967, and Vesic, 1972). Baligh (1975) combined these two approaches in approximate form. The solutions involve several simplifying assumptions, such as neglect of undrained strength anisotropy and strain softening behavior. The former can be adequately approximated by using the average of the vertical and horizontal strengths. Neglecting strain-softening, on the other hand, can lead to a serious error for sensitive

clays, Ladanyi (1972). Other factors such as cone type and rate of penetration may significantly affect the penetration resistance.

N_k is generally obtained from empirical correlations. The reference s_u should be measured from field vane tests or direct simple shear tests. The overburden pressure (σ_o) is usually taken as the in-situ total vertical stress (σ_{vo}) since the in-situ horizontal stress is usually not known.

Data presented by Lunne and Kleven (1981) shows that for normally consolidated marine clays using field vane strength, the cone factor N_k falls between 11 and 19 with an average of 15. These results were obtained using a standard 10 cm² electric cone at a standard rate of penetration of 2 cm/sec.

It is more difficult to establish similar correlations in stiff overconsolidated clays because of the important effects of fabric and fissures on the response of the clay (Powell and Quarterman, 1988).

Investigations by Kjekstad et al (1978) in non-fissured over-consolidated clays indicate an average cone factor $N_k = 17$. In this case, the reference s_u was obtained by triaxial compression tests. The value of N_k appears to be independent of overconsolidation ratio.

The s_u value determined as a function of cone resistance (q_c) in highly overconsolidated clay deposits must be considered with great caution since it is difficult to establish the extent fissures affect drainage and their effect on progressive failure.

Some people have had good experience using the relationship

$$s_u = \frac{q_c}{N_c} \qquad (4.8)$$

where N_c varies from 9 to 20, with an average of 15, although in general it is not recommended.

In general, the undrained shear strength, s_u, has been estimated from the measured cone bearing, q_c, using Equation 4.7, where N_k is an empirical cone factor and σ_o is generally taken to be the total overburden pressure (σ_{vo}). With the corrected cone resistance, q_T, the cone factor has been expressed (Lunne et al, 1985) as:

$$N_{KT} = \frac{q_T - \sigma_{vo}}{s_u} \tag{4.9}$$

Using effective bearing to estimate s_u - Senneset et al (1982) have suggested the use of the effective cone resistance, q_E, to determine s_u. Where q_E is defined as follows:

$$q_E = q_c - u \tag{4.10}$$

and u = total pore pressure measured immediately behind the cone tip.

Campanella et al (1982) redefined the effective cone bearing using the corrected cone resistance, q_T. The undrained shear strength can then be determined as follows,

$$s_u = \frac{q_E}{N_{KE}} = \frac{q_T - u}{N_{KE}} \tag{4.11}$$

Senneset et al (1982) proposed that $N_{KE} = 9$ with a likely variation of

±3. Lunne et al (1985) and Robertson et al (1986) showed that N_{KE} varied from 1 to 13 and appeared to correlate with B_q.

One major drawback using the effective cone resistance, q_E, is the reliability to which q_E can be determined. In soft normally consolidated clays, the total pore pressure, u, generated immediately behind the tip during cone penetration is often approximately 90 percent or more of the measured cone resistance, q_c. Even when q_c is corrected to q_T, the difference between q_T and u is often very small. Thus, q_E is often an extremely small quantity and is therefore sensitive to small errors in q_c measurements.

Using excess pore pressure to estimate s_u - Several relationships have been proposed between excess pore pressure (Δu) and s_u based on theoretical or semi-theoretical approaches using cavity expansion theory (Vesic, 1972, Battaglio et al, 1981; Randolph and Wroth, 1979; Massarch and Broms, 1981; Campanella et al, 1985) using:

$$s_u = \frac{\Delta u}{N_{\Delta u}} \qquad (4.12)$$

where $N_{\Delta u}$ can vary between 2 and 20 (on a global basis).

These methods have the advantage of increased accuracy in the measurement of Δu, especially in soft clays, where Δu can be very large. In soft clays, the cone resistance can be very small and typically the cone tip load cell may be required to record loads less than 1% of rated capacity with an associated inaccuracy of up to 50% of the measured values. However, in soft clays, the pore pressures generated can be very large and the pressure trasnducer may record pressures up to 80% of its rated

capacity with an associated accuracy of better than 1% of the measured value. Therefore, estimates of s_u in soft clays will inherently be more accurate using pore pressure data, as opposed to the tip resistance.

The cone resistance and the excess pore pressures generated during cone penetration into fine grained soils will be dependent on the stress history, sensitivity and stiffness ratio. Low values of stiffness ratio generally apply to highly plastic clays (plasticity index, PI > 80) which tend to generate low pore pressures. High values of stiffness ratio generally apply to low plastic clays and silts (PI ≤ 15) which tend to generate high pore pressures. The excess pore pressures also tend to increase with increasing soil sensitivity and decrease with increasing overconsolidation ratio (stress history). A semi-empirical solution was proposed by Massarch and Broms (1981) based on cavity expansion theories but including the effects of overconsolidation and sensitivity by using Skempton's pore pressure parameter at failure (A_f). Charts illustrating this approach are given in Fig. 4.15. Approximate values for A_f can be estimated from the following:

Saturated Clays	A_f
Very sensitive to quick	1.5 - 3.0
Normally consolidated	0.7 - 1.3
Lightly overconsolidated	0.3 - 0.7
Highly overconsolidated	-0.5 - 0.0

Clearly a knowledge of the plasticity index (PI) would assist in the estimate of s_u.

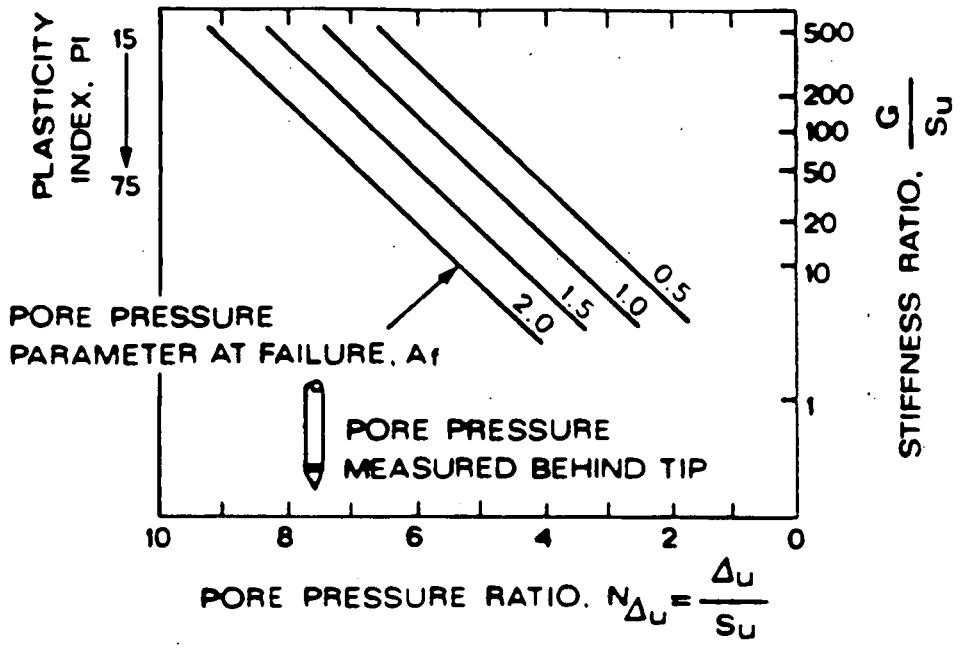

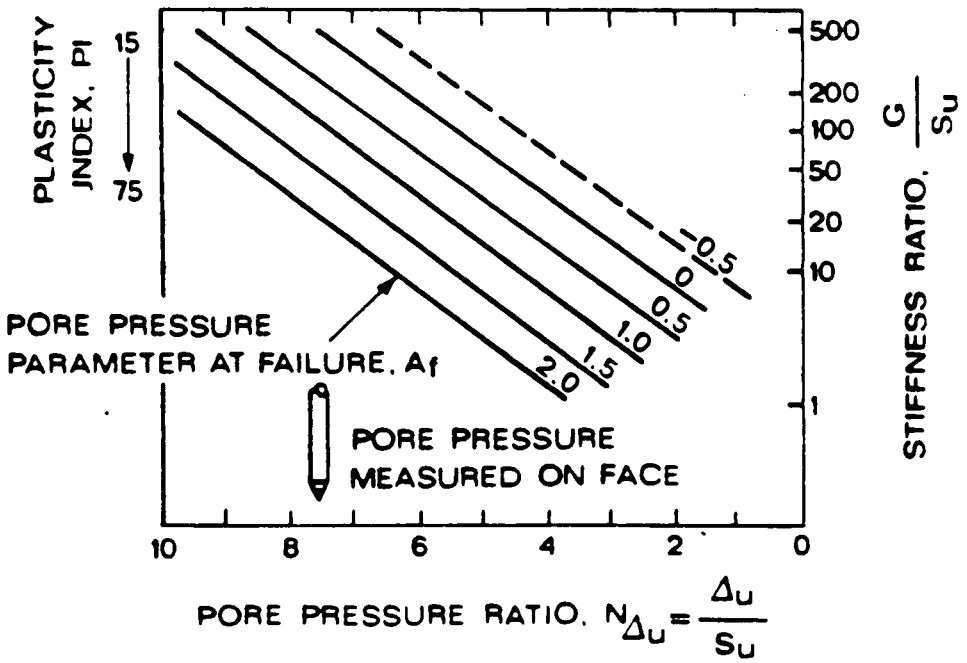

Figure 4.15 Proposed Charts to Obtain s_u from Excess Pore Pressure, Δu, Measured during CPTU (After Campanella et al, 1985)

If pore pressures are measured immediately behind the cone tip, the measured values may not have reached the true cylindrical cavity expansion value. Therefore s_u estimated from the chart with the pore presures behind the tip may be slightly overestimated. Also because of the tendency for low or negative pore pressures measured behind the tip in insensitive, overconsolidated clays (see Fig. 3.3) the chart in Fig. 4.15 is not recommended for highly overconsolidated clays ($-0.5 < A_f < 0$).

Schmertmann (1975) wisely comments that for standard cone testing, the best procedure is to make individual correlations for N_k based on s_u measurements for specific clays and CPT procedures. This, of course, requires a reliable estimate of the in-situ s_u appropriate to the particular design problem.

Recommendations - For standard cone testing it is recommended to use Equation (4.7) with an N_k value of 15 for preliminary assessment of s_u, if no data is available for s_u. For sensitive clays, the N_k value should be reduced to around 10 or less depending on the degree of sensitivity. The overburden pressure can be taken as the total vertical stress. With local experience individual correlations for N_k should be determined for specific clays. **It is also recommended that N_k be defined for a specific method of evaluating s_u, such as by the field vane test, since s_u is not a unique soil parameter.**

The N_k values based on experience will change somewhat as all cone resistance values become corrected to q_T.

For piezometer cone testing, it is recommended to also use Fig. 4.15 and Δu in Equation 4.12. Care is required to use the correct chart relevant to the pore pressure location.

Although the charts in Fig. 4.15 are based on cavity expansion theories, they are basically semi-empirical in nature. The advantage in using the charts is that they provide some rational guide to the correct selection of the cone factor, $N_{\Delta u}$. The charts clearly show how the factor $N_{\Delta u}$ will vary with OCR, sensitivity and stiffness.

Figure 4.16 presents data from the Vancouver area (Robertson et al, 1986) showing how the cone factor $N_{\Delta u}$ varies with the pore pressure parameter B_q. Also included on Fig. 4.16 is the range of North Sea data presented by Lunne et al (1985). The Vancouver area data show the same basic trend but with more scatter. When the data presented in Fig. 4.16 is reviewed a little more closely, it is apparent that trends in the data can be defined. Soils with high OCR have low B_q and low $N_{\Delta u}$ values. Soils with the same OCR but increasing sensitivity (S_t) show a marked increase in $N_{\Delta u}$ and a smaller increase in B_q. Unfortunately, the data shown is for soils of predominantly similar plasticity index (PI) and no clear trend with changing PI can be seen. The trend lines for increasing OCR and S_t have been included on Fig. 4.16 as a guide. These same trends in $N_{\Delta u}$ can be obtained from the chart shown in Fig. 4.15. The data shown in Fig. 4.16 would indicate that increasing sensitivity (S_t) can increase $N_{\Delta u}$ to as high as 18, compared to the maximum value of about 10 shown in Fig. 4.15.

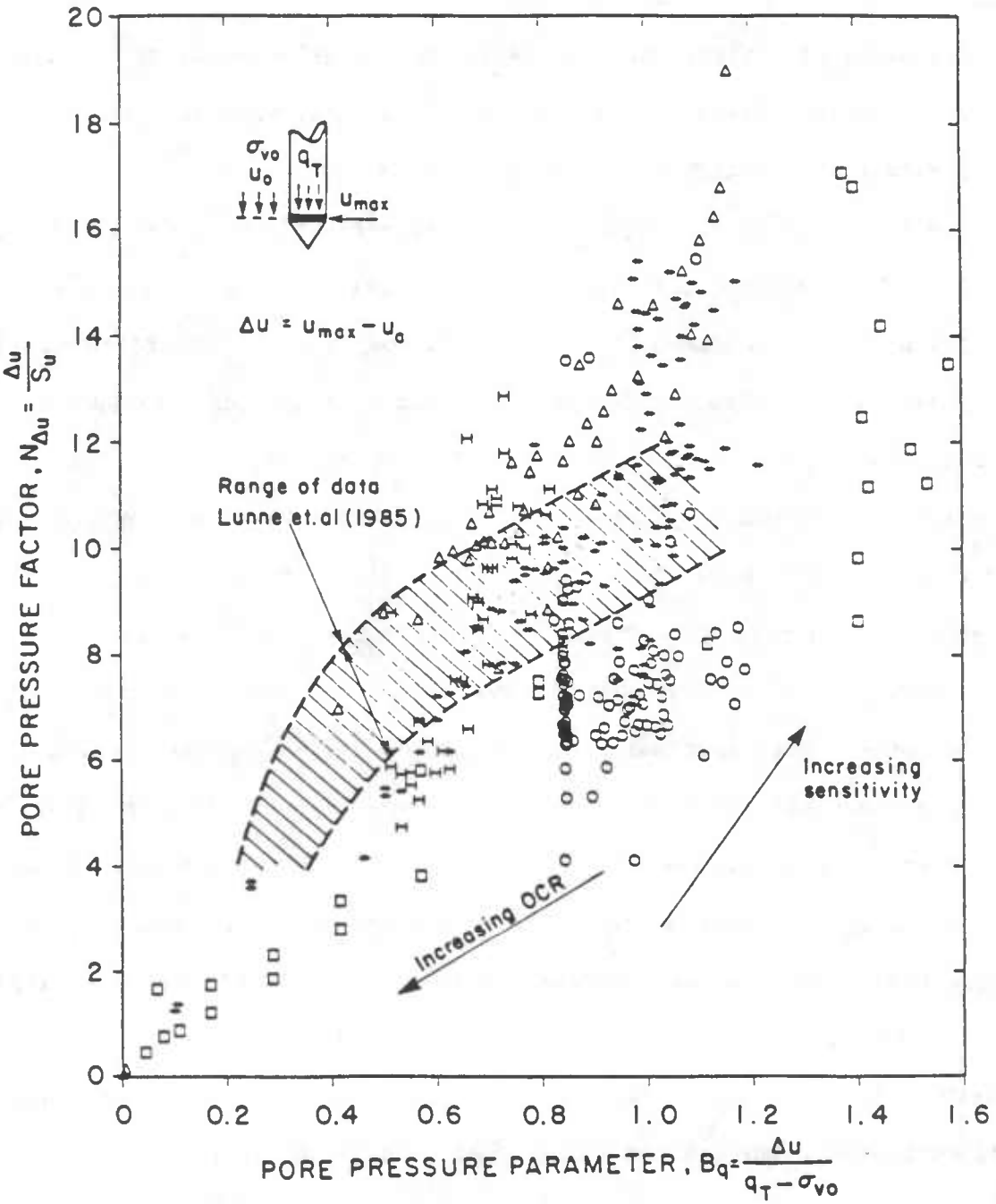

Figure 4.16 Pore Pressure Factor $N_{\Delta u}$ vs. Pore Pressure Parameter B_q for Vancouver Data (After Robertson et al, 1986)

Based on the data shown in Figs. 4.15 and 4.16 the authors suggest the following method for determining the undrained shear strength from CPTU data:

1. Using the CPTU profile estimate the OCR and sensitivity (S_t). Methods to estimate OCR and S_t are discussed in a later section.
2. Estimate appropriate value of A_f.
3. Use Fig. 4.15 to estimate $N_{\Delta u}$.
4. Calculate B_q and use Fig. 4.16 to estimate $N_{\Delta u}$, again use estimated OCR and S_t.
5. Compare $N_{\Delta u}$ values from Figs. 4.15 and 4.16 and use average value to calculate s_u.
6. Using calculated value of s_u re-evaluate OCR using s_u/σ'_{vo} (see Section 4.5.5).
7. Iterate from 1 to 6 until consistent value of s_u is derived.

Experience has shown that no simple unique relationship exists between CPTU data and undrained shear strength, s_u, for all clay type soils. Therefore procedures, such as outlined above, are required to more realistically evaluate s_u for all possible clay soils. However, simple relationships are possible for site specific soils. **If possible, always make a direct measurement of s_u (field vane or even U-U, etc.) and determine $N_{\Delta u}$ for specific clay layers at a given site to determine s_u profiles from CPTU data.**

4.5.2. Sensitivity

The sensitivity (S_t) of a clay, which is the ratio of undisturbed strength to totally remolded strength, can be estimated from the friction ratio (R_f%) using,

$$S_t = \frac{N_s}{R_f\%} \qquad (4.13)$$

Schmertmann (1978) suggested a value of N_s = 15 for mechanical CPT data. Robertson and Campanella (1983) initially suggested N_s = 10 for electronic CPT data. However, recent data (Greig, 1985) collected in the Vancouver area suggest an average of N_s = 6 based on field vane testing. The authors therefore suggest using an average N_s of 6 for an initial estimate of S_t if no direct measurements of S_t are available.

It has been recognized for many years that the sleeve friction stress, f_s, is approximately equal to the remolded undrained shear strength, s_{ur}. Data from the Vancouver area has shown that the friction sleeve stress is generally close to the remolded strength. However, the friction sleeve values are very small and the variation in results are probably due to the inherent difficulty of measuring small sleeve frictions. The observation that soils with a high sensitivity have very low sleeve friction values is also reflected in the R_f classification charts (Figs. 4.1 and 4.2).

4.5.3. Drained Shear Strength

Senneset et al (1982) and Keaveny and Mitchell (1986) have suggested methods to determine the drained effective stress shear strength parameters (c', ϕ'), from the cone penetration resistance and the measured total pore pressures. However, these methods, as with any method for determining effective stress parameters from undrained cone penetration data, can be subject to serious problems. Any method of analyses must make assumptions

as to the distribution of total stresses and pore pressures around the cone. Unfortunately, the distribution of stresses and pore pressures around a cone is extremely complex in all soils and has not adequately been modelled or measured to date except perhaps in soft normally consolidated clays. Also, an important problem, which is not identified by Senneset et al, (1982) is the location of the porous element, since different locations give different measured total pore pressures.

The authors believe that the present state of interpretation and analyses of CPT data has not yet reached a stage to allow reliable estimates of drained shear strength parameters from undrained cone penetration data.

A detailed discussion about limitations of the theories relating to interpretation of CPT data in clays is given by Tavenas et al (1982).

4.5.4. Compressibility and Modulus

4.5.4.1. Constrained Modulus

Mitchell and Gardner (1975) made a comprehensive review of the numerous correlations between cone resistance and constrained modulus, M. Most of these take the general form

$$M = \frac{1}{m_v} = \alpha\, q_c \qquad (4.14)$$

where m_v = volumetric compressibility = $(\Delta v/v/\Delta p)$.

Sanglerat et al (1972) developed a comprehensive array of α values for different cohesive soil types with different cone resistance values. Mitchell and Gardner's (1975) summary of Sanglerat's α values are given in Table 4.3. Schmertmann developed a method that related the s_u/σ'_{vo} ratio

$$M = \frac{1}{m_v} = \alpha q_c$$

q_c < 7 bar	3 < α < 8	
7 < q_c < 20 bar	2 < α < 5	Clay of low plasticity (CL)
q_c > 20 bar	1 < α < 2.5	
q_c > 20 bar	3 < α < 6	Silts of low plasticity (ML)
q_c < 20 bar	1 < α < 3	
q_c < 20 bar	2 < α < 6	Highly plastic silts & clays (MH, CH)
q_c < 12 bar	2 < α < 8	Organic silts (OL)
q_c < 7 bar:		
50 < w < 100	1.5 < α < 4	
100 < w < 200	1 < α < 1.5	Peat and organic clay (P_t, OH)
w > 200	0.4 < α < 1	

TABLE 4.3: Estimation of Constrained Modulus, M, for Clays (Adapted from Sanglerat, 1972) (After Mitchell and Gardner, 1975)

to the overconsolidation ratio (OCR) and then to the one dimensional compression index of the soil, C_c, as shown on Table 4.4.

The coefficient of volume change (m_v) and the compression index (C_c) are related by:

$$m_v = \frac{0.435\ C_c}{(1+e_o)\sigma_{va}} \qquad (4.15)$$

where e_o = initial void ratio,

σ_{va} = average of initial and final stresses.

These methods provide only a rough estimate of soil compressibility. The values by Schmertmann in Table 4.4 appear to give very conservative estimates of C_c and appear to be too large by a factor of about 2. Increasing sensitivity can significantly increse the compressibility of a clay at stresses higher than the preconsolidation stress.

Additional data from Atterberg limit tests (PI) and/or undisturbed sampling and oedometer tests are required for more reliable estimates.

The estimation of drained parameters such as the one dimensional compression index, C_c, or compressibility, m_v, from an undrained test is liable to serious error, especially when based on general empirical correlations. Conceptually, total stress undrained measurements from a cone cannot yield parameters for drained conditions without the addition of pore pressure measurements. The predictions of volume change based on q_c using either Table 4.3 or Table 4.4 may be in error by ±100%. However, with local experience individual correlations can be developed for specific soil types.

s_u/σ'_{vo}	approx. OCR	$C_c/(1 + e_1)$
0 - 0.1	less than 1	greater than 0.4 (still consolidating)
0.1 - 0.25	1	0.4
0.26 - 0.50	1 to 1.5 (assume 1)	0.3
0.51 - 1.00	3	0.15
1 - 4	6	0.10
over 4	greater than 6	0.05

TABLE 4.4: Estimation of Compression Index, C_c, from s_u/σ'_{vo} Ratio (After Schmertmann, 1978)

4.5.4.2. Undrained Young's Modulus E_u.

The estimation of undrained Young's modulus, E_u, is usually made using empirical correlations with the undrained shear strength, s_u, in the form

$$E_u = n\ s_u \qquad (4.16)$$

where n is a constant that depends on stress level, overconsolidation ratio, clay sensitivity and other factors (Ladd et al 1977). As discussed earlier, because soil behaviour is non-linear, the choice of relevant stress level is very important. Fig. 4.17(a) presents data for normally consolidated soils from Ladd et al. (1977) that shows the variation of the ratio E_u/s_u with stress level for seven different cohesive soils, ($15 < PI < 75$). Fig. 4.17(b), shows the variation of E_u/s_u with overconsolidation ratio (OCR) at two stress levels for the same soil types shown in Fig. 4.17(a). Figure 4.17(c) shows the variation of stiffness ratio at 25% of failure stress with OCR as proposed by Duncan and Buchignani, 1976.

The recommended procedure for the estimation of the undrained Young's modulus (E_u) is to first estimate the undrained shear strength (s_u) from CPT profiles, as previously discussed, then estimate the stress history (OCR) using the ratio, s_u/σ'_{vo} (Fig. 4.19). Then, using Fig. 4.17, estimate E_u for the relevent stress level appropriate for the particular problem. A knowledge of the plasticity index (PI) would significantly improve the estimate.

4.5.4.3. Shear Modulus

A tentative correlation between dynamic shear modulus (G_{max}) and q_c

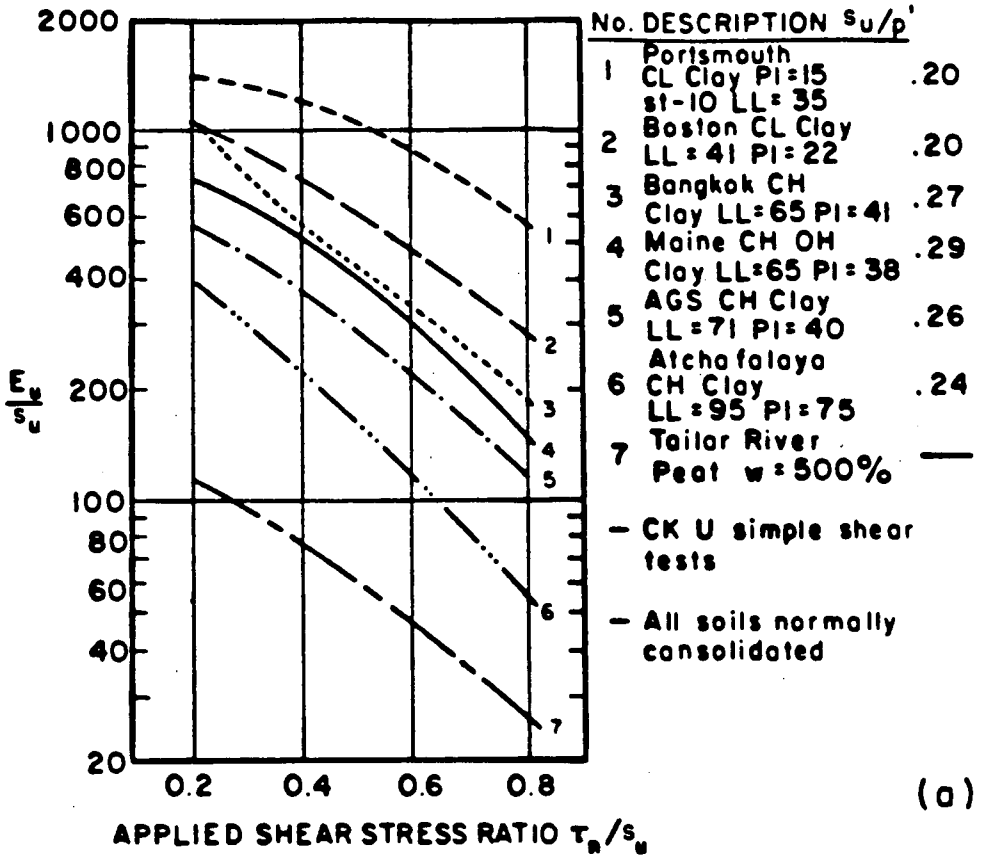

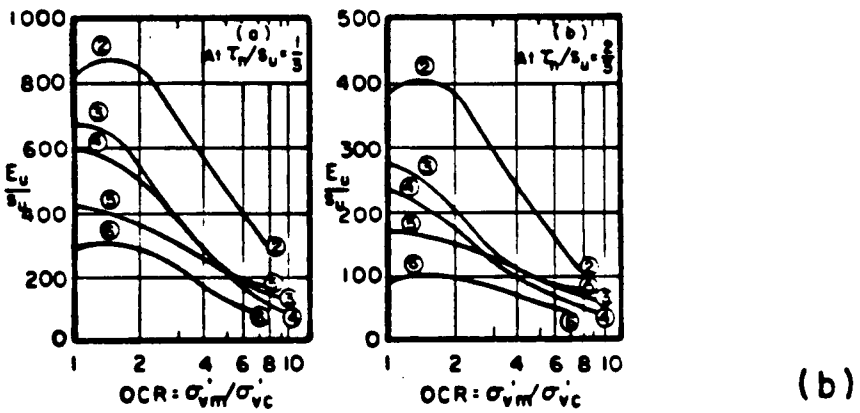

Figure 4.17 (a) and (b) Selection of Soil Stiffness Ratio for Clays (Adapted from Ladd et al, 1977)

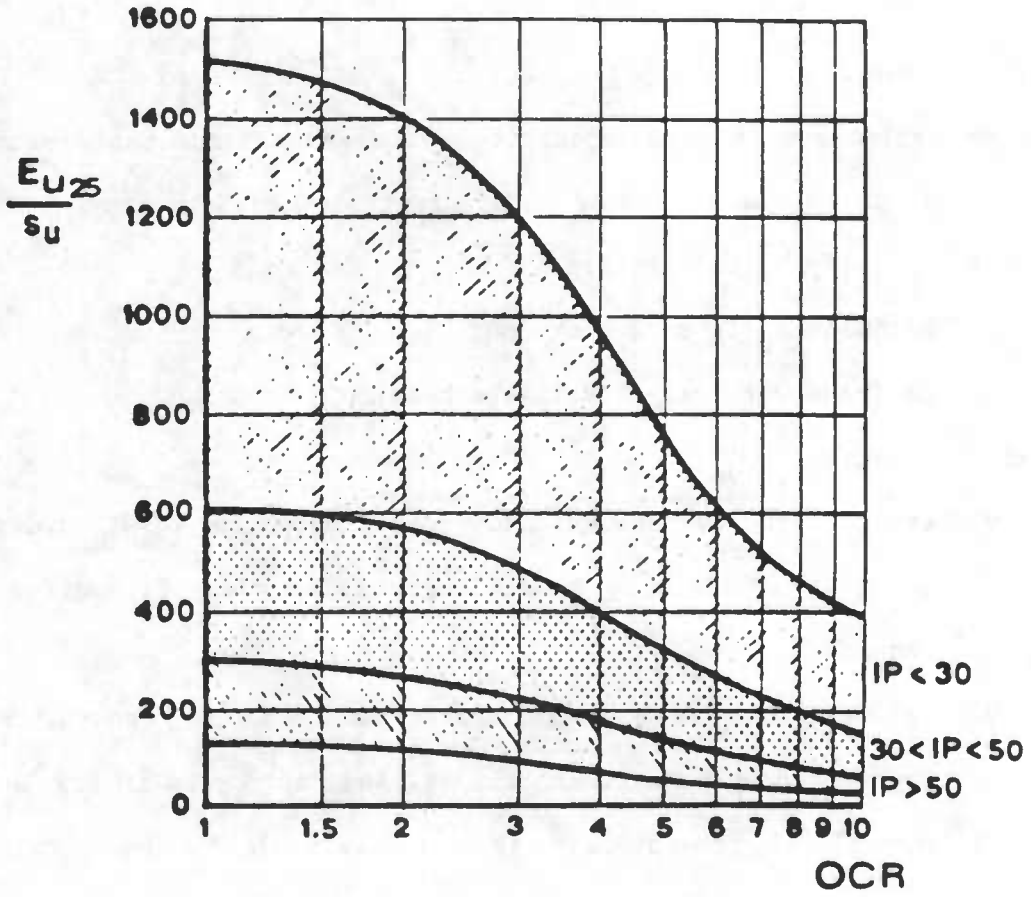

Figure 4.17 (c) Stiffness Ratio as a Function of OCR
(After Duncan and Buchignani, 1976)

for clays is shown in Figure 4.18. A knowledge of plasticity and OCR is important, similar to the estimate of E_u. Note that according to elastic theory $G = 1/3\ E_u$ for undrained elastic deformation at small strains.

4.5.5. Stress History

An estimate of overconsolidation ratio and maximum past pressure may be obtained using the following method suggested by Schmertmann (1975) and modified slightly by the writers:

i) estimate s_u from q_c or Δu;

ii) estimate vertical effective stress, σ'_{vo} from soil profile;

iii) compute s_u/σ'_{vo};

iv) estimate the average normally consolidated $(s_u/\sigma'_{vo})_{NC}$ for the soil using Fig. 4.19(b). A knowledge of the plasticity index (PI) is required.

v) estimate OCR from correlations by Ladd and Foott (1974) and normalized by Schmertmann (1978a) and reproduced in Fig. 4.19(a).

If the PI of the deposit is not available, Schmertmann (1978a) suggests assuming an average normally consolidated $(s_u/\sigma'_{vo})_{NC}$ ratio of 0.33 for most post-pleistocene clays.

It should also be noted that the shape of the tip resistance profile can give an approximate indication of stress history. For normally consolidated clay deposits with hydrostatic groundwater conditions the tip resistance is linearly increasing with depth. For most young clays where overconsolidation has been caused by erosion or desiccation the OCR will decrease with depth until the deposit, at depth, is approximately normally consolidated. In these cases, the tip resistance would be approximately

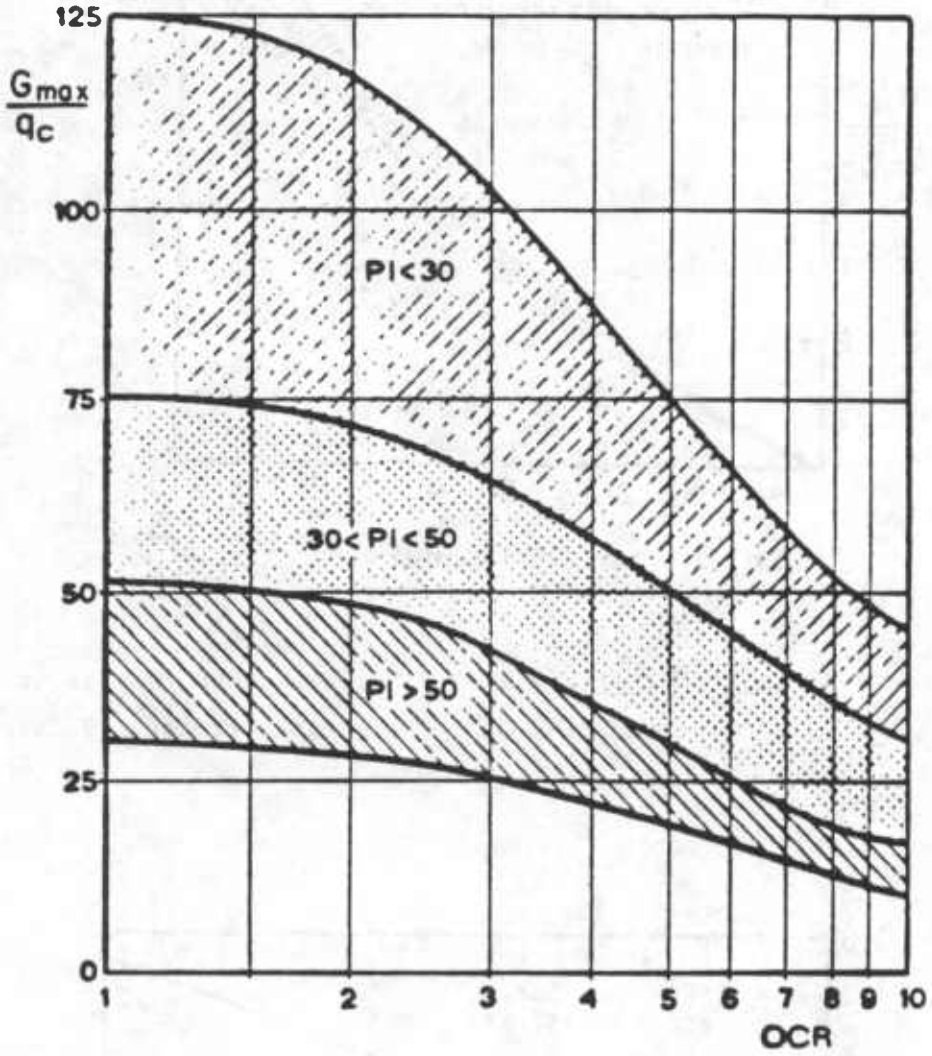

Figure 4.18 Tentative Correlation for Estimating Dynamic Shear Moduli (G_{max}) in Clay Soils

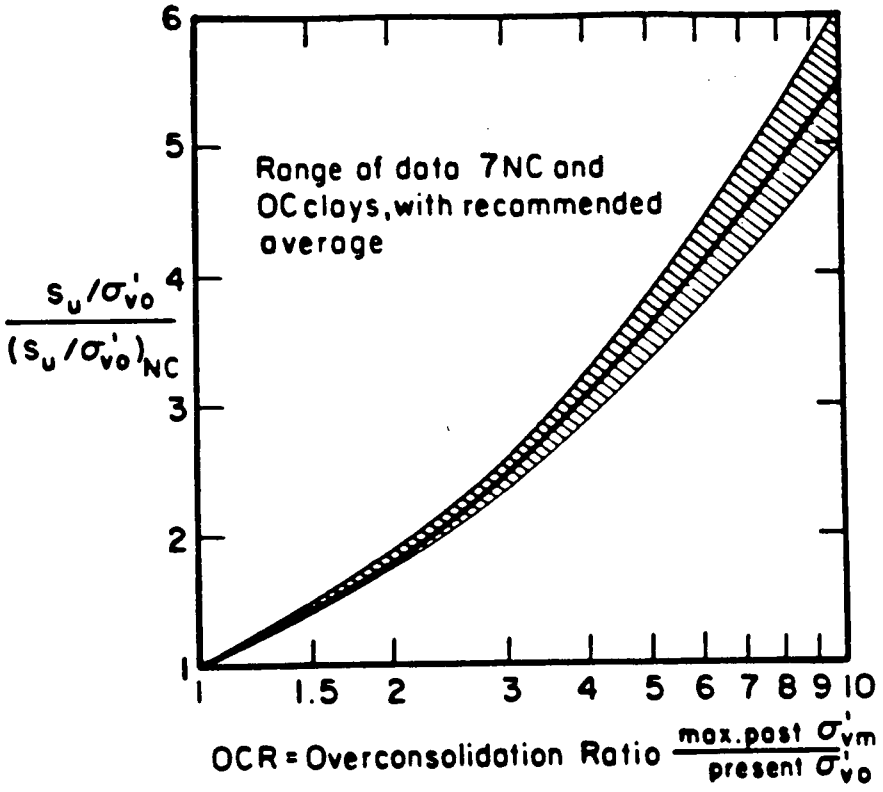

Figure 4.19 (a) Normalized s_u/σ'_{vo} Ratio vs. OCR for Use in Estimating OCR (After Schmertmann, 1978a)

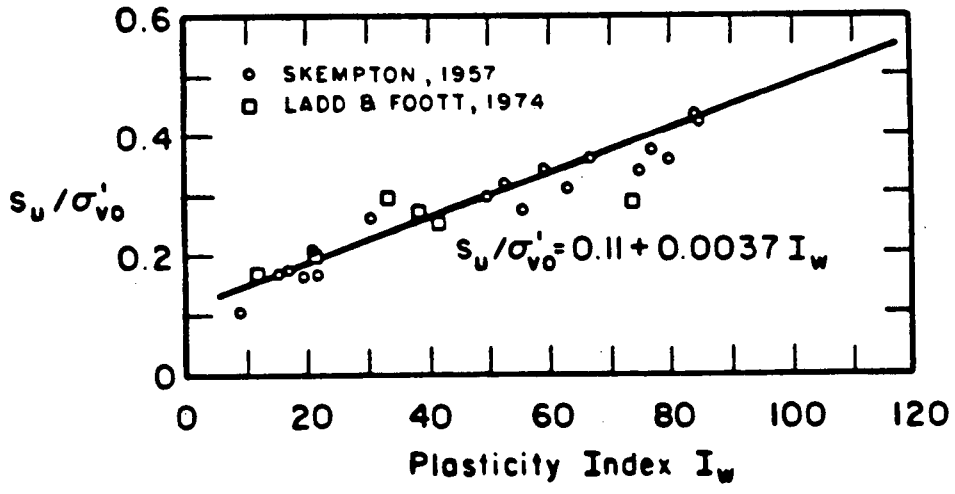

Figure 4.19 (b) Statistical Relation between s_u/σ'_{vo} Ratio and Plasticity Index, for Normally Consolidated Clays

constant or even decrease with depth until the depth where the deposit is normally consolidated and will then increase linearly with depth. For aged clays where the OCR is constant with depth the tip resistance may continue to stay constant with depth.

Baligh et al (1980) suggested that the pore pressure measured during undrained cone penetration may reflect the stress history of a deposit. Since then several methods have been suggested to correlate various pore pressure parameters to OCR. A summary of the main pore pressure parameters is suggested by various authors as follows:

(i) $\frac{u}{q_c}$ Baligh et al (1981)

(ii) $\frac{\Delta u}{q_T}$ Campanella and Robertson (1981)

(iii) $\frac{\Delta u}{q_c - u_o}$ Smits (1982)

(iv) $\frac{\Delta u}{q_c - \sigma_{vo}}$ Senneset et al (1982); Jones and Rust (1982); Jefferies and Funegard (1983); Wroth (1984)

(v) $\frac{q_T - \Delta u - \sigma_{vo}}{\sigma'_{vo}}$ Jamiolkowski et al (1985)

(vi) $\frac{\Delta u}{\sigma'_{vo}}$ Azzouz et al (1983)

It is generally agreed that q_c should always be corrected to q_T whenever possible. Therefore, (iv) becomes B_q (Equation 4.1). Battaglio

et al (1986) presented several examples of the parameters (iv) and (v) for different Italian clays.

Wroth (1984) correctly pointed out that only the shear induced excess pore pressure reveals the nature of the soil behaviour and depends on stress history. Unfortunately, because of the complex nature of cone penetration, it is not possible to isolate the shear induced pore pressures. However, as suggested early, the pore pressures measured immediately behind the cone tip appear to be influenced by shear stresses, although changes in octahedral stresses complicate any quantitative interpretation.

A review of published correlations shows that no unique relationship exists between the above pore pressure ratios and OCR, because pore pressures measured at any one location are influenced by clay sensitivity, preconsolidation mechanism, soil type and local heterogeneity (Robertson et al, 1986; Battaglio et al, 1986).

Since the shear induced pore pressures cannot be isolated with measurements at any one location on the cone, Campanella et al (1985) suggested that the difference between pore pressures measured on the face and somewhere behind the tip may correlate better with OCR (see Fig. 3.3).

At present any empirical relationship should be used to obtain only qualitative information on the variation of OCR within the same relatively homogeneous deposit.

4.5.6 Flow Characteristics

In the last 10 years, much attention has been devoted to the analysis of dissipation tests with the CPTU (Torstensson, 1977; Randolph and Wroth, 1979; Baligh and Levadoux, 1980; Acar et al, 1982; Gupta and Davidson, 1986). A dissipation test consists of stopping cone penetration and

monitoring the decay of excess pore pressures (Δu) with time. From this data an approximate value of the coefficient of consolidation in the horizontal direction (c_h) can be obtained.

A comprehensive study and review of this topic was recently published by Baligh and Levadoux (1986). Relevant conclusions were:

1. The simple uncoupled solutions provide reasonably accurate predictions of the dissipation process.
2. Consolidation is taking place predominantly in the recompression mode, especially for dissipation less than 50%.
3. Initial distribution of excess pore pressures around the cone have a significant influence on the dissipation process.

Based on the findings of Baligh and Levadoux (1986) the following procedure is recommended for evaluating c_h from CPTU dissipation tests:

a) Plot the normalized excess pore pressure with log time.

b) Compare the measured dissipation curve with the theoretical curves (see Fig. 4.20).

c) If the curves are similar in shape, compute c_h from:

$$c_h = \frac{R^2 T}{t} \qquad (4.17)$$

where: T = theoretical time factor for given tip geometry and porous element location

t = time to reach given value of $\Delta u(t)/\Delta u$

R = radius of cone.

An alternate method may be used especially if an initial redistribution of excess pore pressure is apparent:

a) Plot excess pore pressure vs. square root time and fit best straight

line ignoring initial redistribution and extrapolate line to zero time to obtain initial excess pore pressure.

b) Choose appropriate percent dissipation and use corresponding time and Eq. 4.17 to calculate c_h.

If no data exists concerning A_f or I_R (See Fig. 4.20) assume:

A_f = 0.80 for most soft clays

$I_R = 100 = G/s_u$

Note that $G/s_u = 1/3\ E/s_u$ for undrained deformation assuming elastic concepts hold as a first approximation.

The value of c_h determined for $\Delta u(t)/\Delta u = 0.5$ (i.e., 50% consolidation), may be used in problems involving horizontal flow in the overconsolidated range. To obtain c_h in the normally consolidated range, use

$$c_h\ (N.C.) = \frac{RR}{CR} \cdot c_h\ (CPTU) \qquad (4.18)$$

where:

RR = recompression ratio = $C_s/1+e_o$

CR = virgin compression ratio = $C_c/1+e_o$

If no data is available, take $\frac{RR}{CR} = 0.15$ (Jamiolkowski et al, 1983)

At present, because of the difficulties in predicting the initial distribution of excess pore pressures around a cone in stiff, overconsolidated clays (OCR > 4), the theoretical solutions for estimating c_h from dissipation tests is limited to normally to lightly overconsolidated clays (OCR < 4).

In stiff overconsolidated clayey soils the pore pressure gradient around the cone can be extremely large (see Fig. 3.3). This gradient of pore pressure often results in dissipations recorded behind the tip that initially increase before decreasing to the final equilibrium value. This

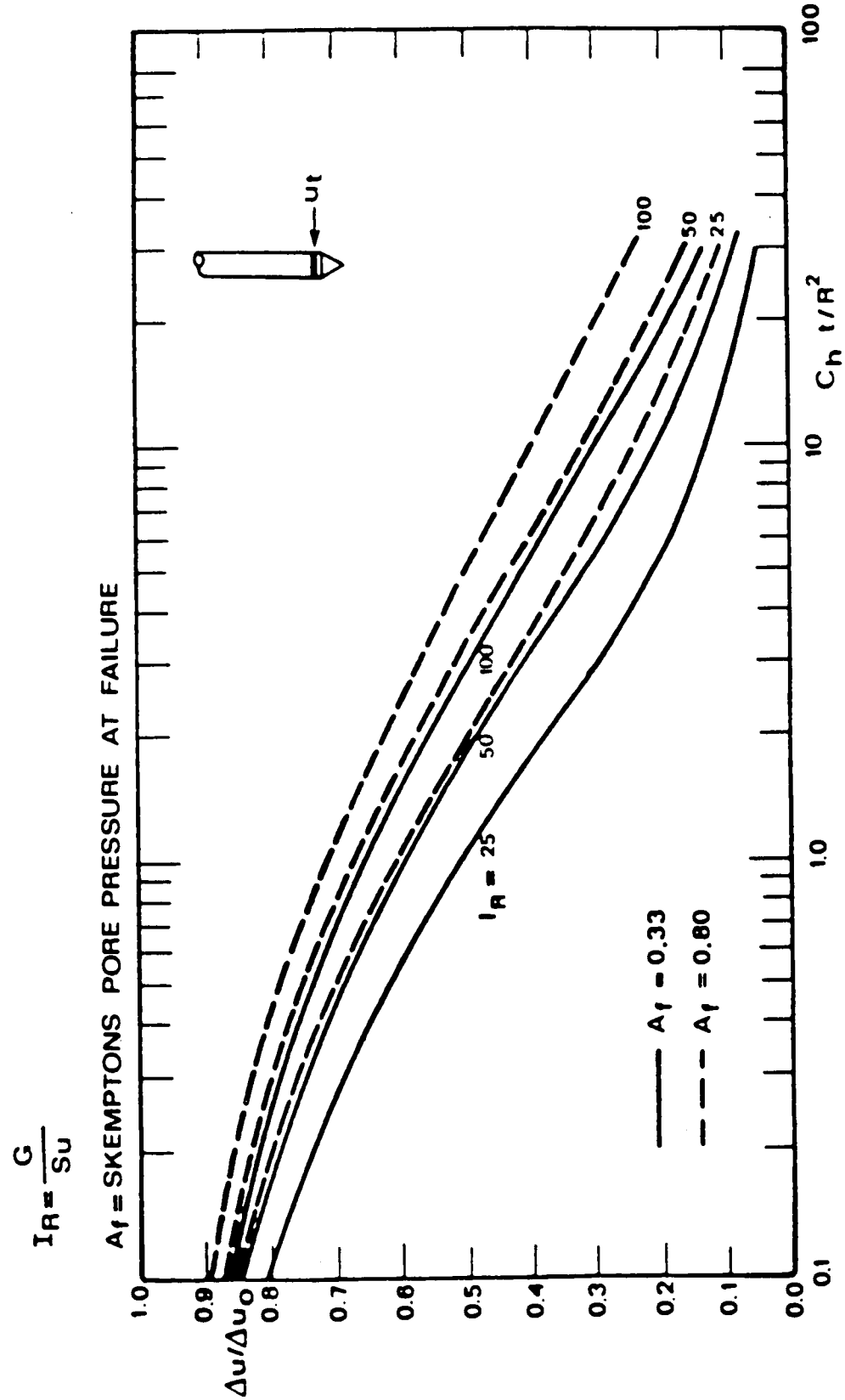

Figure 4.20 Theoretical Curves for Cylindrical Pore Pressure Dissipation for Various Stiffness Ratios (After Battaglio et al, 1981)

type of response is believed to be due to the redistribution of excess pore pressures around the cone before the primarily radial drainage, although poor saturation of the cone can also cause this response.

In spite of the above limitations, the dissipation test provides a useful means of evaluating approximate consolidation properties, soil macrofabric and related drainage paths of natural clay deposits. The test also appears to provide very important information for the design of vertical drains (Battaglio et al, 1981; Robertson et al, 1986).

It is useful here to comment on the procedure used while recording the pore pressure dissipations. Some users have reported that they found it necessary to clamp the penetration rods at the ground surface while recording pore pressure dissipation. It appears that if the rods were not clamped a drop in the measured pore pressure would result when load was released from the tip. It appears the location of the sensing element explains the sensitivity of decay response to procedure used. When load is released, pore pressures at the tip immediately drop in response to the decrease in total stress. Whereas, behind the tip, in the zone of failed soil the stress level does not change significantly when load is released. It therefore appears that, for standard 60° cones, the location of the piezometer element behind the tip is less sensitive to the procedure used. This is an important point because the amount of load applied to the tip, even with the rods clamped, will change with time due to stress relaxation.

A crude estimate of permeability can be made from the soil type classification. A more reliable estimate of permeability, especially for fine grained soils, can be made from the consolidation and compressibility characteristics. Since:

$$k_v = c_v m_v \gamma_w \tag{4.19}$$

$$k_h = c_h m_h \gamma_w \tag{4.20}$$

where k_v and k_h are the coefficient of permeability in the vertical and horizontal directions, respectively. Results of limited past experience suggests that soil compressibility can be regarded as approximately isotropic, $m_v = m_h$ (Mitchell et al, 1978; Ladd et al, 1977) for the purposes of estimating permeability.

Since an estimate of m_v can be made, then estimates of vertical permeability can be obtained. Estimates of m_v can be made using Table 4.3 or using an α factor based on local experience.

If it is assumed that soil compressibility is isotropic, then:

$$c_v = c_h \times \frac{k_v}{k_h} \tag{4.21}$$

An estimate of the ratio k_v/k_h can be obtained from Table 4.5, after Baligh and Levadoux, (1980). Evidence of the soil heterogeneity can be obtained from examination of the bearing, friction and dynamic pore pressure records.

4.6. Problem Soils

Correct interpretation of CPT or CPTU data requires some knowledge that the penetration is predominatly drained or undrained. Problem soils

	Nature of Clay	k_h/k_v
1.	No evidence of layering	1.2 ± 0.2
2.	Slight layering, e.g., sedimentary clays with occasional silt dustings to random lenses	2 to 5
3.	Varved clays in north-eastern U.S.	10 ± 5

TABLE 4.5: Anisotropic Permeability of Clays
(After: Baligh and Levadoux, 1980)

are often soils where penetration is taking place under partially drained conditions, such as fine sands and silts and some organic soils.

One of the major advantages of CPTU data is the ability to distinguish between drained, partially drained and undrained penetration. The dissipation of excess pore pressures during a pause in penetration can provide valuable additional information regarding drainage conditions. If the excess pore pressures dissipate fully in a time from about 30 seconds to 3 minutes for a standard 10 cm^2 cone, the penetration process was most likely partially drained and quantitative interpretation is very difficult. Other factors, such as stratigraphy and poor saturation of the sensing element can also influence the pore pressure response.

If CPTU data is not available, Fig. 4.2 can be used to estimate drainage conditions during penetration. Soils that fall within zones 7, 8, 9, 10 and 12 tend to have drained penetration. Soils that fall within zones 1, 2, 3, 4 and 5 tend to have undrained penetration. Caution should be used when soils fall in or close to zones 6 and 11, since penetration may be partially drained and quantitative interpretation is very difficult.

Fibrous organic soils can sometimes be difficult to interpret. The shear strength is often controlled by the fibrous nature of the soil mass. Often instability is generated in thin layers of soft organic (non-fibrous) clays or silts that exist immediately above or below the fibrous deposit. Therefore, the CPT data should be studied carefully to look for the possibility of such soft layers, since often they will control stability.

Gravelly soils also present a problem for interpretation of CPT data. Appreciable gravel content can make penetration with a cone impossible.

Small gravel content can allow cone penetration but can cause large spikes in the q_c and f_s profile. These spikes cannot be interpreted to give realistic geotechnical parameters, such as D_r, ϕ or E. Caution should be exercised when interpreting CPT data in gravelly soils. Additional data, such as shear wave velocity, can be useful to evaluate the extent of gravel content.

4.7. Groundwater Conditions

It is almost impossible to determine the groundwater conditions from the cone bearing data, q_c. In some soils, particularly older relatively free draining soils, a higher q_c layer can form around present or past groundwater levels. This may be due to chemical precipitation which produces cementation between grains. In clays, past or present groundwater levels are normally associated with overconsolidation above groundwater level from drying. However, these methods can only provide an indication of possible past or present groundwater levels.

The addition of pore pressure measurements during cone testing provides a direct measure of groundwater conditions. The equilibrium piezometric profile can be measured directly during a stop in the penetration. Experience gained by the writers has shown this to be an extremely important feature for the piezometer cone for penetration in both drained and undrained soils. It has been common practice to obtain the height of water in a borehole but rarely are the groundwater conditions hydrostatic. Often there is a slight upward or downward gradient of water pressures resulting from overall regional groundwater conditions. The ability to measure equilibrium piezometric pressures during a stop in the penetration

is useful for evaluating consolidation conditions or unusual hydraulic gradients. Identifying the actual groundwater conditions can be extremely valuable for investigations of slopes, embankments, tailings disposal and tidal areas.

The time required to reach full equilibrium pore pressure during a stop in penetration will depend mainly on the soil permeability. For many investigations, it is sufficient to take equilibrium measurements at the end of the profile before pulling the rods and during rod breaks in any sand layers or purposely stopping in a coarser layer to obtain a rapid dissipation to an equilibrium pore pressure.

A poorly saturated piezometer element and cavity will not affect the accuracy of the measured equilibrium pore pressure, but will lengthen the time it takes to reach equilibrium.

4.8. SPT-CPT Correlations

The Standard Penetration Test (SPT) is still the most commonly used in-situ test in North America. However, despite continued efforts to standardize the SPT procedure there are still problems associated with its repeatability and reliability. Many geotechnical engineers have developed considerable experience with design methods based on local SPT correlations. With time, direct CPT design correlations will also be developed based on local experience and field observation. However, with the initial introduction of CPT data there is a need for better SPT-CPT correlations so that CPT data can be used in existing SPT data based design correlations.

A considerable number of studies have taken place over the years to quantify the relationship between SPT N value and CPT cone bearing resistance, q_c. A wide range of q_c/N ratios have been published leading to much confusion. The variations in published q_c/N ratio can be clarified by reviewing the derived q_c/N ratios, as a function of mean grain size (D_{50}), as shown in Fig. 4.21. It is clear from Fig. 4.21 that the q_c/N ratio increases with increasing grain size. The scatter in results appears to increase with increasing grain size. This is not surprising since penetration in gravelly sand (D_{50}= 1.0 mm) is significantly influenced by the larger gravel sized particles, not to mention the variability of delivered energy in the SPT data. Also sand deposits in general are usually stratified or non-homogeneous causing rapid variations in CPT tip resistance. There is also some difficulty in defining the D_{50} from some of the references. Additional data has been collected from calibration chamber tests (Baldi et al, 1985) which confirms the data shown in Fig. 4.21.

Robertson et al (1982) discussed how the q_c/N ratio varies with the amount of energy delivered to the drill rods. Kovacs et al (1981) and Robertson et al (1982) have shown that the energy delivered to the rods during a SPT can vary from about 20% to 90% of the theoretical maximum, 475 J (4,200 in.lb.). The energy delivered to the drill stem varies with the number of turns of rope around the cathead and varies with the fall height, drill rig type, hammer and anvil type, and operator characteristics.

When using the rope and cathead procedure with two turns of the rope, the typical energy delivered from a standard donut type hammer is about 50% to 60% of the theoretical maximum (Kovacs and Salomone, 1982). Schmertmann (1976) and Seed and Idriss (1986) have has suggested that based on limited

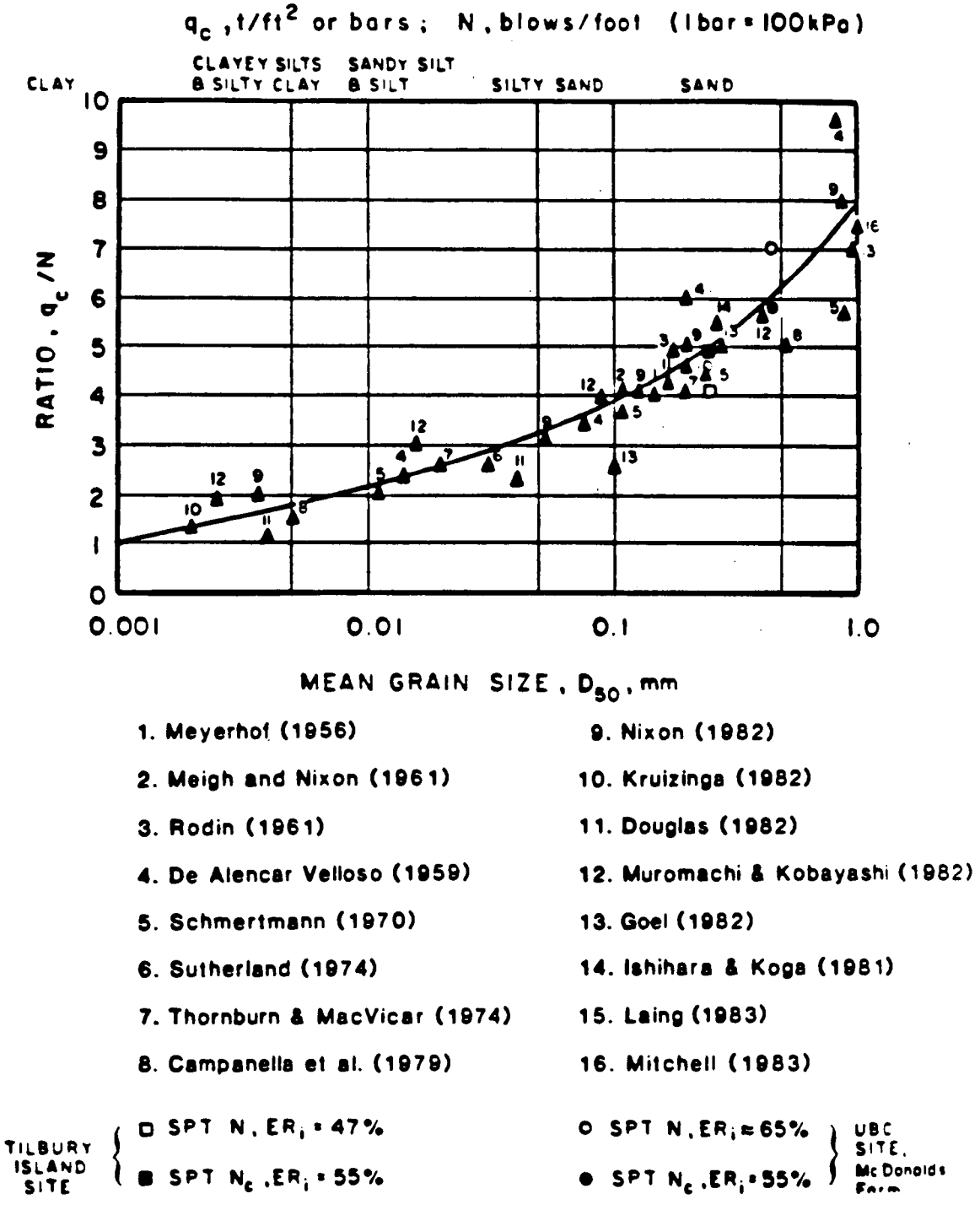

Figure 4.21 Variation of q_c/N Ratio with Mean Grain Size at SPT Energy Level 55-60% (After Robertson et al, 1983)

data, an efficiency of about 55% to 60% may be the norm for which it can be assumed that many North American SPT correlations were developed. Most of the data presented in Fig. 4.21 was obtained using the standard donut type hammer with a rope and cathead system.

Robertson et al (1982) presented energy measurements on SPT data that indicate that the average energy ratio of 55% to 60% may represent the average energy level associated with the q_c/N correlation shown in Fig. 4.21.

Fig. 4.21 can therefore be used to convert CPT data to equivalent SPT N values. To estimate the mean grain size from CPT data use can be made of the simplified classification chart shown in Fig. 4.2. The classification chart in Fig. 4.2 should be used as a guide to grain size. Included on Fig. 4.2 are the suggested q_c/N ratios for each soil zone. The addition of pore pressure measurements during cone penetration would significantly improve the soil classification. For mechanical cone data use can be made of classification charts by Schmertmann (1978a), Searle (1979) or Muromachi and Atsuta (1980).

If local design correlations have been developed based on SPT data obtained using alternative procedures such as a trip hammer or procedures other than the rope and cathead technique, the q_c/N ratios shown in Fig. 4.21 may be slightly in error. If a trip hammer was used it is likely that the energy level would be higher than the average 55% to 60% level by a factor of about 1.4 (Douglas, 1982). Thus q_c/N ratios would be slightly higher than those shown in Fig. 4.21. Blow count varies inversely with energy level.

4.9. Summary

4.9.1. General

- Interpretation of CPT and CPTU data is based on empirical and semi-empirical correlations.
- Primary purpose of CPT and CPTU is stratigraphic logging. Preliminary estimates of geotechnical paramaters can be made and critical areas defined. These critical areas may then require further testing that may include DMT soundings and/or selective sampling and laboratory testing.
- If at all possible, always verify correlations used with direct local or site specific measurements and adjust as necessary. Site specific correlations provide the most reliable assessment of geotechnical parameters.
- Cone resistance may not reach full value within thin stiff layers (<70cm).

4.9.2. Soil Type (Section 4.2)

Figure 4.2 (Electric CPT data)

Figure 4.3 (Electric CPTU data)

- Charts are global in nature, therefore they provide only a guide to soil behavior type.
- Expect some overlap in zones.
- Local correlations are preferable.
- Based on data obtained at depths of <100 ft. (30 m)
- Thin stiff layers (<70 cm), q_c may not respond fully.

4.9.3. **Stratigraphy (Section 4.3)**

- Look for normally consolidated clay deposits where q_c increases linearly with depth.
- Look for major layers consistent with project requirements.
- Look for details in layers, thin lenses, general homogeneity in layers.
- Look for possible influence of low horizontal stresses (near cavity or adjacent borehole) and high stresses (OCR or after compaction).

4.9.4. **Drainage Conditions (Section 4.7)**

- Determine average depth of the groundwater table where equilibrium porewater pressure equals zero.

- Define layers of drained or undrained cone penetration.
- Use Fig. 4.2 as a guide or CPTU data.
- Review available data before interpretation of CPT data for geotechnical paramaters.
    - Geologic origin of deposit.
    - Major mineral composition to estimate compressibility.
    - Review plasticity of fine grained soils.
    - Review potential for stress history;
        - old deposits have high potential of stress history
        - young deposits have possibility of underconsolidation.
    - Review possibility of cementation and/or gravel content.

Drained Penetration

4.9.5. **Relative Density (D_r) (Section 4.4.1)**

- Fig. 4.6 for relatively uniform, uncemented, clean, predominantly quartz, unaged sands.
- Use Fig. 4.5 to adjust correlation based on estimated compressibility;
  - rounded, well graded, quartz sands - lowest compressibility
  - increased angularity, mica content or uniformity in grading - increases compressibility
  - carbonate sands are significantly more compressible.
- For overconsolidated sands (K_o >0.45) estimate σ'_{ho} and use in Fig. 4.6
  - Estimate K_o from Equation 4.6.
- In thin layers (<70 cm), q_c may underestimate D_r.
- In general, D_r is a poor indicator of soil behaviour.
- The correlations are sensitive for horizontal stress (i.e., K_o) and soil compressibility (i.e., grain mineralogy).

4.9.6. **Friction Angle (ϕ) (Section 4.4.2)**

- Fig. 4.8 for relatively uniform, uncemented, clean, predominantly quartz, unaged sands.
- Use Fig. 4.7 to adjust correlation based on estimate of increased compressibility. However, correlation is not sensitive to variation in compressibility for most quartz sands.
- For overconsolidated sands (K_o >0.45) ϕ' will be slightly overpredicted using Fig. 4.8 (see Fig. 4.7).

- ϕ' in Fig. 4.8 is related to in situ initial horizontal effective stress before cone penetration.

- ϕ' varies with stress level due to curvature of strength envelope

  - ϕ' decreases with increasing confining stress level. A <u>one-log cycle increase</u> in confining stress produces the following approximate <u>decrease</u> in ϕ':

D_r <35%	0 to 1°
35% <D_r <65%	2° to 3°
65% <D_r <85%	3° to 5°
85% <D_r	5° to 8°

- In thin layers (<70 cm), q_c may underestimate ϕ'.

4.9.7. **Deformation Moduli (Section 4.4.3)**

- Constrained Modulus (M)
  - Fig. 4.9 for normally consolidated, uncemented, predominantly quartz, unaged sands.
  - Fig. 4.10 for overconsolidated, uncemented, predominantly quartz sands.
  - Modulus is very sensitive to OCR (Fig. 4.10).
- Young's Modulus (E)
  - Fig. 4.11 for normally consolidated, uncemented, predominantly quartz sands.

  - Fig. 4.12 for overconsolidated, uncemented, predominantly quartz sands.
  - E very sensitive to OCR (Fig. 4.12).
  - Important to define stress level of required E.
  - Fig. 4.9 and 4.11 (N.C. Deposits) will give conservatively low moduli if OCR unknown.
- Dynamic Shear Modulus (G_{max})
  - Fig. 4.13 for N.C. and O.C., uncemented, unaged, predominantly quartz sands.
  - G_{max} insensitive to OCR.

4.9.8. **Stress History (Section 4.4.4)**

- Presently impossible to quantify stress history from only CPT or CPTU data during <u>drained</u> penetration,
- Combined DMT (K_D) and CPT (q_c/σ'_{vo}) data useful to estimate K_o, Fig. 4.14.
- Indication of high K_o if D_r >>100%.

<u>Undrained Penetration</u> (Section 4.5)

4.9.9. **Undrained Shear Strength (s_u) (Section 4.5.1)**

Important to remember there is no unique value of s_u. Depends on stress path followed, type of test, strain rate, etc. Whenever possible, verify correlation factor with field vane test to directly measure s_u.

- For CPT Data
  - s_u estimated from empirical correlation, Eq. 4.7

$$s_u = \frac{q_c - \sigma_{vo}}{N_K}$$

where σ_{vo} = total overburden stress

$N_K = 15 \pm 5$

s_u = field vane undrained shear strength

- N_K depends on: OCR, sensitivity, stiffness.
- For sensitive clays ($S_t > 5$) N_K may be <10.
- Large scatter in N_K for very soft clays, where q_c <5 t/ft² due to possible poor resolution of q_c.
- For stiff fissured clays the macrofabric is a major factor and

$$N_K = 25 \pm 5$$

- For CPTU Data
  - Correct q_c to q_T

$$q_T = q_c + u(1-a)$$

where:

u = pore pressure behind tip

a = net area ratio (Section 3.1.1).

  - s_u estimated from empirical correlation, Eq. 4.9

$$s_u = \frac{q_T - \sigma_{vo}}{N_{KT}}$$

  - Calculate $B_q = \frac{u-u_o}{q_T-\sigma_{vo}}$.
  - Estimate sensitivity (S_t) and OCR.
  - Use Fig. 4.15 to estimate $N_{\Delta u}$.
  - Use B_q and Fig. 4.16 to estimate $N_{\Delta u}$.
  - Compare $N_{\Delta u}$ and use average to calculate s_u, Equation 4.12.

$$s_u = \frac{\Delta u}{N_{\Delta u}}$$

- Use s_u to re-evaluate OCR (Fig. 4.19) and sensitivity.
- Iterate until consistent s_u is derived.
  - Δu from CPTU is good for very soft clays.
  - Not recommended for stiff clays.
- Whenever possible measure s_u by field vane to directly determine N_{KT} and $N_{\Delta u}$ for a given clay.

4.9.10. **Sensitivity (Section 4.5.2)**

- Assume friction sleeve stress $f_s = s_u$ (remolded).
- Calculate $S_t = s_u$ (undisturbed) above ÷ s_u (remolded).
- Estimate S_t from Equation 4.13. $S_t = N_s/R_f(\%)$ and try $N_s = 6$.

4.9.11. **Stress History (OCR) (Section 4.5.5)**

- Estimate s_u, then calculate s_u/σ'_{vo}.
- Compare with s_u/σ'_{vo} estimated from Fig. 4.19(b) for N.C. deposit. Use $s_u/\sigma'_{vo} = 0.3$ if no better estimate available.
- Use Fig. 4.19 to estimate OCR.
  - Pore pressure ratio from CPTU data is a useful guide to variations in OCR within a homogeneous deposit.

4.9.12. **Deformation Moduli (Section 4.5.4)**

- Constrained Moduli (M)
  - Table 4.3, where: $M = \frac{1}{m_v} = \alpha \cdot q_c$.
  - Applicable for stress increment ≤1 t/ft².

  - Crude estimate only, better to measure m_v from oedometer test or estimate from DMT.
- Undrained Young's Moduli (E_u)
  - Estimate s_u, then use Fig. 4.17.
  - Knowledge of plasticity and OCR important.
- Dynamic Shear Moduli (G_{max})
  - Use Fig. 4.18.
  - Knowledge of plasticity and OCR important.

4.9.13. **Flow Characteristics (Section 4.5.6)**

- Plot normalized excess pore pressure from dissipation test versus log time.
- Compare shape of normalized dissipation curve with theoretical curves (Fig. 4.20).
- If similar shape, calculate (Eq. 4.17)

$$c_h = \frac{R^2 T}{t}$$

where:

T = time factor (Fig. 4.20)

c_h = coefficient of consolidation

t = time to reach a given value of $\Delta u(t)/\Delta u$

R = radius of cone (usually R = 17.85 mm or 0.7 in.).

If no data exists, assume $A_f = 0.8$

$$I_R = 100.$$

  - c_h determined for $\Delta u(t)/\Delta u = 0.5$ (i.e., 50% consolidation) may be used in problems involving horizontal flow in OC range.

- For c_h in N.C. range, use

$$c_h \text{ (N.C.)} = \frac{RR}{CR} \cdot c_h \text{ (OC)}$$

where:

RR = recompression ratio

CR = virgin compression ratio.

If no data available, assume $\frac{RR}{CR} = 0.15$.

- Approximate estimate of k from

$$k_h = c_h \, m_h \, \gamma_w$$

$$k_v = c_v \, m_v \, \gamma_w$$

Assume $m_v = m_h$.

4.9.14. **Equivalent SPT N Value (Section 4.8)**

- Fig. 4.21. Requires D_{50} or estimated soil type.
- Fig. 4.2 for direct estimate of q_c/N.
- SPT N value at approx. 55 to 60% energy.

5. DESIGN RECOMMENDATIONS

5.1. Foundation Engineering

There are basically two main methods for the application of cone data to geotechnical design,

i) Use of cone data to evaluate soil parameters, e.g. evaluation of ϕ, D_r, s_u and E.

ii) Direct use of cone data for design, e.g. cone resistance for pile capacity.

Much of the early use of cone data for geotechnical design was through the direct application to pile design. This approach has the advantage that it is based on observed field experience. Thus, these methods, when applied in similar situations can produce reliable results. In recent years, direct CPT based design methods have also been developed for other applications, such as, design of shallow foundations and liquefaction assessment. The direct methods have a particular advantage in granular soils, such as sand, where use of parameters like relative density can produce misleading results.

The evaluation of soil parameters can be useful for design in cases where little design experience exists and a more fundamental analysis is applied.

In areas like North America, many geotechnical engineers have developed considerable experience with design based on local SPT correlations. In the initial introduction of CPT data, many of these engineers will feel more comfortable converting the CPT data to equivalent SPT N values and then applying them to their existing SPT based design

methods. Section 4.8 in this report can provide a basis for the required CPT-SPT correlation. However, the q_c/N ratios shown in Fig. 4.21 appear to represent SPT N values obtained with an average energy ratio of about 55% to 60%. If local design correlations have been developed based on SPT data obtained using alternative procedures with resulting different average energy levels, Fig. 4.20 should be adjusted to reflect local practise and experience.

5.2. Shallow Foundations (Footings and Rafts)

5.2.1. Shallow Foundations on Sand

Settlement, rather than bearing capacity criteria, usually controls design, except for narrow foundations (<3 feet) on loose sand.

A quick estimate of settlements can be made using the chart in Fig. 5.1, which has been adapted from the SPT method of Burland and Burbidge (1984, 1985). Fig. 5.1 indicates the probable extent of a settlement problem. Burland and Burbidge reviewed over 200 settlement records to develop a simple empirical relationship between the average SPT N-value, foundation pressure and settlement. Correction factors were also developed to account for footing shape, thickness of sand layer and time-dependent (creep) deformations (see Burland and Burbidge, 1984 or 1985 for details). The correlations are valid for predominantly silica sands where the factor of safety against bearing capabity is greater than 3. To use the Burland and Burbidge correlation the CPT q_c values should be converted to equivalent SPT N-values using Fig. 4.21 or for sand by assuming $q_c/N = 5.0$, where q_c is in bars or tons/ft^2.

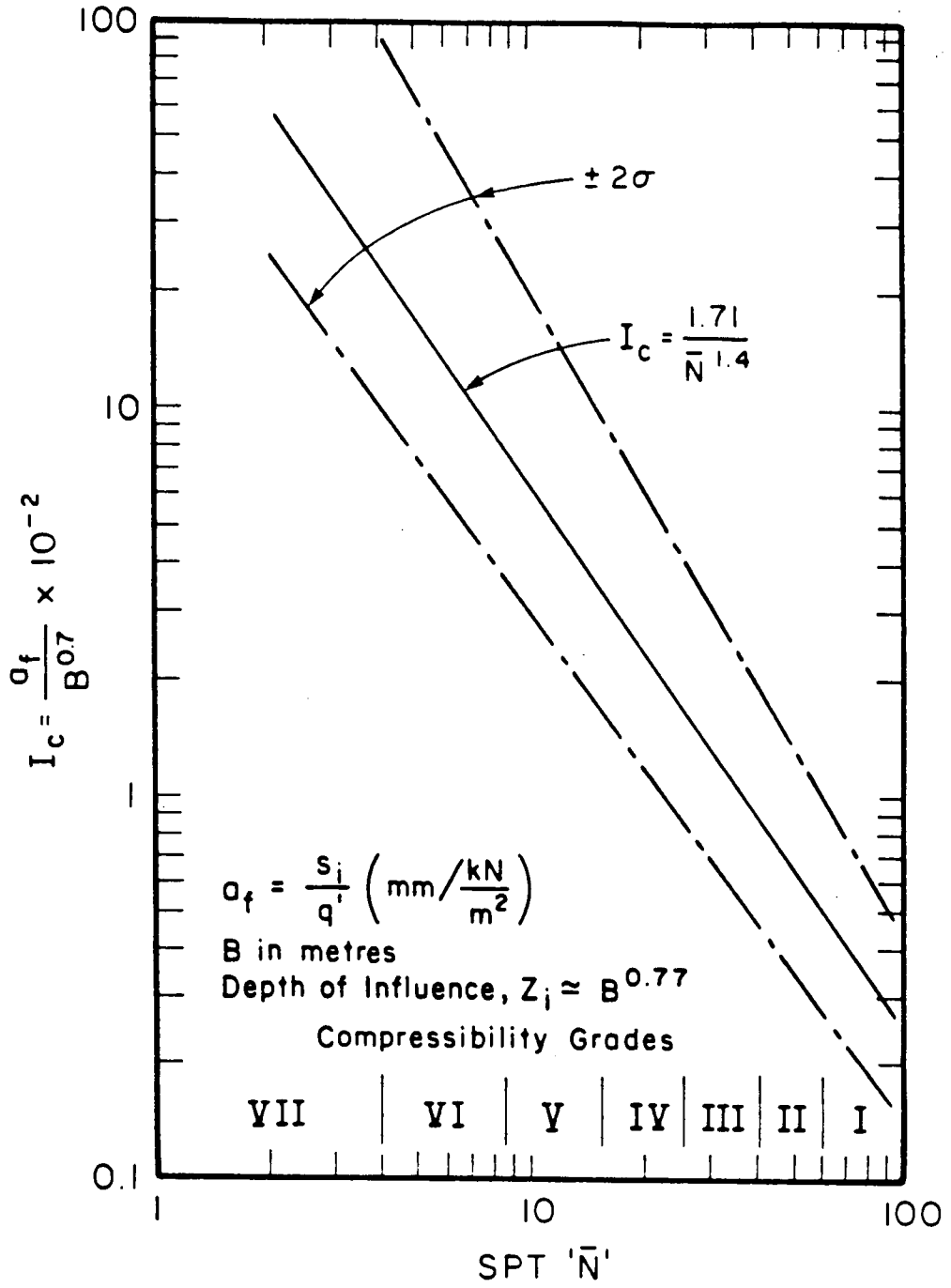

Figure 5.1 Relationship between Compressibility (I_c) and Mean SPT Blow Count ($\bar{N}$) over Depth of Influence (Z_i)
(After Burland and Burbidge, 1984 and 1985)

A rapid conservative estimate of settlement of footings on sand can be obtained directly from q_c using the empirical relationship proposed by Meyerhof (1974):

$$S = \frac{P_n \cdot B}{2 \cdot \bar{q}_c} \qquad (5.1)$$

where S = settlement

P_n = net applied loading

B = footing width

$\bar{q}_c$ = average value of q_c over a depth equal to B.

For direct use of CPT data in calculating settlements of footings on sand, the method by Schmertmann (1970) is considered to be a good approach. Schmertmann found that for normal foundation loads (1 t/ft² to 3 t/ft²)an almost linear relationship exists between E and q_c. He also proposed an E/q_c ratio of 2.0 for circular footings over normally consolidated sand. The method was later modified by distinguishing between square and strip footings by incorporating shape factors of 1.25 and 1.75, respectively (Schmertmann, 1978c). The recent chamber test studies by Baldi et al (1981) appear to confirm these values for normally consolidated sands (see Fig. 4.11). The ratio's suggested by Schmertmann require some modification for such effects as the magnitude of foundation pressure and soil stress history. Section 4.4.3 should provide some guidance for any such

modification. The following E/q_c values are recommended for use in the method by Schmertmann (1970): 2.5 to 3.5 for recent N.C. silica sand fills (age <100 years), 3.5 to 6.0 for N.C. aged (>3000 years) and 6.0 to 10.0 for overconsolidated silica sands. Caution should be exercised before increasing the E/q_c ratio appreciably for overconsolidated sands because of the uncertainty in estimating OCR for a sand. Details of Schmertmann's (1970) method and a worked example are given in the Worked Examples Volume.

For very narrow footings bearing capacity may govern design. The bearing capacity calculations are based on friction angle values which can be estimated using cone data from Fig. 4.7.

5.2.2. Shallow Foundations on Clay

The two main calculations for shallow foundation on clay are related to stability and settlement. Stability is assessed from bearing capacity calculations using the undrained shear strength, s_u. The undrained shear strength can be estimated from cone bearing or pore pressure data as discussed in Section 4.5.1. Settlement is estimated using the compressibility of a clay. Unfortunately, the compressibility of a clay is not reliably estimated from cone data. However, a variety of crude empirical methods are discussed in Section 4.5.4. These methods serve only as a first approximation of a settlement problem. For a more accurate prediction of compressibility, it remains necessary to obtain samples and perform laboratory consolidation tests. The methods, however, can be adjusted based on local experience for any particular clay based on field settlement observations.

The piezometer cone offers the potential to estimate the rate of consolidation, as discussed in Section 4.5.6. The rate of pore pressure dissipation, during a pause in the penetration, provides a measure of the coefficient of horizontal consolidation, c_h. However, the theories related to these measurements make many simplifying assumptions. The method therefore requires local adjustment for any particular clay by an adequate number of field settlement observations.

It should be made clear that because the CPT provides continuous profiles of soil variability judgement and experience should be applied to adequately account for the soil variability. However, the continuous nature of the CPT in-situ data provides a good basis for this judgement to be applied.

5.3. Deep Foundations (Piles)

Determination of pile capacity from the CPT is one of the earliest applications of the cone test. Pile foundations have been designed more or less successfully, using empirical approaches, for a large number of years. The problem of estimating pile capacity, however, is complicated by the large variety of pile types and installation procedures, as well as soil type. The present state-of-the-art in pile design using cone penetration test data is highly empirical. A full discussion of all the various methods is beyond the scope of this section. However, a recent paper by Robertson et al (1988), provides a useful evaluation of 13 different CPT methods.

5.3.1. Piles in Clay

Nearly all the working load capacity of driven piles in clay comes from the shaft. Until relatively recently, the prevalent design philosophy was that some bond or adhesion existed between the pile shaft and the soil. It was natural to correlate the strength of this bond with the undrained shear strength of the soil, s_u. This led to what is commonly referred to as the 'total stress method' for predicting pile capacity. The limiting skin friction, τ_s, on the pile shaft is expressed as a proportion of the in-situ shear strength of the soil, s_u, as

$$\tau_s = \alpha s_u \, . \qquad (5.2)$$

Experience from pile tests has provided a variety of correlations of the parameter α with soil type and strength (Tomlinson, 1980).

Burland (1973) advanced from this approach by arguing that soil behaviour is controlled by effective stresses. The new 'effective stress' approach relates skin friction to in-situ effective stress state. This led to a relationship between skin friction and the in-situ effective overburden pressure according to

$$\tau_s = \beta \, \sigma'_{vo} \qquad (5.3)$$

The parameter β thus reflects not only the friction angle between the pile and the soil, but also the ratio of the horizontal and vertical effective stresses.

Both of the above approaches involve empirical correlations to estimate α and β. The existing correlations are related to the undrained shear strength of the soil, s_u.

Randolph and Wroth (1982) provide an excellent outline of the recent developments that have occurred in the effective stress approach to pile design. In particular, they provide some insight into the three main events in the history of a driven pile. These are:

i) pile installation,

ii) consolidation, as excess pore pressure generated during installation dissipate, and

iii) pile loading.

Randolph and Wroth (1982) suggest that the design parameters α and β should be related to soil overconsolidation ratio (OCR) and hence to the s_u/σ'_{vo} ratio and provide tentative design charts. However, more data from pile tests are needed to confirm their design charts.

The improvements in understanding of the performance of piles using effective stress concepts may not lead to radical changes in empirically based design rules, but will increase confidence in those design rules and their ability to extrapolate them to new situations.

5.3.2. Piles in Sand

One of the major problems with the prediction of pile capacity in sands is associated with the large variety of pile installation techniques and their influence on the ultimate capacity. Sands are very sensitive to variations in cyclic or vibration loading. Thus, CPT related methods should take account of installation technique for the prediction of

ultimate capacity. However, these effects are often difficult to quantify and further research is required in this direction.

A large portion of the working load capacity of many driven piles in sand comes from end bearing. The scale effects for relating cone data to pile end bearing are complex but reasonably well understood. A consistent method to account for scale effects was developed by DeBeer (1963). Empirical correlations for end bearing were developed in Holland (Heijnen, 1974) and later confirmed by other investigations (Schmertmann, 1975). A recent development in the calculations of pile capacity has been the introduction of a correction for overconsolidation and gradation in cohesionless soils. The method is based on the results of a number of pile load tests in Holland in overconsolidated sands (Beringen et al, 1979). However, the major problem in many cases is related to the difficulty in estimating the overconsolidation ratio in sand. Conservatism is usually applied, especially for shallow penetrations into dense sand layers where scale effects predominate. The influence of overconsolidation on pile end bearing is one of the reasons a limit value to pile end bearing is usually applied. A limit pile end bearing of 150 t/ft^2 (15 MN/m^2) is generally accepted (de Ruiter and Beringer, 1979), although in dense sands cone resistance values may be greater than 500 t/ft^2 (50 MN/m^2). It is likely that in dense normally consolidated sands, higher ultimate end bearing values than 150 t/ft^2 (15 MN/m^2) can occur, but this has not been adequately confirmed by load tests (de Ruiter, 1982).

5.3.3. CPT Design Methods

There are many methods available to determine pile capacity from CPT data. The three popular direct CPT methods for driven piles are those described by de Ruiter and Beringen (1979), Schmertmann (1978a) and LCPC (1982). A summary of these three main methods for using CPT data to predict vertical pile capacity is given in the following sections. A worked example for each is given in the Worked Examples Volume.

European Method (de Ruiter and Beringen, 1979)

The CPT method used in Europe and especially for design of piles in the North Sea is summarized in Table 5.1.

The unit end bearing for piles in sand is based on pile load test data and is governed by the q_c in a zone of between 0.7D to 4D (where D = pile diameter) below the pile tip and 8D above the pile tip, as shown in Fig. 5.2.

Schmertmann Method (1978a)

The Schmertmann CPT method for design of piles is summarized in Table 5.2. The pile tip resistance in sand is the same as that recommended by de Ruiter and Beringen (1979) using Fig. 5.2. Shaft friction in sands is estimated using Fig. 5.3 where D/B is pile length to width ratio, and in clay using Fig. 5.4.

LPC Method (Bustamante and Gianeselli, 1982)

The method developed at LCPC (France) is summarized in Tables 5.3, 5.4, and 5.5. The unit end bearing is calculated using an equivalent cone resistance at the pile tip, as shown in Fig. 5.5.

Generally, it is recommended to use all three methods and the lowest value of ultimate capacity should be adopted.

5.3.4. Factor of Safety

The choice of factor of safety to be applied to the calculated ultimate pile capacity depends on many factors, including reliability and sufficiency of the site investigation data, confidence in the method of calculation, previous experience with similar piles in same ground conditions and whether or not pile loading tests are to be performed. Where there are appreciable differences in CPT profiles, a reasonable lower bound profile should be adopted or the site should be divided into similar regions. In cases where no specific estimate of settlement is to be made, the factor of safety may also be intended to limit settlements to reasonable values. In which case due allowance should be made for the type of loading, which may affect settlement; i.e., cyclic live loads will give larger settlements than single (or few) load applications, particularly if the live load is large compared with the dead load.

The recommended factors of safety for the above CPT methods are 2.25 for standard electric CPT and 3.0 for mechanical CPT. The LCPC Method recommends a factor of safety of 2 for skin friction and 3 for point resistance (standard electric CPT).

5.3.5. Non-displacement Piles (Bored Piles)

Non-displacement piles include bored cast-in-situ piles, precast piles placed in a pre-bored hole, piles placed with the aid of jetting and piles constructed by pumping grout through the hollow stem of a continuous-flight auger. With bored piles, horizontal stresses will decrease rather than

	SAND	CLAY
Unit Skin Friction, f_p	Minimum of: f_1 = 0.12 MPa (1.2 t/ft²) f_2 = CPT sleeve friction, f_s $f_3 = q_c/300$ (compression) $f_4 = q_c/400$ (tension)	$f = \alpha\, s_u$ where: α = 1 for N.C. Clay = 0.5 for O.C. Clay
Unit End Bearing, q_p	Minimum: q_p from Fig. 5.2	$q_p = N_c \cdot s_u$ where: N_c = 9 $s_u = q_c/N_k$, N_k = 15 to 20

TABLE 5.1: European CPT Design Method
(After de Ruiter and Beringer, 1979)

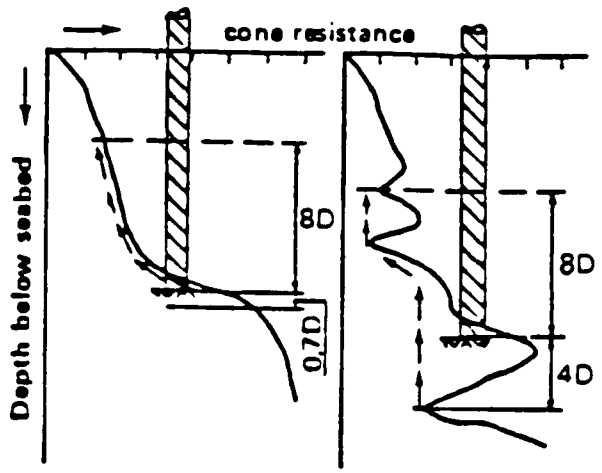

$$q_p = \frac{(I + II)/2 + III}{2}$$

Key

D : Diameter of the pile

I : Average cone resistance below the tip of the pile over a depth which may very between 0.7D and 4D

II : Minimum cone resistance recorded below the pile tip over the same depth of 0.7D to 4D

III : Average of the envelope of minimum cone resistances recorded above the pile tip over a height which may very between 6D and 8D. In determining this envelope, values above the minimum value selected under II are to be disregarded

q_p : Ultimate unit point resistance of the pile

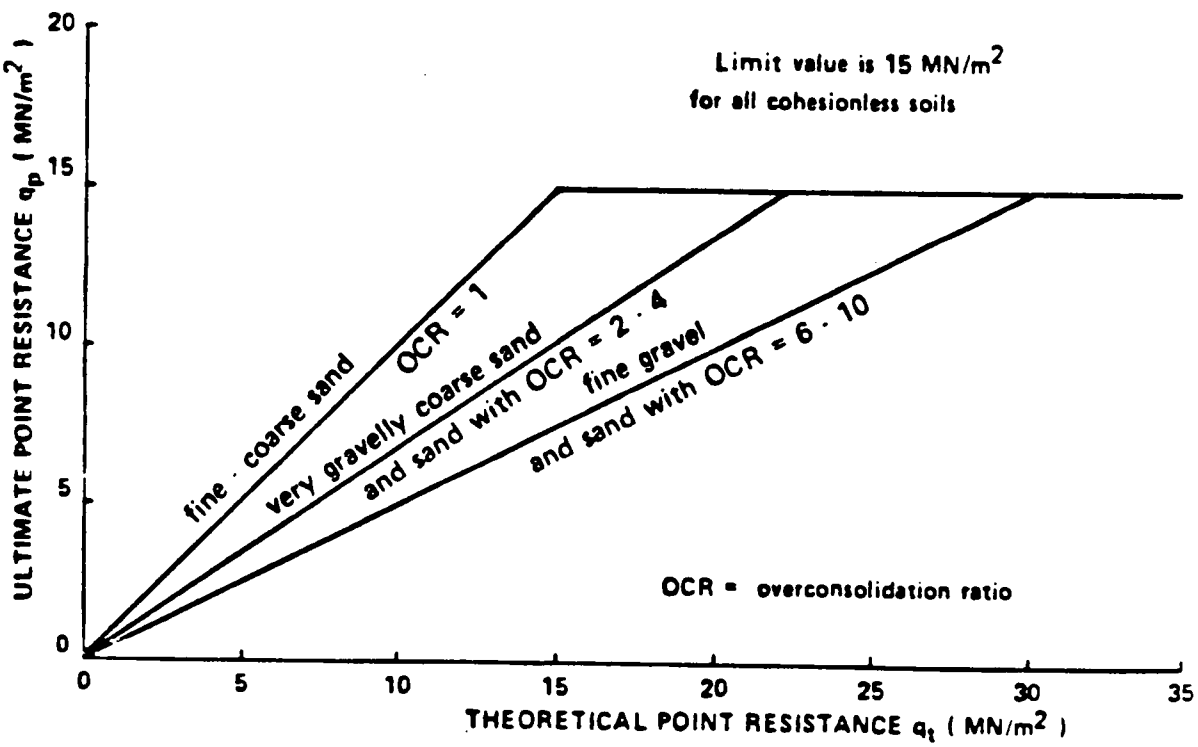

Figure 5.2 Application of CPT to Pile Design (After de Ruiter and Beringer, 1979)

	SAND	CLAY
Unit Skin Friction, f_p	Minimum of: $f_1 = K[\sum_{o}^{8D} (\frac{\ell}{8D}) \cdot f_s + \sum_{8D}^{L} \cdot f_s]$ where: K = ratio of f_p/f_s (Fig.5.3) ℓ = depth to f_s considered D = pile width L = pile length f_2 = 0.12 MPa (1.2 t/ft²) $f_3 = c \cdot q_c$ C Precast concrete 0.012 Concrete enlarged base 0.018 Steel displacement 0.012 Open-ended steel 0.008 For tension capacity take $f = 0.7\ f_p$	Minimum of: $f_1 = \alpha' s_u$ (see Fig. 5.4) $f_2 = \lambda(\bar{p}' + 2\bar{s}_u)$ where: $\bar{p}'$ = ave. σ'_{vo} along pile length $\bar{s}_u$ = ave. s_u along pile length λ = 0.3 for L/B = 10 = 0.2 for L/B = 20 = 0.14 for L/B > 60 $f_3 = \alpha'[\sum_{o}^{8D} (\frac{\ell}{8D}) \cdot f_s + \sum_{8D}^{L} f_s]$
Unit End Bearing, q_p	Minimum q_p from Fig. 5.2	

TABLE 5.2: Schmertmann CPT Design Method
(After Schmertmann 1978a)

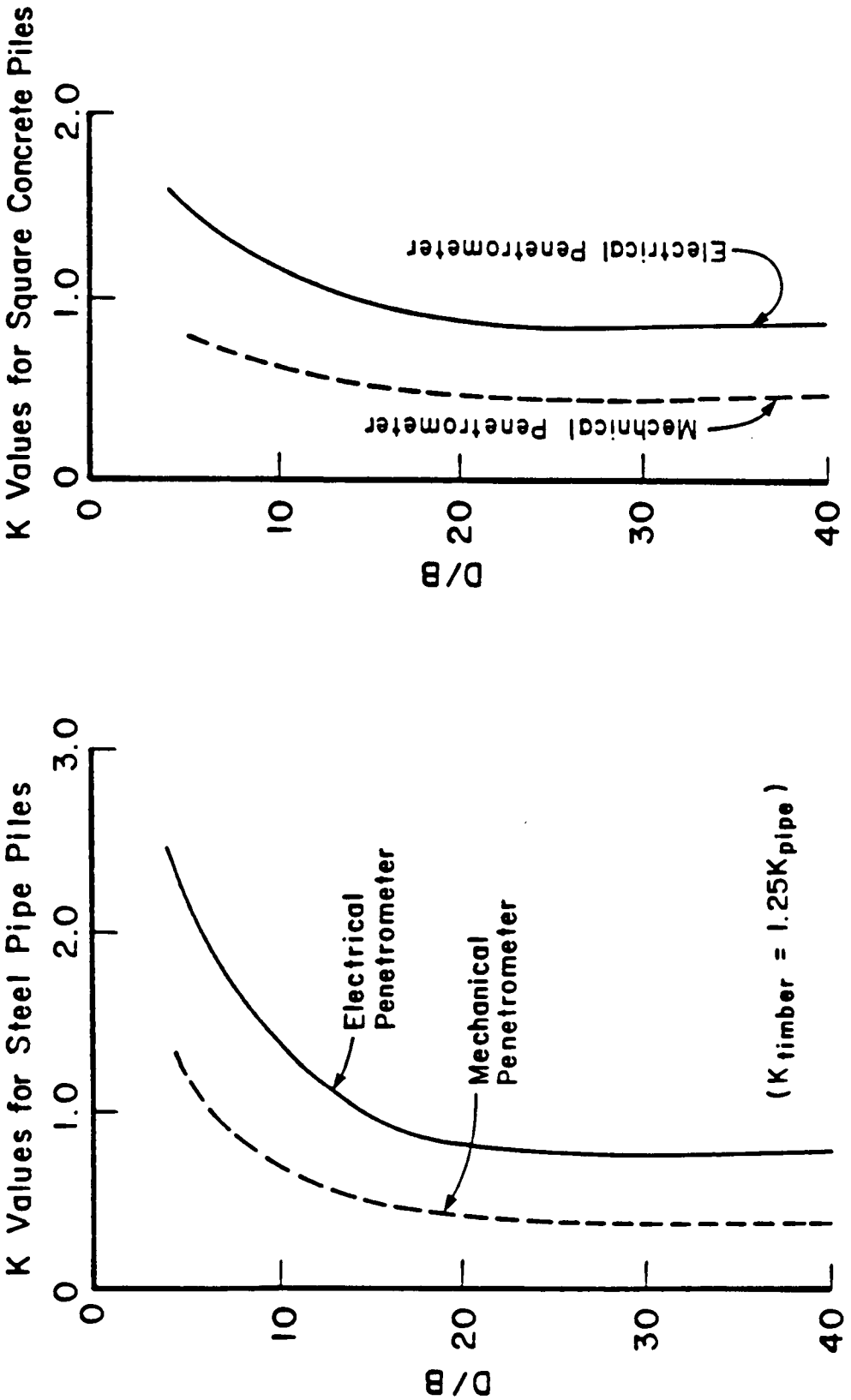

Figure 5.3 Design Curves for Pile Side Friction in Sand (After Schmertmann, 1978)

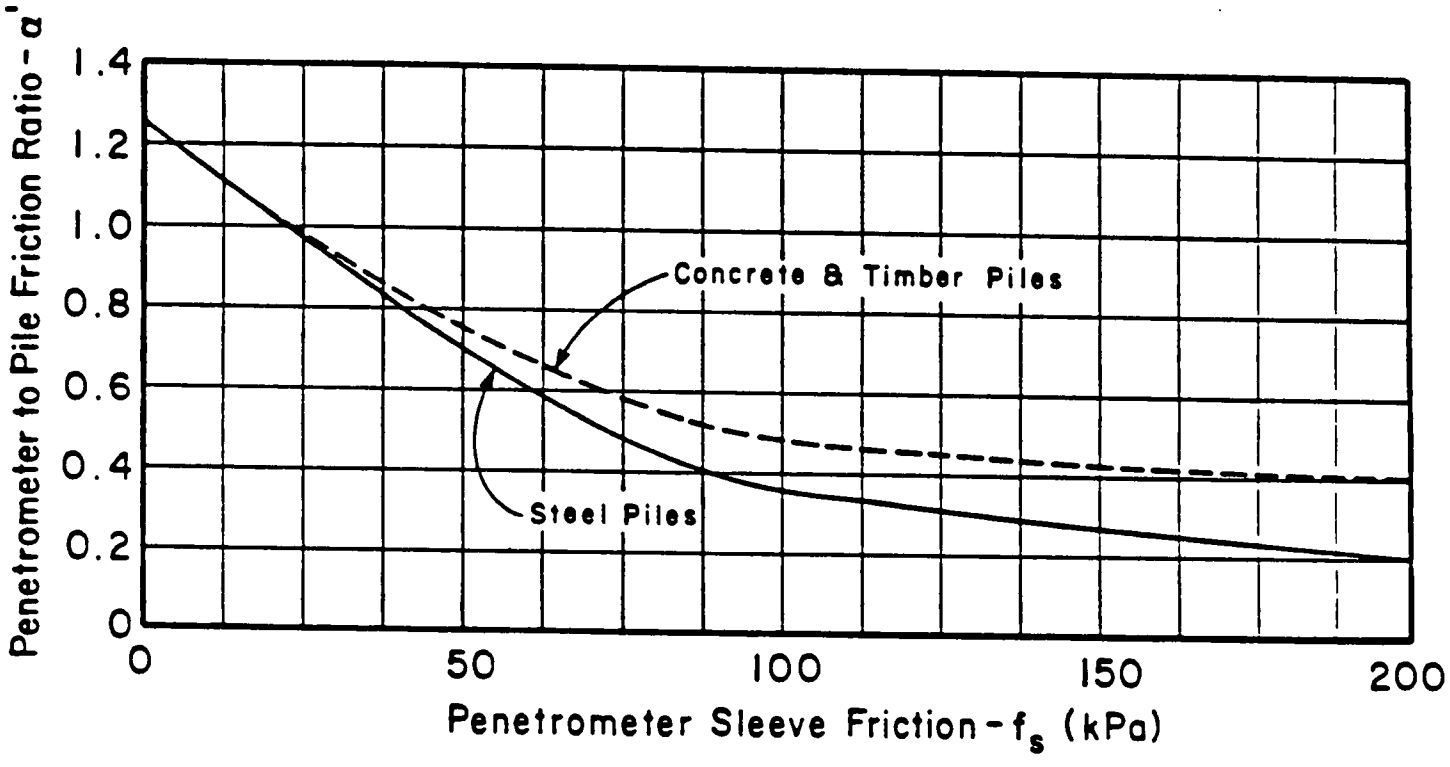

Figure 5.4 Design Curves for Pile Side Friction in Clay (After Schmertmann, 1978)

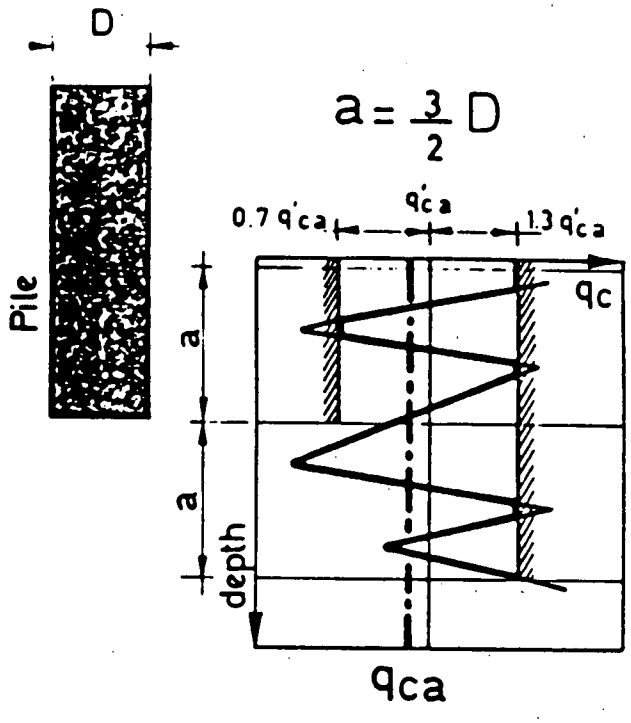

Figure 5.5 LCPC CPT Method to Determine Equivalent Cone Resistance at Pile Tip (After Bustamante and Gianeselli, 1982)

	Sand and Clay
Unit Skin Friction f_p	$f_p = \frac{q_c}{\alpha}$ α = friction coefficient (Table 5.5)
Unit End q_p	$q_p = k_c \cdot q_{ca}$ q_{ca} = equivalent cone resistance at level of pile tip (Fig. 5.5) k_c = bearing capacity factor (Table 5.4)

TABLE 5.3: LCPC CPT Method
(Bustamante and Gianeselli, 1982)

Nature of Soil	q_c (MPa)	Factors k_c	
		Group I	Group II
Soft clay and mud	<1	0.4	0.5
Moderately compact clay	1 to 5	0.35	0.45
Silt and loose sand	≤5	0.4	0.5
Compact to stiff clay and compact silt	>5	0.45	0.55
Soft chalk	≤5	0.2	0.3
Moderately compact sand and gravel	5 to 12	0.4	0.5
Weathered to fragmented chalk	<5	0.2	0.4
Compact to very compact sand and gravel	<12	0.3	0.4

Group I - Plain bored piles
Mud bored piles
Micro piles (grouted under low pressure)
Cased bored piles
Hollow auger bored piles
Piers
Barrettes

Group II - Cast screwed piles
Driven precast piles
Prestressed tubular piles
Driven cast piles
Jacked metal piles
Micropiles (small diameter piles grouted under high pressure with diameter <250 mm)
Driven grouted piles (low pressure grouting)
Driven metal piles
Driven rammed piles
Jacked concrete piles
High pressure grouted piles of large diameter

TABLE 5.4: Bearing Capacity Factors, k_c

Nature of Soil	q_c (MPa)	Coefficients, α				Maximum Limit of f_p (MPa)					
		Category									
		I		II		I		II		III	
		A	B	A	B	A	B	A	B	A	B
Soft clay and mud	<1	30	30	30	30	0.015	0.015	0.015	0.015	0.035	-
Moderately compact clay	1 to 5	40	80	40	80	0.035 (0.08)	0.035 (0.08)	0.035 (0.08)	0.035	0.08	≥0.12
Silt and loose sand	≤5	60	150	60	120	0.035	0.035	0.035	0.035	0.08	-
Compact to stiff clay and compact silt	>5	60	120	60	120	0.035 (0.08)	0.035 (0.08)	0.035 (0.08)	0.035	0.08	≥0.20
Soft chalk	≤5	100	120	100	120	0.035	0.035	0.035	0.035	0.08	-
Moderately compact sand and gravel	5 to 12	100	200	100	200	0.08 (0.12)	0.035 (0.08)	0.08 (0.12)	0.08	0.12	≥0.20
Weathered to fragmented chalk	>5	60	80	60	80	0.12 (0.15)	0.08 (0.12)	0.12 (0.15)	0.12	0.15	≥0.20
Compact to very compact sand and gravel	>12	150	300	150	200	0.12 (0.15)	0.08 (0.12)	0.12 (0.15)	0.12	0.15	≥0.20

CATEGORY:

IA - Plain bored piles
Mud bored piles
Hollow auger bored piles
Micropiles (grouted under low pressure)
Cast screwed piles
Piers
Barettes

IB - Cased bored piles
Driven cast piles

IIA - Driven precast piles
Prestressed tubular piles
Jacked concrete piles

IIIA - Driven grouted piles
Driven rammed piles

IIB - Driven metal piles
Jacked metal piles

IIIB - High pressure grouted piles with diameter >250 mm
Micro piles grouted under high pressure

Note:

Max. limit unit skin friction, f_p: bracket values apply to careful execution and minimum disturbance of soil due to construction.

TABLE 5.5: Friction Coefficient, α

increase as they do with a displacement pile. With pre-bored or jetted piles any increase in stress will be less than will occur with a driven parallel-sided pile, the reduction depending on the extent to which the pile is driven below the pre-bored or jetted depth. Stress increase may also be less with a pile which is vibrated into the ground or is cast within a vibrated open-ended casing. Hence, non- displacement piles should have lower shaft resistance than displacement piles of the same diameter considering this factor only. However, the soil/pile interface is much rougher which compensates. In bored piles there may also be a reduction in end bearing capacity because of loosening of soil below pile tip level, but then the tip might be enlarged which again partially compensates.

Although some bored piles have been constructed in the Netherlands in recent years, they are few in number compared with driven piles, and hence there is no large body of experience for bored piles as there is with driven piles. Pile capacities of non-displacement piles are sometimes calculated by the CPT methods (see Section 5.3.3), but a higher factor of safety is often applied. The LCPC method was based on the results of 55 bored piles and is therefore recommended for bored piles.

Because of the uncertainties concerning non-displacement piles, especially in sand, and the considerable effect that installation procedures can have on bearing capacity and settlement, it is recommended that pre-construction pile load tests should be performed. It may be feasible to dispense with these on very small projects where there is considerable local experience, but in such cases factors of safety should be increased by some 50 percent.

5.3.6. Settlement of Piles

Although installation of piles changes the deformation and compressibility characteristics of the soil mass governing the behaviour of single piles under load, this influence extends only a few pile diameters below the pile tip. Meyerhof (1976) therefore suggests that the total settlement of a group of driven or bored piles under safe design load (not exceeding about one-third the ultimate group capacity) can generally be estimated, assuming an equivalent foundation (Terzaghi and Peck, 1967).

For a group of shaft resistance piles, the equivalent foundation is assumed to act on the soil at an effective depth of two-thirds the pile embedment. For a group of point-bearing piles the equivalent foundation is taken at the elevation of the pile points.

Meyerhof (1976) suggested the following relationship to estimate the settlement of pile groups in sand.

$$S = \frac{P_n \cdot B \cdot I}{2 \cdot \bar{q}_c} \qquad (5.4)$$

where $\bar{q}_c$ = average q_c within zone of settlement

B = width of pile group

P_n = net foundation pressure

I = influence factor of effective group embedment

$I = 1 - \frac{D'}{8B} \geq 0.5$

D' = effective embedment.

This formula is an extention of Meyerhof's relationship for shallow foundations on sand (see Section 5.2.1).

If the thickness of sand below the effective foundation depth is less than the foundation width (B), the estimated settlement can be reduced approximately linearly with the corresponding stratum thickness.

If the sand is overconsolidated, the above relationship will considerably overestimate settlement, similar to the influence of OCR on the E/q_c ratio (see Section 4.4.3).

The settlement of a pile group in clay or above a clay stratum is estimated from the initial deformation (E_u) and consolidation properties (m_v) of the clay and treating the foundation as an equivalent foundation as mentioned for pile groups in sand. The rate of settlement for pile groups in clay is controlled by the coefficient of consolidation of the deposit, similar to shallow foundation (see Section 5.2).

A recent publication by Fellenius (1989) suggests that <u>all</u> piles will, in the long term, be subjected to downdrag along their upper portions due to relative settlements of the surrounding soil. Fellenius (1989) suggests a unified approach to pile design incorporating downdrag.

5.3.7. Negative Shaft Friction (Downdrag)

Negative shaft friction and subsequent dragload are rarely a problem of capacity but one of settlement. The magnitude of the dragload generally has no influence on the bearing capacity of a pile, since the capacity of a pile is based on a plunging failure when the pile is assumed to be moving down relative to all the soil. Exceptions to this are end bearing piles driven into a very strong layer such as rock where large negative friction forces can cause damage to the piles. In general, a rigid, high capacity pile will experience a large dragload, but small settlements, whereas a less rigid, smaller capacity pile will experience a smaller dragload, but larger settlements. No pile will settle more than the ground surface nearest the pile. For further details, see Fellenius (1989).

5.4. Embankment and Slope Stability

The stability of slopes and embankments depends upon the shear strength of the soil. For embankments placed on soft, low permeability soils (clays, silts, etc.), the stability is usually assessed using a total stress analysis. Thus, the key parameter is the relevant undrained shear strength. A full discussion on the design of embankments is beyond the scope of this report. The reader is, therefore, encouraged to read the recent Terzaghi lecture by C.C. Ladd (1986).

The CPT is ideally suited to a preliminary evaluation of stability along a proposed embankment route. Critical areas, defined by the CPT, may require selective testing (field vane test) or sampling.

Details on the evaluation of undrained shear strength and friction angle are given in Sections 4.5.1 and 4.4.2.

5.5. Seismic Liquefaction Assessment

Some of the most comprehensive recent work on liquefaction assessment has been reported by Seed (1979, 1981, 1985). The method suggested by Seed involves two parts:

i) Estimate of the average cyclic stress ratio, τ/σ'_{vo}, developed in the field due to earthquake shaking.

ii) Estimate of the average cyclic stress ratio to cause liquefaction of the soil, τ_ℓ/σ'_{vo} .

The cyclic stress ratio developed in the field due to earthquake shaking can be computed from an equation of the form:

$$\tau/\sigma'_{vo} = 0.65 \frac{a_{max}}{g} \frac{\sigma_o}{\sigma'_{vo}} \cdot r_d \qquad (5.5)$$

where a_{max} = maximum acceleration at the ground surface,

σ_o = total overburden pressure on sand layer under condolidation

σ'_{vo} = initial effective overburden pressure on sand layer under consideration,

r_d = a stress reduction factor varying from a value of 1 at the ground surface to a value of 0.9 at a depth of about (10 m) 30 ft.

A convenient relationship proposed by the Japanese (Iwasaki et al, 1981) for the reduction factor, r_d is given by:

$$r_d = 1 - 0.015\ z \qquad (5.6)$$

where z is the depth in meters.

The current practise in North America for the determination of the cyclic stress ratio to cause liquefaction of the soil is either:

i) by use of field correlations using in-situ tests,

or ii) by means of laboratory tests on representative samples of the soil deposit.

Because of the great difficulty in obtaining undisturbed samples of sand deposits, most engineers prefer to adopt the field performance correlation approach, (Peck, 1979).

The existing field correlation most widely used is that proposed by Seed (1979) and Seed et al (1985) which involves the Standard Penetration Test (SPT). Recent work (Zhou, 1980; Douglas et al 1981; and Robertson and Campanella, 1985; Seed et al, 1983) has shown that similar correlations can be developed using the static cone penetration test (CPT).

The work by Douglas et al (1981) involved conversion of CPT data to equivalent SPT blowcounts. The work by Zhou (1980) and Robertson and Campanella (1985) involves a direct correlation between cone resistance and cyclic stress ratio to cause liquefaction. The correlation by Zhou (1980) is based on data from Chinese earthquakes using an electric cone that is different in dimensions and design than the European standard and thus may not be completely valid for standard electric cone data. The correlation proposed by Robertson and Campanella (1985) is shown in Fig. 5.6. Values

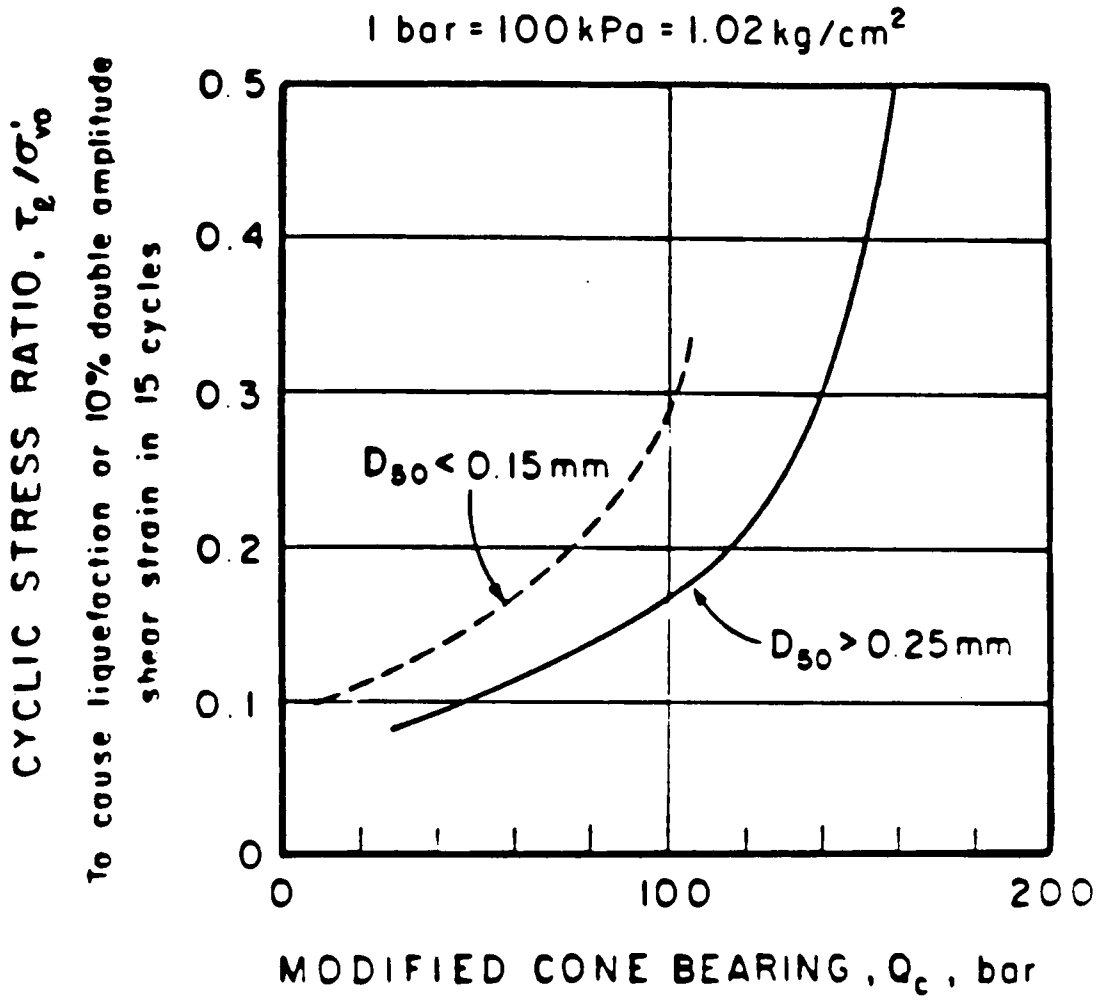

Figure 5.6 Correlation between Liquefaction Resistance under Level Ground Conditions and Cone Penetration Resistance for Sands and Silty Sands (After Robertson and Campanella, 1985)

of average cyclic stress ratio to cause liquefaction or 10 percent peak to peak strain in 15 cycles are plotted as a function of the normalized penetration resistance Q_c. This is similar in form to the correlation proposed by Seed using the normalized SPT blowcount, N_1. In this form, the measured cone resistance, q_c, is corrected to an effective overburden pressure of 100 kPa (1 kg/cm²) and can be determined from the relationship:

$$Q_c = C_Q \cdot q_c \qquad (5.7)$$

where C_Q is a function of the effective overburden pressure at the depth where the penetration test is conducted. The values of C_Q can be read from the chart shown in Fig. 5.7, which is based on a review of large calibration chamber test results (Baldi et al, 1982).

The correlation proposed by Seed et al (1985) is based on a direct correlation with their previous SPT method. The resulting design curves are very similar to those shown in Figs. 5.6 and 5.7. However, the latest correlation (Seed et al, 1985) uses the SPT N-value corrected to an average energy level of 60%, $(N_1)_{60}$. This allows more confidence in the conversion of CPT-Q_C to SPT-$(N_1)_{60}$ using the proposed q_C/N ratios in Figure 4.21.

The CPT methods proposed by Robertson and Campanella (1985) and Seed et al (1983) can be used in the same way as the SPT method. For any given site with <u>level ground</u> and a given value of maximum ground surface acceleration, the possibility of cyclic mobility or liquefaction is evaluated on an empirical basis with the aid of Figs. 5.6 and 5.7 by determining the appropriate values of Q_c for the sand deposit and obtaining lower bound values of the cyclic stress ratio, τ_l/σ'_{vo}, to cause

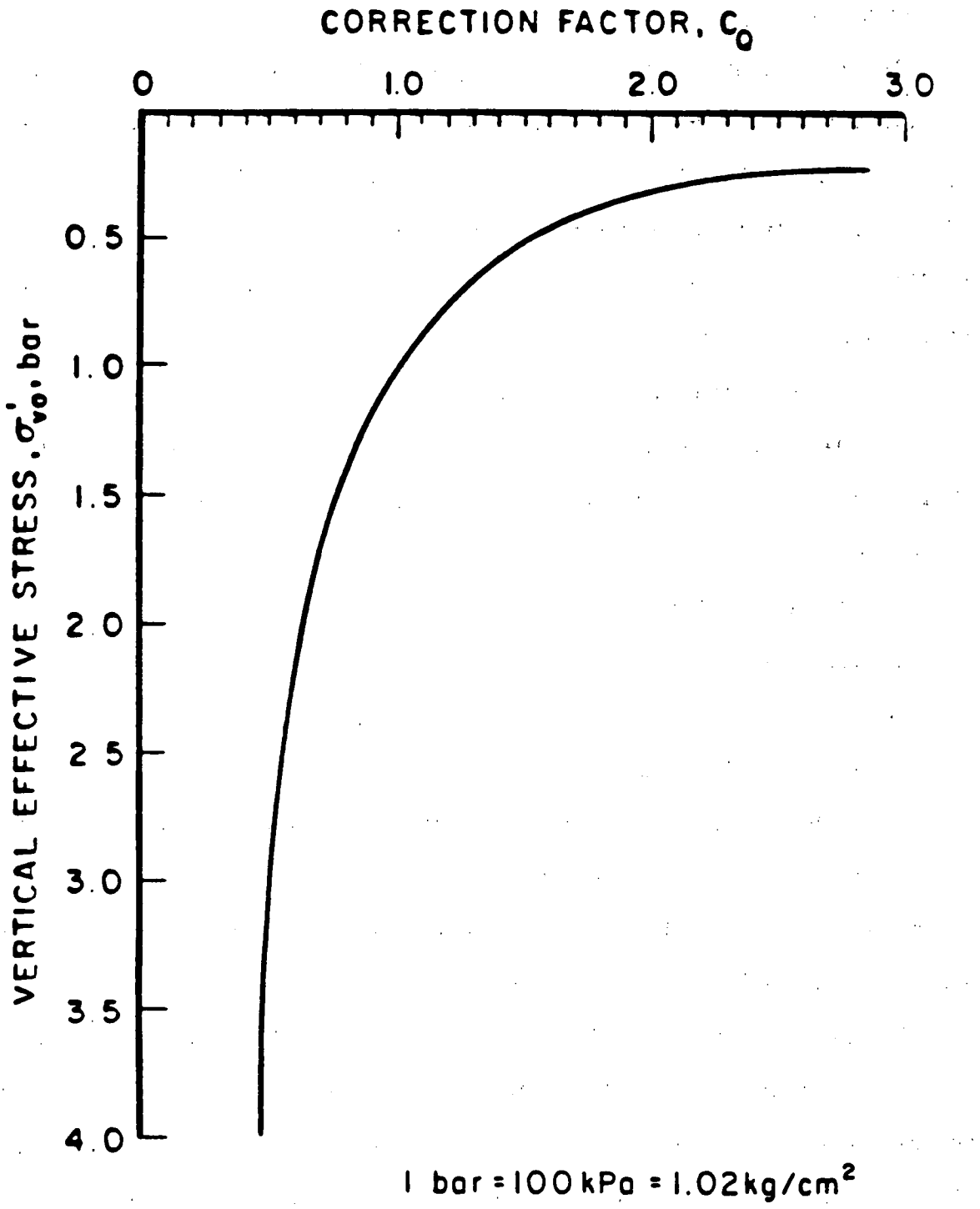

Figure 5.7 Relationship Between Correction Factor C_Q and Effective Overburden Pressure (After Robertson and Campanella, 1985)

liquefaction, and comparing these values with that induced by the design earthquake (τ/σ'_{vo}).

In a similar manner to that proposed by Seed et al (1983) the correlations shown in Fig. 5.6 applies to sands with an average grain size, $D_{50} > 0.25$ mm. For silty sands and silts that plot below the A-line on the plasticity chart and with a $D_{50} < 0.15$ mm, Robertson and Campanella (1983) have also proposed a second correlation (see Fig. 5.6), similar to Seed and Idriss (1981).

Seed and Idriss (1981) proposed, based on recent studies in China, that certain clayey soils may be vulnerable to severe strength loss as a result of earthquake shaking. These soils appear to have the following characteristics:

Percent finer than 0.005 mm	<	15%
Liquid Limit	<	35
Water Content	>	0.9 x liquid limit

(i.e. Liquidity Index close to 1.0)

It is interesting to note that these soil types tend to plot in the lower left corner of the classification chart, shown on Fig. 4.1 (Douglas and Olsen, 1981). These soil types have a liquidity index close to one and tend to generate high positive pore pressures during shear.

To identify sand and silts that may be liquefiable, use can be made of the classification chart shown in Fig. 5.8. Work by Douglas (1982) and experience at UBC would suggest that soils susceptable to liquefaction fall within an area on the soil classification chart designated Zone A. Loose clean quartz sands with a $D_{50} \geq 0.25$ mm tend to fall within the upper area of Zone A with 30 bar $< q_c <$ 150 bar and friction ratio, $R_f \leq$

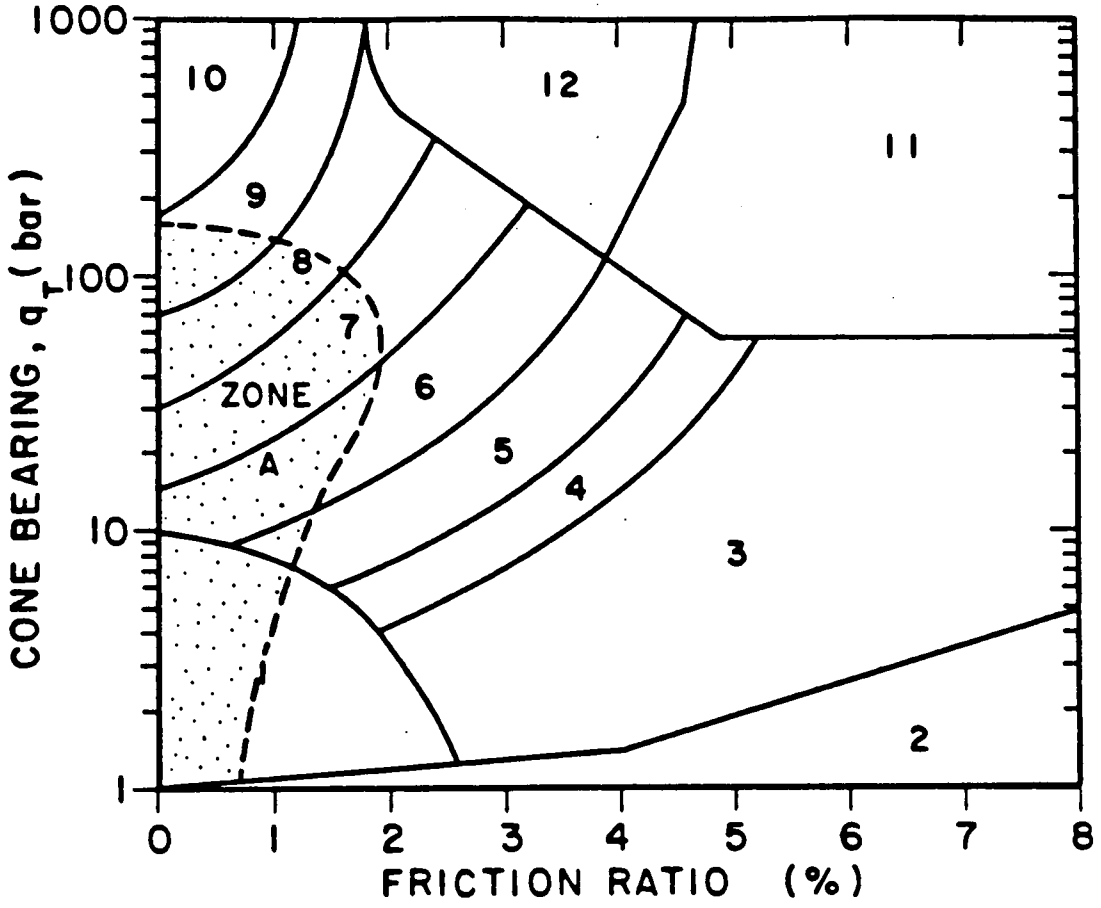

Zone	Soil Behaviour Type
1	sensitive fine grained
2	organic material
3	clay
4	silty clay to clay
5	clayey silt to silty clay
6	sandy silt to clayey silt
7	silty sand to sandy silt
8	sand to silty sand
9	sand
10	gravelly sand to sand
11	very stiff fine grained*
12	sand to clayey sand*

* overconsolidated or cemented.

Figure 5.8 Soil Classification Chart for Electronic Cone Showing Proposed Zone of Liquefiable Soils (After Robertson, 1986)

1.0. Soils that fall within the lower area of Zone A are the loose silty sands and silts, since a decrease in mean grain size tends to cause a decrease in penetration resistance. These soils tend to have higher resistance to liquefaction for the same penetration resistance values and tend to develop more pore pressures during penetration because of their lower permeability. Soils that fall outside of zone A, and have higher friction ratios, will tend to have a higher resistance to cyclic loading. However, the size of the cyclic loading (earthquake) will control their final susceptibility to liquefaction.

The correlations proposed for the CPT data and shown in Fig. 5.6 are based on empirical relationships supported by a limited number of field and laboratory data points and should therefore, at present, be used only as an estimate of liquefaction potential. Field performance data from Japan (Shibata, 1985) shows that the correlation does appear reasonable. The CPT does have the advantage of providing a continuous and repeatable measure of penetration resistance and with experience should prove a valuable tool for in-situ assessment of liquefaction resistance.

The existing SPT and CPT methods use the penetration resistance to assess liquefaction resistance in sands and silty sands. However, in silts, and to come extent silty sands, penetration often takes place under undrained conditions and large pore pressures can be generated. The penetration resistance in these soils is often extremely small and becomes sensitive to instrument or test errors. Also, these methods that use penetration resistance cannot be applied directly to problems where static shear exists, such as sloping ground or adjacent to structures.

For soils with static shear, the volume change characteristics are very important. The concept of a dilative or contractive soil is embodied in the steady-state approach to seismic liquefaction (Castro, 1975). For sloping ground conditions, the concept of Steady State Strength (Castro, 1975; Poulos, 1981) is more applicable. The Steady State Line (SSL) represents a condition of zero dilation during shear (Poulos, 1981). However, the major drawback of this approach is the requirement to measure the in-situ void ratio, e, or relative density, D_r. This has proven to be an extremely difficult task since it usually involves the use of undisturbed samples and laboratory testing. However, several correlations have recently been developed to correlate CPT data directly to Steady State concepts (Been and Jefferies, 1985). The approach developed by Been and Jefferies (1985) has used a 'State Parameter', ψ. The state parameter, ψ, is then correlated directly to cone penetration resistance, q_c, using existing calibration chamber results on different sands. Robertson (1986) has developed an approach which is similar to that of Been et al (1985) but uses dilation angle, ν, (see Fig. 5.9). The dilation angle is derived from existing correlations between cone penetration resistance and friction angle and uses the concept of stress dilatancy (Rowe, 1962).

The concept of liquefaction proposed by Castro (1975) for soils subjected to static shear, implies that soils that exist to the right of the steady state line (i.e., contractive) may liquefy and flow. However, the methods by Been et al (1985) and Robertson (1985) show that only extremely loose sands exist on the contractive side of the steady state line. Therefore, for most sands where $q_c \geq 40$ t/ft^2 flow liquefaction

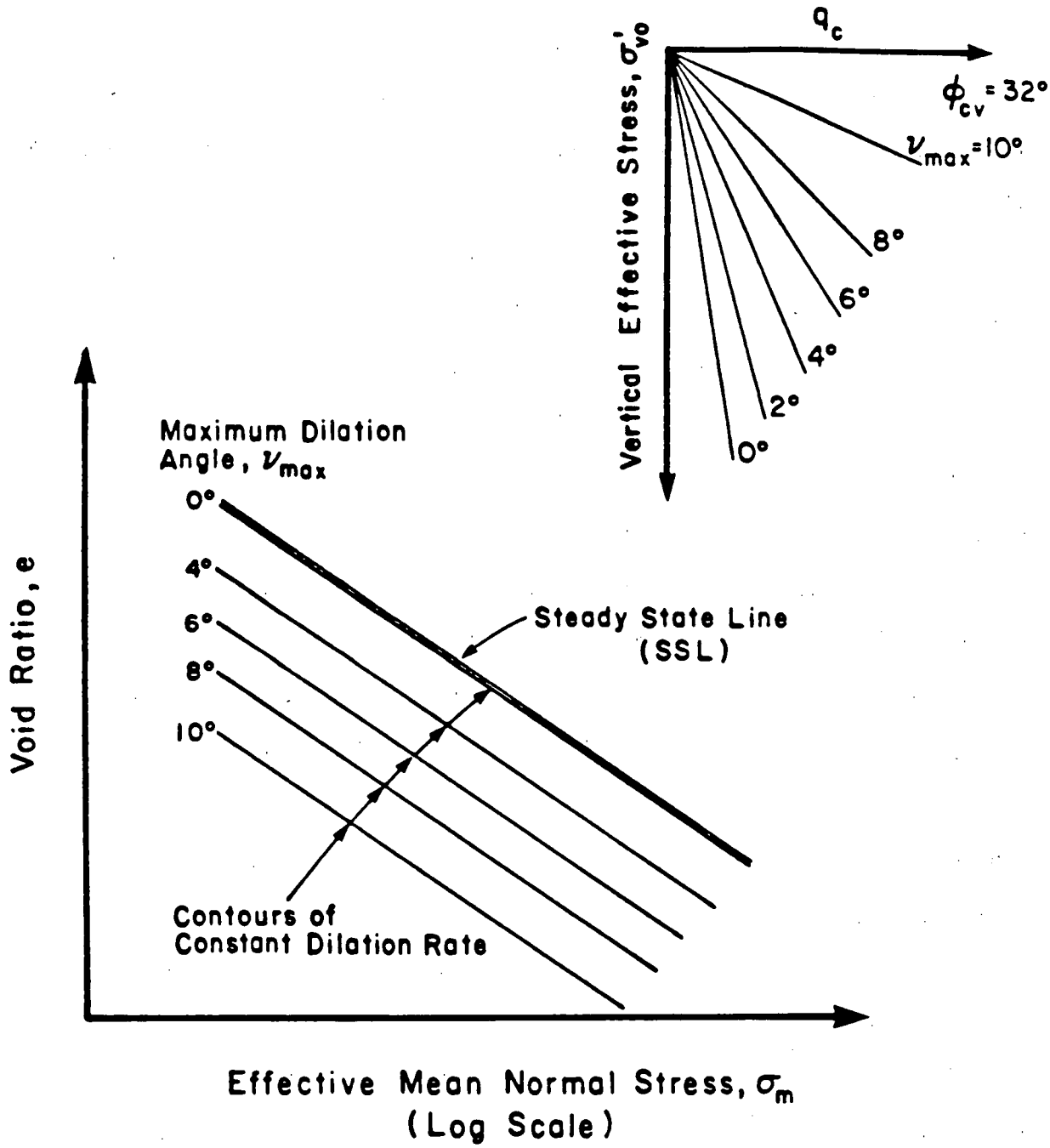

Figure 5.9 Schematic Outline to Show Use of Maximum Dilation Angle to Represent State of Soil Relative to Steady State (After Robertson, 1986)

is unlikely and deformation developing during cyclic loading becomes critical (i.e., cyclic mobility).

The concept of assessing deformation due to cyclic loading has been incorporated into the latest "liquefaction" curves developed by Seed et al (1984).

The recent addition of continuous pore pressure measurements has improved the interpretation and understanding of CPT data for liquefaction assessment. Pore pressure parameters (B_q) provide an indication of both the volume change characteristics and relative permeabiilty. The pore pressure parameter is useful in the fine grained soils such as silty sands and silts where the relative permeability is low enough to enable significant pore pressure response to be measured. From the standpoint of liquefaction resistance, volume change characteristics are very important.

Nobody has yet completely quantified the measured pore pressure response during cone penetration to liquefaction resistance. Recent work by Campanella et al, (1983) has shown that the differential pore pressure ratio can provide an excellent indicator of changes in liquefaction resistance in silts after compaction. However, the location of the pore pressure element is extremely important. It has been demonstrated that the location of the porous element immediately behind the cone tip encourages the measurement of low or negative dynamic pore pressures in fine sands and silts which appear to reflect the volume change character of the soil under shear which is essential in assessing susceptibility to liquefaction.

A new approach to liquefaction analysis using CPT data has been proposed by Olsen (1984). This approach also uses a SPT-CPT correlation similar to that proposed by Seed et al (1983) and Robertson and Campanella

(1985), but includes the friction sleeve stress, f_s, as a measure of soil sensitivity. This approach appears to be highly sensitive to the accuracy of the CPT friction measurement, which is known to be highly variable for cones of different designs. Olsen's approach is essentially very similar to the approach shown in Figs. 5.6, 5.7 and 5.8 in that low bearing soils (silts) with high friction stress (i.e. high friction ratio) have a higher resistance to liquefaction than a soil with the same friction but somewhat higher bearing (i.e., sand with smaller friction ratio).

5.6. Other Applications

5.6.1. General

The CPT is often an ideal tool for evaluating many aspects of a soil investigation. However, for optimum use of CPT data for various applications, it is always important to remember the factors that influence the interpretation of the data. The significant factors that influence CPT data in sands are, in-situ stress (σ'_{ho}), compressibility, density, and cementation.

A common problem in applying CPT data in sands is the investigation of sand density. As discussed at length in section 4.4.1, relative density is a poor parameter to represent the behaviour characteristics of a sand. It is also a very difficult parameter to measure in-situ since no unique relationship exists between cone resistance and relative density for all sands. The relationships are influenced significantly by soil compressibility and in-situ horizontal stress. The final application for many problems in sand relate to the shear strength. Thus, it is often more logical to investigate the shear strength or friction angle, ϕ, of a sand,

rather than relative density. The friction angle correlations are much less influenced by soil compressibility and in- situ stress.

In many cases the interpretation of CPT data to estimate intermediate parameters, such as, density or friction angle, is unnecessary if the cone data is affected in the same manner as the soil characteristic being investigated. A good example of this approach is the assessment of liquefaction resistance in sands using cone penetration resistance. The liquefaction resistance and cone resistance both increase with increasing soil density, K_o, aging and prior seismic history. Often the CPT data can be correlated directly to the soil characteristic required.

5.6.2. Compaction Control

CPT data has been found to be extremely useful for evaluation of deep compaction techniques such as, vibroflotation, dynamic compaction, vibratory rollers and vibrocompaction (stone columns). However, as mentioned above, cone resistance is influenced by soil density and in-situ stresses. Most of the deep compaction techniques induce significant changes in the horizontal stresses. However, the ultimate aim of most compaction techniques are usually to improve the soil strength or resistance to some loading condition or to improve the soil compressibility characteristics. Thus, after suitable calibration the CPT data can be used directly to monitor changes in these behaviour characteristics. Sometimes this may involve the use of the term 'apparent relative density', since the real relative density is not known or required but the apparent change in relative density is of more importance.

Recent studies have also shown the importance of time effects after deep compaction techniques. Cone resistance values have been observed to increase several weeks after compaction of clean sands (Mitchell, 1986, Schmertmann et al, 1986). This behaviour appears to be more pronounced after deep compaction by blasting dynamic compaction and vibro-densification and appears to be related to the structure and cementation of the sand.

5.6.3. Other Applications

Other applications of CPT data include:

i) checking the adequacy and uniformity of placed fill

ii) locating bedrock

iii) checking the amount of undesirable material for excavation

iv) locating cavities in soft rocks, e.g. chalk

v) locating permafrost

vi) pipeline investigations.

5.7. Summary - Design

5.7.1. **General**

Fig. 5.10 summarizes the basic concepts followed when using CPT data for geotechnical design.

5.7.2. **Shallow Footings (Section 5.2)**

- Shallow Foundations on Sand

  Safe Bearing Capacity:

  1. Use standard bearing capacity formula and bearing capacity factors (Terzaghi and Peck, 1967).

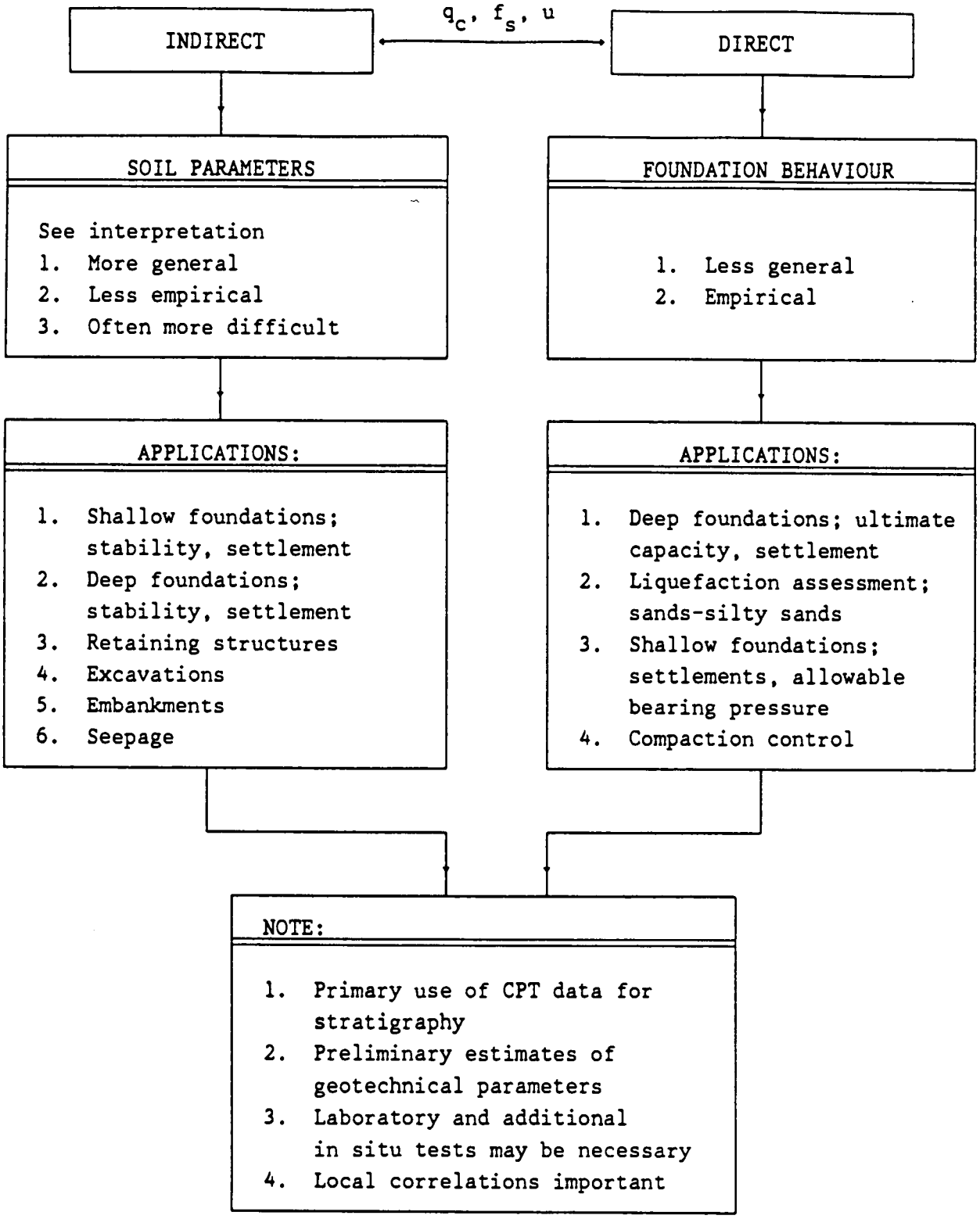

Figure 5.10: Geotechnical Design from CPT Data

Settlements:

1. Convert q_c to equivalent SPT N value (Fig. 4.21 with Fig. 4.2).
2. Use Fig. 5.1 (Burland et al, 1977) for approximate estimate (or see Burland and Burbidge, 1984, 1985)

or

3. Directly from CPT using (Meyerhof, 1974)

$$S = \frac{P_n \cdot B}{2 \cdot \bar{q}_c}$$

where S = settlement

P_n = net applied loading

B = footing width

$\bar{q}_c$ = average value of q_c over a depth equal to B

or

4. Detail calculation using Schmertmann (1970) method:

$$S = C_1 \cdot C_2 \cdot \Delta_p \cdot \Sigma \frac{I_z \cdot \Delta z}{C_3 \cdot \alpha \cdot q_c}$$

where C_1 = depth to base of footing correction

$$= 1 - 0.5 \frac{\sigma_1'}{\Delta_p}$$ where: σ' = at footing depth

C_2 = long term creep correction

$= 1 + 0.2 \log (t \cdot 10)$ where t = time in years

C_s = shape correction

= 1.0 circular footing

= 1.75 strip footing

= 1.25 square footing

Δ_p = net footing pressure

I_z = strain influence factor

Δz = soil layer thickness

q_c = cone bearing

α = empirical factor

= 2.5 to 3.5 (recent N.C. silica sand, age <100 yrs)

= 3.5 to 6.0 (N.C. aged silica sand, age >3000 yrs)

= 6.0 to 10.0 (O.C. silica sands)

- Based on load increment between 1 t/ft² and 3 t/ft².

- Shallow Footings on Clay

Safe Bearing Capacity

1. Use standard bearing capacity formula (Skempton 1951) and s_u calculated from CPT data (Section 4.5.1).

Settlements:

1. Use standard settlement calculation (i.e., Skempton and Bjerrum, 1957) and E_u and m_v estimated from q_c (Section 4.5.4).

5.7.3. Deep Foundations (Section 5.3)

Estimate axial pile capacity using empirical direct CPT methods:

1. European Method (deRuiter and Beringen, 1979)
2. Schmertmann (1978)
3. LCPC (Bustamante and Gianesalli, 1982).

Generally, it is recommended to use all three methods and select the lowest capacity. Generally, a factor of safety of 2.25 is applied for electronic CPT data.

6. REFERENCES

Acar, Y., 1981, "Piezocone Penetrating Testing in Soft Cohesive Soils", Louisiana State University, Dept. of Civil Eng., Fugro Postdoctoral Fellowship, Activity Report No. 4.

Al-Awkati, Z.A., 1975, "On Problems of Soil Bearing Capacity at Depth", Ph.D. Thesis, Duke University, Department of Civil Engineering.

ASTM Designation: D3441, 1986, American Society for Testing and Materials, Standard Method for Deep Quasi-Static, Cone and Friction-Cone Penetration Tests of Soil.

ASTM, 1973, "Evaluation of Relative Density and its Role in Geotechnical Projects Involving Cohesionless Soils", STP. 523, 510 p.

Baldi, G., Bellotti, R., Ghionna, V., Jamiolkowski, M. and Pasqualini, E., 1981, "Cone Resistance of a Dry Medium Sand", 10th International Conference on Soil Mechanics and Foundation Engineering, Stockholm, Vol. 2, pp. 427-432.

Baldi, G., Bellotti, R., Ghionna, V., Jamiolkowski, M. and Pasqualini, E., 1982, "Design Parameters for Sands from CPT", Proceedings of the Second European Symposium on Penetration Testing, ESOPT II, Amsterdam, Vol. 2, pp. 425-438, May 1982.

Baldi, G., Bellotti, R., Ghionna, V., Jamiolkowski, M. and Pasqualini, E., 1985, "Penetration Resistance and Liquefaction of Sands", Proceedings XI Int. Conf. Soil Mech. and Foundation Eng., San Francisco, Vol. 4, p. 1891.

Baldi, G., Bellotti, R., Ghionna, V., Jamiolkowski, M. and Pasqualini, E., 1986, "Interpretation of CPT's and CPTU's, 2nd Part: Drained Penetration of Sands", 4th Int. Geotechnical Seminar, Nenying Technological Institute, Singapore, Field Inst. & In Situ Measurements, pp. 143-162.

Baligh, M.M., 1975, "Theory of Deep Site Static Cone Penetration Resistance", Report No. R.75-76 Massachusetts Institute of Technology, Cambridge, Mass., 02139.

Baligh, M.M., 1976, "Cavity Expansion in Sand with Curved Envelopes", Journal of the Geotechnical Engineering Division, ASCE, Vol. 102, No. GT11, Nov. 1976, pp. 1131-1146.

Baligh, M.M., Azzouz, A.S., Wissa, A.Z.E., Martin, R.T. and Morrison, M.J., 1981, "The Piezocone Penetrometer", ASCE, Geotechnical Division, Symposium on Cone Penetration Testing and Experience, St. Louis, pp. 247-263.

Baligh, M.M. and Levadoux, J.N., 1980, "Pore Pressure Dissipation After Cone Penetration", Massachusetts Institute of Technology, Department

of Civil Engineering, Construction Facilities Division, Cambridge, Massachusetts 02139.

Baligh, M.M., Vivatrat, V., and Ladd, C.C., 1978, "Exploration and Evaluation of Engineering Properties for Foundation Design of Offshore Structures", Massachussetts Institute of Technology, Department of Civil Engineering, Research Report No. R78-40, December, 1978.

Baligh, M.M., Vivatrat, V., and Ladd, C.C., 1980, "Cone Penetration in Soil Profiling", ASCE, Journal of Geotechnical Engineering Division, Vol. 106, GT4, April, pp. 447-461.

Battaglio, M., Jamiolkowski, M., Lancellotta, R., Maniscalco, R., 1981, "Piezometer Probe Test in Cohesive Deposits", ASCE, Geotechnical Division, Symposium on Cone Penetration Testing and Experience, pp. 264-302.

Been, K., Crooks, J.H.A., Becker, D.E. and Jefferies, M.G., 1985, "State Parameter Interpretation of the Cone Penetration Test in Sands", Geotechnique, I.C.E., Vol. XXXV.

Been, K. and Jefferies, M.G., 1985, "A State Parameter for Sands", Geotechnique, Vol. 35, No. 2, June, pp. 99-112.

Beringen, F.L., Windle, D. and Hooydonk, W.R. van, 1979, "Results of Loading Tests on Driven Piles in Sands", Proceedings of the Conference on Recent Developments in Design and Construction of Piles, ICE London.

Bjerrum, L., 1972, "Embankment on Soft Grounds", ASCE Proceedings of the Specialty Conference on Performance of Earth and Earth-Supported Structures", Vol. 2, pp. 1-54, Lafayette.

Burland, J.B., 1973, "Shaft Friction of Piles in Clay - A Simple Fundamental Approach", Ground Engineering, 6, No. 3, pp. 30-42.

Burland, J.B., Broms, B.B. and De Mello, V.F.B., 1977, "Behaviour of Foundations and Structures", Proceedings of the 9th International Conference on Soil Mechanics and Foundation Engineering, Volume 2, Tokyo, Japan.

Burland, J.B. and Burbidge, M.C., 1984, "Settlement of Foundations on Sand and Gravel", Inst. of Civil Engineers, London, Invited Lecture, Centenary Celebrations, pp. 5-66.

Burland, J.B. and Burbidge, M.C., 1985, "Settlement of Foundations on Sand and Gravel", Proceedings of the Institution of Civil Engineers, Part 1, 78, December, pp. 1325-1381.

Bustamante, M. and Gianeselli, L., 1982, "Pile Bearing Capacity Prediction by Means of Static Penetrometer CPT", Proceedings of the Second European Symposium on Penetration Testing, Amsterdam, May, pp. 493-500.

Byrne, P.M. and Eldridge, T.L., 1982, "A Three Parameter Dilatant Elastic Stress-strain Model for Sand", Civil Engineering Department Soil Mechanics Series No. 57, University of British Columbia, May 1982.

Campanella, R.G. and Robertson, P.K., 1981, "Applied Cone Research", Symposium on Cone Penetration Testing and Experience, Geotechnical Engineering Division, ASCE, Oct. 1981, pp. 343-362.

Campanella, R.G., Robertson, P.K. and Gillespie, D., 1981, "In-Situ Testing in Saturated Silt, (Drained or Undrained?)" Proceedings, 34th. Canadian Geotechnical Conference, Fredericton, Canada.

Campanella, R.G. and Robertson, P.K., 1982, "State of the Art in In-situ Testing of Soils: Developments since 1978", Engineering Foundation Conference on Updating Subsurface Sampling of Soils and Rocks and Their In-situ Testing, Santa Barbara, California, January, pp. 245-267.

Campanella, R.G., Gillespie, D., and Robertson, P.K., 1982, "Pore Pressures during Cone Penetration Testing", Proc. of 2nd European Symposium on Penetration Testing, ESOPT II, pp. 507-512, A.A. Balkema.

Campanella, R.G., Robertson, P.K. and Gillespie, D., 1983, "Cone Penetration Testing in Deltaic Soils", Canadian Geotechnical Journal, Vol. 20, No. 1, February, pp. 23-35.

Campanella, R.G. and Robertson, P.K., 1984, "A Seismic Cone Penetrometer to Measure Engineering Properties of Soil", Society of Exporation Geophysics, Annual Meeting, Atlanta, Dec.

Campanella, R.G., Robertson, P.K., Gillespie, D.G. and Greig, J., 1985, "Recent Developments in In-Situ Testing of Soils", Proceedings of XI ICSMFG, San Francisco, Vol. 2, pp. 849-854.

Campanella, R.G. and Robertson, P.K., 1988, "Current Status of the Piezocone Test", Invited Lecture, First Internatinal Conf. on Penetration Testing, ISOPT-1, Disney World, March, A.A. Balkema, pp. 93-116.

Castro, G., 1975, "Liquefaction of Cyclic Mobility of Saturated Sands", Journal of the Geotechnical Eng. Div., ASCE , Vol. 101, No. GT6, pp. 551-569.

Chapman, G.A. and Donald, I.B., 1981, "Interpretation of Static Penetration Tests in Sand", 10th International Conference on Soil Mechanics and Foundation Eng., Stockholm, Vol. 2, pp. 455-458.

Cone Penetration Testing and Experience, 1981, Edited by G.M. Norris and R.D. Holtz, Proceedings of a Symposium sponsored by the Geotechnical Division of ASCE, St. Louis, Missouri, Oct. 1981.

Dahlberg, R., 1974, "Penetration, Pressuremeter and Screw Plate Tests in a Preloaded Natural Sand Deposit", Proceedings of the European Symposium on Penetration Testing, ESOPT I, Stockholm, Vol. 2.2.

Davidson, J.L. and Bloomquist, D.G., 1986, "A Modern Cone Penetration Testing Vehicle", Proceedings of In-Situ 86, ASCE Specialty Conference, Blacksburg, Virginia, pp. 502-513.

Davisson, M.T., 1973, "High Capacity Piles", Lecture Series, Innovations in Foundation Construction, ASCE, Illinois Section, Chicago, 52 pp.

de Beer, E.E., 1963, "The Scale Effect in the Transposition of the Results of Deep-Sounding Tests on the Ultimate Bearing Capacity of Piles and Caisson Foundations", Geotechnique, 13, pp. 39-75.

de Ruiter, J., 1971, "Elastic Penetrometer for Site Investigations", Journal of Soil Mechanics and Founation Engineering Division, ASCE, Vol. 97, SM-2, Feb., pp. 457-472.

de Ruiter, J., 1982, "The Static Cone Penetration Test State-of-the-Art Report", Proceedings of the Second European Symposium on Penetration Testing, ESOPT II, Amsterdam, May 1982, Vol. 2, pp. 389-405.

de Ruiter, J. and Beringen, F.L., 1979, "Pile Foundations for Large North Sea Structures", Marine Geotechnology, Vol. 3, No. 3, pp. 267-314.

Douglas, B.J., 1982, "SPT Blowcount Variability Correlated to the CPT", Proceedings of the 2nd European Symposium on Penetration Testing, ESOPT II, Amsterdam, Vol. 1, pp. 41.

Douglas, B.J., and Olsen, R.S., 1981, "Soil Classification Using Electric Cone Penetrometer", Symposium on Cone Penetration Testing and Experience, Geotechnical Engineering Division, ASCE, Oct. 1981, St. Louis, pp. 209-227.

Douglas, B.J., Olsen, R.S. and Martin, G.R., 1981, "Evaluation of the Cone Penetrometer Test for SPT Liquefaction Assessment", Geotechnical Engineering Div., ASCE, National Convention, St. Louis, Session No. 24.

Douglas, B.J., Strutynsky, A.I., Mahar, L.J. and Weaver, J., 1985, "Soil Strength Determinations From the Cone Penetration Test", Proceedings of Civil Engineering in the Arctic Offshore, San Francisco.

Durgunoglu, H.T. and Mitchell, J.K., 1975, "Static Penetration Resistance of Soils: I-ANALYSIS", Proceedings, ASCE Specialty Conference on In-Situ Measurement of Soil Parameters, Raleigh, Vol. I.

Fellenius, B.H., 1989, "Unified Design of Piles and Pile Groups", Transportation Research Board, Washington, TRB Reord 1169, pp. 75-82.

Gillespie, D.G., 1981, "The Piezometer Cone Penetration Test", M.A.Sc. Thesis, Department of Civil Engineering, University of British Columbia, December 1981.

Gillespie, D. and Campanella, R.G., 1981, "Consolidation Characteristics from Pore Pressure Dissipation after Piezometer Cone Penetration", Soil Mechanics Series No. 47, Department of Civil Engineering, The University of British Columbia, 17 pgs.

Goel, M.C., 1982, "Correlation of Static Cone Resistance with Bearing Capacity", Proceedings of the Second European Symposium on Penetration Testing, Amsterdam, May, Vol. 2.

Gupta, R.C. and Davidson, J.L., 1986, "Piezoprobe Determined Coefficient of Consolidation," Soils and Foundations, Vol. 26, No. 3.

Hardin, B.O., Drnevich, V.P., 1972, "Shear Modulus and Damping in Soils: Design Equations and Curves", Proceedings of ASCE, Journal of the Soil Mechanics and Foundation Division, Vol. 98, SM7, pp. 667-692.

Heijnen, W.J., 1974, "Penetration Testing in the Netherlands", Proceedings of the First European Symposium on Penetration Testing, Stockholm, ESOPT I, Vol. I, pp. 79-83.

Holden, J.C., 1971, "Laboratory Research on Static Cone Penetrometers", University of Florida, Gainsville, Department of Civil Engineering, Internal Report, CE-SM-71-1.

Hogentogler and Co., Inc., "Operator's Manual for CPT and CPTU Testing", P.O. Box 385, Gaithersburg, MD 20877-0385, Phone: (301) 948-3271, FAX: (301) 869-4148.

Hughes, J.M.O. and Robertson, P.K., 1984, "Full-displacement Pressuremeter Testing in Sand", Submitted to Geotechnique, April 1984.

Huntsman, S.R., Mitchell, J.K., Klejbuk, L.W. and Shinde, S.B., 1986, "Lateral Stress Measurement During Cone Penetration", Proceedings of In-Situ 86, Specialty Conference, ASCE, Blacksburg, Virginia, pp. _.

Imai, T. and Tonouchi, K., 1982, "Correlation of N Value with S-wave Velocity and Shear Modulus", Proceedings of the Second Symposium on Penetration Testing, ESOPT II, Amsterdam, Vol. 1, pp. 67-72.

In-situ Measurement of Soil Properties, 1975, Proceedings of the Specialty Conference on In-Situ Measurement of Soil Parameters of the Geotechnical Division, ASCE., Raleigh, North Carolina, June 1975.

ISSMFE, 1977, International Society for Soil Mechanics and Foundation Engineering. Report of the Subcommittee on Standardization of Penetration Testing in Europe, Proceedings 9th International Conference on Soil Mechanics and Foundation Engineering, Tokyo, Vol. 3, Appendix 5, pp. 95-152.

Iwasaki, T., Tatsuoka, F., Tokida, K. and Yasuda, S., 1978, "A Practical Method for Assessing Soil Liquefaction Potential Based on Case Studies at Various Studies in Japan", 2nd International Conference on Microzonation for Safer Construction Research and Application.

Iwasaki, T., Tokida, K. and Tatsuoka, F., 1981, "Soil Liquefaction Potential Evaluation with Use of the Simplified Procedure", Proceedings of the International Conference on Recent Advances in Geotechnical Earthquake Engineering and Soil Dynamics, St. Louis, April.

Jamiolkowski, M., Lancellotta, R., Tordella, L. and Battaglio, M., 1982, "Undrained Strength from CPT", Proceedings of the European Symposium on Penetration Testing, ESOPT II, Amsterdam, May 1982, Vol. 2, pp. 599-606.

Jamiolkowski, M., Lancellotta, R. and Wolski, W., 1983, "Recompression and Speeding Up Consolidation", S.O.A. and General Report, VIII European Conf. SMFE, Helsinki, May.

Jamiolkowski, M., Ghionna, V.N., Lancellotta, R. and Pasqualini, 1988, "New Correlations of Penetration Test for Design Practice", Invited Lecture, ISOPT-1, Disney World, March, Balkema Publ., pp. 263-196.

Janbu, N., 1963, "Soil Compressibility as determined by Oedometer and Triaxial Tests", Proceedings, 4th European Conference on Soil Mechanics and Foundation Engineering.

Janbu, N. and Senneset, K., 1974, "Effective Stress Interpretation of In Situ Static Penetration Tests", Proceedings of the European Symposium on Penetration Testing, ESOPT I, Stockholm, Sweden, Vol. 2.2, pp. 181-193.

Jefferies, M.G. and Funegard, E., 1983, "Cone Penetration Testing in the Beaufort Sea", ASCE Specialty Conference, Geotechnical Practice in Offshore Engineering, Austin, Texas, pp. 220-243.

Jones, G.A. and Rust, E.A., 1982, "Piezometer Penetration Testing CUPT", Proceedings of the 2nd European Symposium on Penetration Testing, ESOPT II, Amsterdam, Vol. 2, pp. 607-613.

Jones, G.A., Van Zyl, D. and Rust, E., 1981, "Mine Tailings Characterization by Piezometer Cone", Symposium on Cone Penetration Testing and Experience, Geotechnical Engineering Division, ASCE, Oct. 1981, pp. 303-324

Joustra, K. and de Gijt, J.G., 1982, "Results and Interpretation of Cone Penetration Tests in Soils of Different Mineralogic Composition", Proceeding of the European Symposium on Penetration Testing, ESOPT II, Amsterdam, Vol. 2, pp. 615-626.

Kjekstad, O., Lunne, T. and Clausen, C.J.F., 1978, "Comparison Between In-situ Cone Resistance and Laboratory Strength for Overconsolidated North Sea Clays", Marine Geotechnology, Vol. 3, No. 4.

Kovacs, W.D. and Salomone, L.A., 1982, "SPT Hammer Energy Measurements", Journal of the Geotechnical Engineering Division, ASCE, April, Vol. 108, No. GT4, pp. 599-620.

Kovacs, W.D., Salomone, L.A. and Yokel, F.Y., 1981, "Energy Measurements in the Standard Penetration Test", U.S. National Bureau of Standards, Building Science Series 135.

Kroezen, M., 1981, "Measurement of In-situ Density in Sandy/Silty Soil", Canadian Geotechnical Society Newsletter, Sept. Vol. 18, No. 4.

Ladanyi, B., 1967, "Deep Punching of Sensitive Clays", Proceedings of 3rd Pan American Conference on Soil Mechanics and Foundation Engineering, Caracas.

Ladanyi, B., 1972, "In-situ Determination of Undrained Stress-Strain Behaviour of Sensitive Clays with the Pressuremeter", Canadian Geotechnical Journal, Vol. 9, No. 3.

Ladd, C.C. and Foott, R., 1974, "New Design Procedure for Stability of Soft Clays", Journal of the Geotechnical Engineering Division, ASCE, Vol. 100, No. GT7, pp. 763-786.

Ladd, C.C., Foott, R., Ishihara, K., Schlosser, F., and Poulos, H.G., 1977, "Stress-Deformation and Strength Characteristics", Proceedings, Ninth International Conference on Soil Mechanics and Foundation Engineering, Tokyo, Japan, Vol. 11, pp. 421-494.

Ledoux, J.L., Menard, J. and Soulard, P., 1982, "The Penetro-gammadensimeter", Proceedings of the Second European Symposium on Penetration Testing, Amsterdam, May, Vol. 2.

Levadoux, J.-N. and Baligh, M.M., 1986, "Consolidation After Undrained Piezocone Penetration. I: Prediction", Journal of Geotechnical Division, ASCE, Vol. 112, No. 7, pp. 707-726.

Lunne, T. and Kleven, A., 1981, "Role of CPT in North Sea Foundation Engineering", Symposium on Cone Penetration Testing and Experience, Geotechnical Engineering Division, ASCE, Oct. 1981, pp. 49-75.

Lunne, T., Christoffersen, H.P., and Tjelta, T.I., 1985, "Engineering Use of Piezocone Data in North Sea Clays", Proceedings XI ICSMFE, San Francisco.

Lunne, T., Eidsmoen, T., Gillespie, D. and Howland, J.D., 1986, "Laboratory and Field Evaluation of Cone Penetrometers", Proceedings of InSitu 86, Specialty Conference, ASCE, Blacksburg, Virginia.

Marchetti, S., 1985, "On the Field Determination of K_o in Sand", Panel Discussion to Session 2A, In-Situ Testing Techniques, 11th Int. Conference on SMFE, San Francisco.

Marr, L.S., 1981, "Offshore Application of the Cone Penetrometer", ASCE, Symposium on Cone Penetration Testing and Experience, Oct., pp. 456-476.

Massarsch, K.R., and Broms, B.B., 1981, "Pile Driving in Clay Slopes", Proceeding ICSMFE, Stockholm.

Meyerhof, G.G., 1961, "The Ultimate Bearing Capacity of Wedge Shaped Foundations", Proceedings of 5th International Conference on Soil Mechanics and Foundation Engineering, Paris, Vol.2.

Meyerhof, G.G., 1974, "State of the Art of Penetration Testing in Countries Outside Europe", General Report, Proceedings of the European Symposium on Penetration Testing, Stockholm, Volume 2.1, pp. 40-48.

Meyerhof, G.G., 1976, "Bearing Capacity and Settlement of Pile Foundations", Journal of Geotechnical Engineering Division, ASCE, Vol. 102, No. GT3, March, pp. 195-228.

Mikasa, M. and Takada, N., 1974, "Significance of Centrifugal Model Tests in Soil Mechanics", Proceedings of the 8th International Conference on Soil Mechanics and Foundation Engineering, Vol. 1, Part 2, Moscow.

Mitchell, J.K. and Gardner, W.S., 1975, "In-Situ Measurement of Volume Change Characteristics", State-of-the-Art Report, Proceedings of the Conference on In-situ Measurement of Soil Properties, Specialty Conference of the Geotechnical Division, North Carolina State University, Raleigh, Vol. II.

Mitchell, J.K., Guzikowski, F., and Villet, W.C.B., 1978, "The Measurement of Soil Properties In-situ", Report prepared for U.S. Department of Energy Contract W-7405-ENG-48, Lawrence Berkeley Laboratory, University of California, Berkeley, Ca. 94720, March 1978, 67 pgs.

Mitchell, J.K., 1986, "Practical Problems from Surprising Soil Behaviour", 12th Terzaghi Lecture, Journal of Geotechnical Div., Vol. 112, No. 3, pp. 1259-1289.

Muromachi, T., 1981, "Cone Penetration Testing in Japan", Symposium on Cone Penetration Testing and Experience, Geotechnical Engineering Division, ASCE, October, St. Louis, pp. 76-107.

Muromachi, T. and Atsuta, K., 1980, "Soil Classification with R_f Value of Dutch Cone", Sounding Symposium, Tokyo, Japanese Society of Soil Mechanics and Foundation Engineering.

Nieuwenhuis, J.K. and Smits, F.P., 1982, "The Development of a Nuclear Density Probe in a Cone Penetrometer", Proceedings of the Second European Symposium on Penetration Testing, Amsterdam, May, Vol. 2.

Olsen, R.S., 1984, "Liquefaction Analysis Using the Cone Penetration Test", Proceedings of the 8th World Conf. on Earthquake Engineering, San Francisco.

Parkin, A.K. and Arnold, M., 1977, "An Analysis of Penetration Measurements in the C.R.S. Calibration Chamber", Internal Report 52108-3 Norwegian Geotechnical Institute, Oslo.

Parkin, A., Holden, J., Aamot, K., Last, N. and Lunne, T., 1980, "Laboratory Investigations of CPT's in Sand", Norwegian Geotechnical Institute. Report 52108-9, OSLO.

Parkin, A.K. and Lunne, T., 1982, "Boundary Effects in the Laboratory Calibration of a Cone Penetrometer in Sand", Proceedings of the Second European Symposium on Penetration Testing, ESOPT II, Amsterdam, May 1982, Vol. 2, pp. 761-768.

Peck, R.B., 1979, "Liquefaction Potential: Science versus Practice", Journal of the Geotechnical Engineering Div., ASCE, Vol. 105, No. GT3, March 1979.

Poulous, S.J., 1981, "The Steady State of Deformation", Journal of the Geotechnical Engineering Division, ASCE, Vol. 107, No. GT5, pp. 553-562.

Powell, J.J.M. and Quaterman, R.S.T., 1988, "The Interpretation of CPT in Clays with Particular Reference to Rate Effects", ISOPT-1, Balkema Publ., Vol. 2, pp. 903-910.

Power, P.T., 1982, "The Use of the Electic Static Cone Penetrometer in the Determination of the Engineering Properties of Chalk", Proceedings of the Second European Symposium on Penetration Testing, ESOPT II, Amsterdam, May 1982; Vol. 2, pp. 769-774.

Proceedings of the European Symposium on Penetration Testing, 1974, ESOPT I, Stockholm, Published by National Swedish Building Research, June 1974.

Proceedings of the Second European Symposium on Penetration Testing, 1982, ESOPT II, Amsterdam, The Netherlands, May 1982, A.A. Balkema.

Proceedings 10th International Conference on Soil Mechanics and Foundation Engineering, 1981, Soil Exploration and Sampling, Session 7, Stockholm, Vol. 2, pp. 409-586; also see discussions, Session 7, Vol. 4.

Proceedings of the Conference on "Updating Subsurface Sampling of Soils and Their In-situ Testing", 1982, Engineering Foundation Conference, Santa Barbara, California, Jan. 4-8, 1982, 515 pp.

Randolph, M.F. and Wroth, C.P., 1979, "An Analytical Solution for the Consolidation Around a Driven Pile", International Journal for Numerical and Analytical Methods in Geomechanics, Vol. 3, pp. 217-229.

Randolph, M.F. and Wroth, C.P., 1983, "Recent Developments in Understanding the Axial Capacity of Piles in Clay", Ground Engineering, October.

Rigden, W.J., Thorburn, S., Marsland, A. and Quartermain, A., 1982, "A Dual Load Range Cone Penetrometer", Proceedings of the Second European Symposium on Penetration Testing, Amsterdam, May, Vol. 2.

Robertson, P.K., 1983, Ph.D. Dissertation, "In-situ Testing of Soil with Emphasis on its Application to Liquefaction Assessment", Department of Civil Engineering, University of British Columbia, Vancouver, Canada, March, 395 pgs.

Robertson, P.K. and Campanella, R.G., 1983a, "Interpretation of Cone Penetration Tests - Part I (Sand)", Canadian Geotechnical Journal, Vol. 20, No. 4., pp. 718-733.

Robertson, P.K. and Campanella, R.G., 1983b, "Interpretation of Cone Penetration Tests - Part II (Clay)", Canadian Geotechnical Journal, Vol. 20, No. 4., pp. 734-745.

Robertson, P.K., Campanella, R.G. and Wightman, A., 1983, "SPT-CPT Correlations", Journal of the Geotechnical Division, ASCE, Vol. 109, No. GT11, Nov., pp. 1449-1460.

Robertson, P.K. and Campanella, R.G., 1985, "Evaluation of Liquefaction Potential of Sands Using the CPT", Journal of Geotechnical Division, ASCE, Vol. III, No. 3, Mar., pp. 384-407.

Robertson, P.K., Campanella, R.G., Gillespie, D. and Grieg, J., 1986, "Use of Piezometer Cone Data", Proceedings of InSitu 86, ASCE Specialty Conference, Blacksburg, Virginia.

Robertson, P.K., 1986, "In-Situ Testing and Its Application to Foundation Engineering", 1985 Canadian Geot. Colloquium, Canadian Geot. Journal, Vol. 23, No. 23, No. 4, pp. 573-594.

Robertson, P.K., 1986a, "In-Situ Stress Determination in Sands Using Penetration Devices", Proceedings from Seminar on Calibration Chamber Testing, Milano, Italy, March 1986, also UBC, Soil Mechanics Series No. 99, Civil Eng. Dept., Vancouver, B.C.

Robertson, P.K. and Campanella, R.G., 1986, "Guidelines for Use, Interpretation and Application of the CPT and CPTU", UBC, Soil Mechanics Series No. 105, Civil Eng. Dept., Vancouver, B.C., V6T 1W5, Canada; also available from Hogentogler and Co., P.O. Box 385, Gaithersburg, MD 20877, 3rd Edition, 197 pp.

Robertson, P.K., Campanella, R.G., Gillespie, D. and Rice, A., 1986, "Seismic CPT to Measure In-Situ Shear Wave Velocity", Journal of Geotechnical Engineering, ASCE, Vol. 112, No. 8, pp. 791-803.

Robertson, P.K., Campanella, R.G., Brown, P.T. and Robinson, K.E., 1988, "Prediction of Wick Drain Performance Using Piezometer Cone Data", Canadian Geotechnical Journal, Vol. 25, No. 1, Feb.

Robertson, P.K., Campanella, R.G., Davies, M.P. and Sy, A., 1988, "Axial Capacity of Driven Piles in Deltaic Soils Using CPT", 1st International Symposium on Penetration Testing, ISOPT-1, Disney World, March, A.A. Balkema.

Robinsky, E.I., and Morrison, C.F., 1964, "Sand Displacement and Compaction Around Model Friction Piles", Canadian Geotechnical Journal, Vol. 1, No. 2, March 1964, pp. 81-93.

Roy, M., Tremblay, M., Tavenas, F. and La Rochelle, P., 1982, "Development of Pore Pressures in Static Penetration Tests in Sensitive Clay", Canadian Geotechnical Journal, Vol. 19, No. 2, May 1982, pp. 124-138.

Rowe, P.W., 1962, "The Stress-Dilatancy Relation for Static Equilibrium of an Assembly of Particles in Contact", Proc. Royal Society, Vol. 269, Series A, pp. 500-527.

Sanglerat, G., 1972, "The Penetrometer and Soil Exploration", Elsevier.

Schaap, L.H.J. and Zuidberg, H.M., 1982, "Mechanical and Electrical Aspects of the Electric Cone Penetration Tip", Proceedings of the Second European Symposium on Penetration Testing, ESOPT II, Amsterdam, Vol. 2, pp. 841-851, A.A. Balkema.

Schmertmann, J., 1970, "Static Cone to Compute Static Settlement Over Sand", Journal of Geotechnical Engineering Division, ASCE, Vol. 96, SM3, pp. 1011-1043.

Schmertmann, J.H., 1975, "Measurement of In-Situ Shear Strength", Proceedings of the Specialty Conference on In Situ Measurement of Soil Properties, ASCE, Vol. 2, pp. 57-138, Raleigh.

Schmertmann, J.H., 1976, "Predicting the q_c/N Ratio", Final Report D-636, Engineering and Industrial Experiment Station, Department of Civil Engineering, University of Florida, Gainesville.

Schmertmann, J.H., 1978a, "Guidelines for Cone Penetration Test, Performance and Design", Federal Highway Administration, Report FHWA-TS-78-209, Washington, July 1978, 145 pgs.

Schmertmann, J.H., 1978b, "Study of Feasibility of Using Wissa-Type Piezometer Probe to Identify Liquefaction Potential of Saturated Sands", U.S. Army Engineer Waterways Experiment Station, Report S-78-2.

Schmertmann, J.H., Hartman, J.P. and Brown, P.R., 1978c, "Improved Strain Influence Factor Diagrams", Journal of the Geotechnical Engineering Division, ASCE, Vol. 104, No. GT8, August, pp. 1131-1135.

Schmertmann, J.H., Baker, W., Gupta, R. and Kessler, K., 1986, "CPT/DMT QC of Ground Modification at a Power Plant", Proceedings, In Situ 86, ASCE Specialty Conference, Use of In Situ Tests in Geotechnical Engineering, Blacksburg, PA, June, pp. 985-1001.

Searle, I.W., 1979, "The Interpretation of Begemann Friction Jacket Cone Results to Give Soil Types and Design Parameters", Proceedings of 7th European Conference on Soil Mechanics and Foundation Engineering, Brighton, Vol. 2, pp. 265-270.

Seed, H.B., 1976, "Evaluation of Soil Liquefaction Effects on Level Ground During Earthquakes", Liquefaction Problems in Geotechnical Engineering, ASCE Preprint 2752, Philadelphia, PA.

Seed, H.B., 1979, "Soil Liquefaction and Cyclic Mobility Evaluation for Level Ground During Earthquakes", Journal of the Geotechnical Engineering Division, ASCE, Vol. 105, No. GT2, February 1979, pp. 201-255.

Seed, H.B. and Idriss, I.M., 1970, "Soil Moduli and Damping Factors for Dynamics Response Analysis", Report No. EERC 70-10, Univ. of California, Berkeley, Dec.

Seed, H.B. and Idriss, I.M., 1971, "Simplified Procedure for Evaluating Soil Liquefaction Potential", Journal of the Soil Mechanics and Foundations Division, ASCE, Vol. 97, No. SM9, September 1971.

Seed, H.B. and Idriss, I.M., 1981, "Evaluation of Liquefaction Potential of Sand Deposits Based on Observations of Performance in Previous Earthquakes", Geotechnical Engineering Division, ASCE National Convention, St. Louis, Session No. 24.

Seed, H.B., Idriss, I.M. and Arango, I., 1983, "Evaluation of Liquefaction Potential Using Field Performance Data", Journal of Geotechnical Engineering Division, ASCE, Vol. 109, No. 3, March 1983, pp. 458-482.

Seed, H.B., Tokimatsu, K., Harder, L.F. and Chung, R.M., 1985, "Influence of SPT Procedures in Soil Liquefaction Resistance Evaluations", Journal of Geotechnical Division, ASCE, Vol. III, No. 12, pp. 1425-1448.

Semple, R.W. and Johnson, J.W., 1979, "Performance of 'Stingray' in Soil Sampling and In-Situ Testing", Int. Conf. on Offshore Site Investigation, Soc. for Underwater Technology, London, Paper 13, pp. 169-181.

Senneset, K., Janbu, N. and Svanϕ, G., 1982, "Strength and Deformation Parameters from Cone Penetrations Tests", Proceedings of the European Symposium on Penetration Testing, ESOPT II, Amsterdam, May 1982, pp. 863-870.

Senneset, K. and Janbu, N., 1984, "Shear Strength Parameters Obtained from Static Cone Penetration Tests", ASTM STP 883, Symposium, San Diego.

Shibata, T., 1985, "Evaluation of Soil Liquefaction by Cone Penetration Tests", Proceedings of the ROC-JAPAN Joint Seminar on Multiple Hazards Mitigation, Taiwan, Vol. 1, pp. 505-512.

Skempton, A.W., 1951, "The Bearing Capacity of Clays", Proceedings of the British Building Research Congress, 1, pp. 180-189.

Skempton, A.W., 1957, "Discussion: The Planning and Design of the New Hong Kong Airport", Proceedings, Institution of Civil Engineers, London, 7, pp. 305-307.

Skempton, A.W. and Bjerrum, L., 1957, "A Contribution to the Settlement Analysis of Foundations on Clay", Geotechnique, Vol. 7, No. 4, December, pp. 168-178.

Smits, F.P., 1982, "Penetration Pore Pressure Measured with Piezometer Cones", Proceedings of the Second European Symposium on Penetration Testing, ESOPT II, Amsterdam, Vol. 2, pp. 877-881.

Soderberg, L.O., 1962, "Consolidation Theory Applied to Foundation Pile Time Effects", Geotechnique, Vol. 12, pp. 217-232.

Tavenas, F., Leroueil, S. and Roy, M., 1982, "The Piezocone Test in Clays: Use and Limitations", Proceedings of the Second European Symposium on Penetration Testing, ESOPT II, Amsterdam, pp. 889-894.

Terzaghi, K. and Peck, R.B., 1967, "Soil Mechanics in Engineering Practice", Second Edition, John Wiley & Sons, Inc., New York, 729 pp.

Tomlinson, M.J., 1980, "Foundation Design and Construction", 4th edition, Pitman, London.

Torstensson, B.-A., 1975, "Pore Pressure Sounding Instrument", Proceedings, ASCE Spec. Conf. on In-situ Measurement of Soil Properties", Vol. II, Raleigh, N.C., pp. 48-54.

Torstensson, B.-A., 1977, "The Pore Pressure Probe", Nordiske Geotekniske Mφte, Oslo, Paper No. 34.1-34.15.

Torstensson, B.-A., 1982, "A Combined Pore Pressure and Point Resistance Probe", Proceedings of the Second European Symposium on Penetration Testing, ESOPT II, Amsterdam, Vol. 2, pp. 903-908.

Treadwell, D.D., 1975, "The Influence of Gravity, Prestress, Compressibility, and Layering on Soil Resistance to Static Penetration", Ph.D. Dissertation, Graduate Division of the University of California, Berkeley, 210 pgs.

Tringale, P.T. and Mitchell, J.K., 1982, "An Acoustic Cone Penetrometer for Site Investigations", Proceedings of the Second European Symposium on Penetration Testing, Amsterdam, May, Vol. 2.

Tumay, M.T., Acar, Y. and Deseze, E., 1982, "Soil Exploration in Soft Clays with the Quasi-static Electric Cone Penetrometer", Proceedings of the Second European Symposium on Penetration Testing, ESOPT II, Amsterdam, Vol. 2, pp. 915-921.

USGS Open-File Report No. 81-284, 1980, "Evaluation of the Cone Penetrometer for Liquefaction Hazard Assessment", Prepared by Fugro, Inc.

Van de Graaf, H.C. and Jekel, J.W.A., 1982, "New Guidelines for the Use of the Inclinometer with the Cone Penetration Test", Proceedings of the Second European Symposium on Penetration Testing, Amsterdam, May, Vol. 2.

Veismanis, A., 1974, "Laboratory Investigation of Electrical Friction-cone Penetrometers in Sand", Proceedings of the European Symposium on Penetration Testing, ESOPT I, Stockholm, Vol. 2.2.

Vesic, A.S., 1963, "Bearing Capacity of Deep Foundations in Sand", Highway Research Report 39, Highway Research Board, National Research Council, Washington, D.C.

Vesic, A.S., 1970, "Tests on Instrumented Piles, Ogeechee River Site", Journal of the Soil Mechanics and Foundation Division, ASCE, Vol. 96, SM2, pp. 561-584.

Vesic, A.S., 1972, "Expansion of Cavities in Infinite Soil Masses", Journal of the Soil Mechanics and Foundation Division, ASCE, Vol. 98, SM3, pp. 265-290.

Vesic, A.S., and Clough, G.W., 1968, "Behaviour of Granular Materials under High Stresses", Journal of the Soil Mechanics and Foundations Division, ASCE, SM3, May 1968, pp. 661-688.

Villet, W.C.B. and Mitchell, J.K., 1981, "Cone Resistance, Relative Density and Friction Angle", Symposium on Cone Penetration Testing and Experience, Geotechnical Engineering Division, ASCE, Oct. 1981, pp. 178-208.

Wissa, A.E.Z., Martin, R.T. and Garlanger, J.E., 1975, "The Piezometer Probe", Proceedings ASCE Spec. Conf. on In-situ Measurement of Soil Properties, Raleigh, N.C., Vol. 1, pp. 536-545.

Zhou, S., 1980, "Evaluation of the Liquefaction of Sand by Static Cone Penetration Test", Proceedings of the 7th World Conference on Earthquake Engineering, Vol. 3, Istanbul, Turkey.

Zhou, S.G., 1981, "Influence of Fines on Evaluating Liquefaction of Sand by CPT", International Conference on Recent Advances in Geotechnical Earthquake Engineering and Soil Dynamics, Vol. 1, St. Louis, Mo., pp. 167-172.

Zuidberg, H.M, 1985, "Seacalf, a Submersible Cone Penetrometer Rig", Marine Geotechnology, Vol. 1, pp. 15-32.

7.1 APPENDIX A

ASTM DESIGNATION: D3441, 1986

STANDARD TEST METHOD FOR

DEEP, QUASI-STATIC, CONE AND FRICTION-CONE

PENETRATION TESTS OF SOIL

Designation: D 3441 - 86

Standard Test Method for Deep, Quasi-Static, Cone and Friction-Cone Penetration Tests of Soil[1]

This standard is issued under the fixed designation D 3441; the number immediately following the designation indicates the year of original adoption or, in the case of revision, the year of last revision. A number in parentheses indicates the year of last reapproval. A superscript epsilon (ε) indicates an editorial change since the last revision or reapproval.

1. Scope

1.1 This test method covers the determination of end bearing and side friction, the components of penetration resistance which are developed during the steady slow penetration of a pointed rod into soil. This method is sometimes referred to as the "Dutch Cone Test," or "Cone Penetration Test" and is often abbreviated as the "CPT."

1.2 This test method includes the use of both cone and friction-cone penetrometers, of both the mechanical and electric types. It does not include data interpretation. It also includes the penetrometer aspects of piezocone soundings, but does not include the details of piezometer construction, location, measurement, or data interpretation.

NOTE 1—The European Standard for the CPT uses a tip of right cylindrical shape as shown in Fig. 3, as their reference test against which other CPTs may be compared.

1.3 Mechanical penetrometers of the type described in this method operate incrementally, using a telescoping penetrometer tip, resulting in no movement of the push rods during the measurement of the resistance components. Design constraints for mechanical penetrometers preclude a complete separation of the end-bearing and side-friction components. Electric penetrometers are advanced continuously and permit separate measurement of both components. Differences in shape and method of advance between cone penetrometer tips may result in significant differences in one or both resistance components.

1.4 *This standard may involve hazardous materials, operations, and equipment. This standard does not purport to address all of the safety problems associated with its use. It is the responsibility of the user of this standard to establish appropriate safety and health practices and determine the applicability of regulatory limitations prior to use.*

2. Definitions

2.1 *cone*—the cone-shaped point of the penetrometer tip, upon which the end-bearing resistance develops.

2.2 *cone penetrometer*—an instrument in the form of a cylindrical rod with a conical point designed for penetrating soil and soft rock and for measuring the end-bearing component of penetration resistance.

2.3 *cone resistance or end-bearing resistance, q_c*—the resistance to penetration developed by the cone, equal to the vertical force applied to the cone divided by its horizontally projected area.

2.4 *cone sounding*—the entire series of penetration tests performed at one location when using a cone penetrometer.

2.5 *electric penetrometer*—a penetrometer that uses electric-force transducers built into a nontelescoping penetrometer tip for measuring, within the tip, the component(s) of penetration resistance.

2.6 *friction-cone penetrometer*—a cone penetrometer with the additional capability of measuring the local side friction component of penetration resistance.

2.7 *friction-cone sounding*—the entire series of penetration tests performed at one location when using a friction-cone penetrometer.

2.8 *friction ratio, R_f*—the ratio of friction resistance to cone resistance, f_s/q_c, expressed in percent.

2.9 *friction resistance, f_s*—the resistance to penetration developed by the friction sleeve, equal to the vertical force applied to the sleeve divided by its surface area. This resistance consists of the sum of friction and adhesion.

2.10 *friction sleeve*—a section of the penetrometer tip upon which the local side-friction resistance develops.

2.11 *inner rods*—rods that slide inside the push rods to extend the tip of a mechanical penetrometer.

2.12 *mechanical penetrometer*—a penetrometer that uses a set of inner rods to operate a telescoping penetrometer tip and to transmit the component(s) of penetration resistance to the surface for measurement.

2.13 *penetrometer tip*—the end section of the penetrometer, which comprises the active elements that sense the soil resistance, the cone, and in the case of the friction-cone penetrometer, the friction sleeve.

2.13.1 *Discussion*—The addition of a piezometer to the electric penetrometer tip permits the measurement of pore water pressure during and after stopping tip penetration. A penetrometer including a piezometer is known as a piezocone penetrometer, or just piezocone.

2.14 *piezocone sounding*—the entire series of penetration tests performed at one location when using a piezocone penetrometer.

2.15 *push rods*—the thick-walled tubes, or other suitable rods, used for advancing the penetrometer tip to the required test depth.

3. Significance and Use

3.1 This test method supplies data on the engineering properties of soil intended to help with the design and construction of earthworks and the foundations for structures.

---

[1] This test method is under the jurisdiction of ASTM Committee D-18 on Soil and Rock and is the direct responsibility of Subcommittee D18.02 on Sampling and Related Field Testing for Soil Investigations.

Current edition approved Oct. 31, 1986. Published December 1986. Originally published as D 3441 - 75 T. Last previous edition D 3441 - 79.

3.2 This test method tests the soil in place and does not obtain soil samples. The interpretation of the results from this method requires knowledge of the types of soil penetrated. Engineers usually obtain this soil information from parallel borings and soil sampling methods, but prior information or experience may preclude the need for borings.

3.3 Engineers often correlate the results of tests by this test method with laboratory or other types of field tests, or directly with performance. The accuracy of such correlations will vary with the type of soil involved. Engineers usually rely on local experience to judge this accuracy.

3.4 Most engineers with offshore experience have also found this test method suitable for offshore use.

4. Apparatus

4.1 *General:*

4.1.1 *Cone*—The cone shall have a 60° (±5°) point angle and a base diameter of 1.406 ± 0.016 in. (35.7 ± 0.4 mm), resulting in a projected area of 1.55 in.^{2} (10 cm^2). The point of the cone shall have a radius less than ⅛ in. (3 mm).

NOTE 2—Cone tips with larger end areas may be used to increase measurement sensitivity in weak soils. Experience with electrical tips with end area between 0.78 in.^{2} (5 cm^2) and 3.10 in.^{2} (20 cm^2) has shown that they produce data similar to the 1.55 in.^{2} (10 cm^2) standard provided they maintain the same tip geometry. Cone tip sizes in this range may be used for special circumstances provided the cone tip and friction sleeve (if any) area is noted.

4.1.2 *Friction Sleeve*, having the same outside diameter +0.024 to −0.000 in. (+0.5 to −0.0 mm) as the base diameter of the cone (see 4.1.1). No other part of the penetrometer tip shall project outside the sleeve diameter. The surface area of the sleeve shall be 23.2 in.^{2} (150 cm^2) ±2 %.

4.1.3 *Steel*—The cone and friction sleeve shall be made from steel of a type and hardness suitable to resist wear due to abrasion by soil. The friction sleeve shall have and maintain with use a roughness of 20 μin. (0.5 μm) AA, ±50 %.

4.1.4 *Push Rods*—Made of suitable steel, these rods must have a section adequate to sustain, without buckling, the thrust required to advance the penetrometer tip. They must have an outside diameter not greater than the diameter of the base of the cone for a length of at least 1.3 ft (0.4 m) above the base, or, in the case of the friction-cone penetrometer, at least 1.0 ft (0.3 m) above the top of the friction sleeve. Each push rod must have the same constant inside diameter. They must screw or attach together to bear against each other and form a rigid-jointed string of rods with a continuous, straight axis.

4.1.5 *Inner Rods*—Mechanical penetrometers require a separate set of steel, or other metal alloy, inner rods within the steel push rods. The inner rods must have a constant outside diameter with a roughness, excluding waviness, less than 10 μin. (0.25 μm) AA. They must have the same length as the push rods (±0.004 in. or ±0.1 mm) and a cross section adequate to transmit the cone resistance without buckling or other damage. Clearance between inner rods and push rods shall be between 0.020 and 0.040 in. (0.5 and 1.0 mm). See 6.8.1.

4.1.6 *Measurement Accuracy*—Maintain the thrust-measuring instrumentation to obtain thrust measurements within ±5 % of the correct values.

NOTE 3—Special, and preferably redundant, instrumentation may be required in the offshore environment to assure this accuracy and the proper operation of all the remote systems involved.

4.2 *Mechanical Penetrometers:*

4.2.1 The sliding mechanism necessary in a mechanical penetrometer tip must allow a downward movement of the cone in relation to the push rods of at least 1.2 in. (30.5 mm).

NOTE 4—At certain combinations of depth and tip resistance(s), the elastic compression of the inner rods may exceed the downward stroke that the thrust machine can apply to the inner rods relative to the push rods. In this case, the tip will not extend and the thrust readings will rise elastically to the end of the machine stroke and then jump abruptly when the thrust machine makes contact with the push rods.

4.2.2 Mechanical penetrometer tip design shall include protection against soil entering the sliding mechanism and affecting the resistance component(s) (see 4.2.3 and Note 5).

4.2.3 *Cone Penetrometer*—Figure 1 shows the design and action of one mechanical cone penetrometer tip. A mantle of reduced diameter is attached above the cone to minimize possible soil contamination of the sliding mechanism.

NOTE 5—An unknown amount of side friction may develop along this mantle and be included in the cone resistance.

4.2.4 *Friction-Cone Penetrometer*—Figure 2 shows the design and action of one telescoping mechanical friction-cone penetrometer tip. The lower part of the tip, including a mantle to which the cone attaches, advances first until the flange engages the friction sleeve and then both advance.

NOTE 6—The shoulder at the lower end of the friction sleeve encounters end-bearing resistance. In sands as much as two thirds of the sleeve resistance may consist of bearing on this shoulder. Ignore this effect in soft to medium clays.

4.2.5 *Measuring Equipment*—Measure the penetration resistance(s) at the surface by a suitable device such as a hydraulic or electric load cell or proving ring.

4.3 *Electric Penetrometers:*

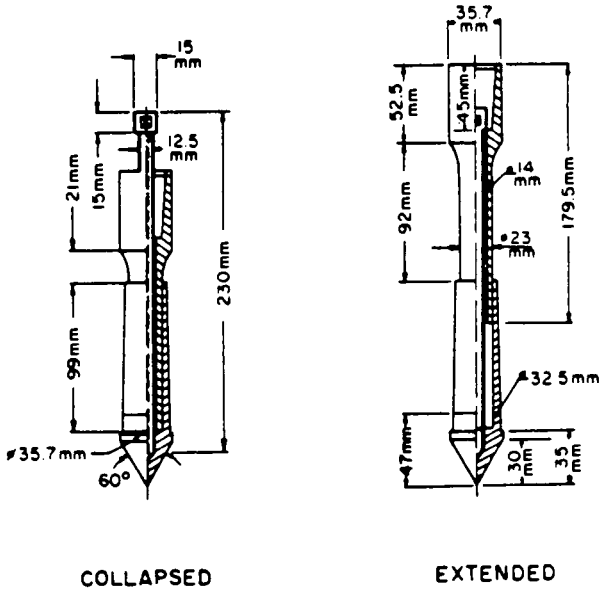

FIG. 1 Example of a Mechanical Cone Penetrometer Tip (Dutch Mantle Cone)

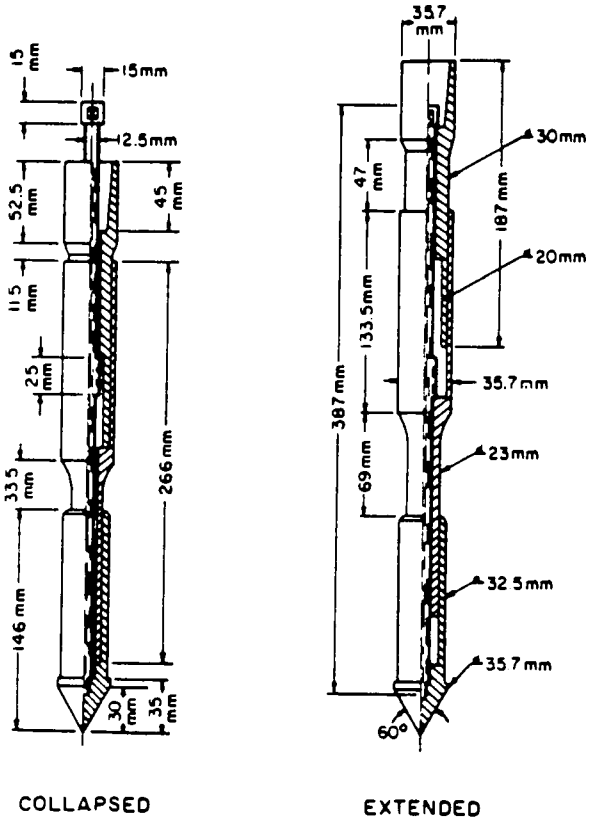

FIG. 2 Example of a Mechanical Friction-Cone Penetrometer Tip (Begemann Friction-Cone)

4.3.1 *Cone Penetrometer*—Figure 3 shows one design for an electric-cone penetrometer tip. The cone resistance is measured by means of a force transducer attached to the cone. An electric cable or other suitable system transmits the transducer signals to a data recording system. Electric-cone penetrometers shall permit continuous advance and recording over each push rod-length interval.

4.3.2 *Friction-Cone Penetrometer*—The bottom of the friction sleeve shall not be more than 0.4 in. (10 mm) above the base of the cone. The same requirements as 4.3.1 apply. Figure 4 shows one design for an electric friction-cone penetrometer tip.

4.3.3 *Other Penetrometers*—Electric penetrometers may include other transducer measurements as well as, or instead of, the friction sleeve measurement. Common ones are inclinometers to assist with the alignment control of the tip (see 6.3) and piezometers to provide additional data on soil stratigraphy and behavior.

4.4 *Thrust Machine*—This machine shall provide a continuous stroke, preferably over a distance greater than one push rod length. The machine must advance the penetrometer tip at a constant rate while the magnitude of the thrust required fluctuates (see 5.1.2).

NOTE 7—Deep penetration soundings usually require a thrust capability of at least 5 tons (45 kN). Most modern machines use hydraulic pistons with 10 to 20-ton (90 to 180-kN) thrust capability.

4.5 *Reaction Equipment*—The proper performance of the static-thrust machine requires a stable, static reaction.

NOTE 8—The type of reaction provided may affect the penetrometer resistance(s) measured, particularly in the surface or near-surface layers.

5. Procedure

5.1 *General:*

5.1.1 Set up the thrust machine for a thrust direction as near vertical as practical.

5.1.2 *Rate of Penetration*—Maintain a rate of depth penetration of 2 to 4 ft/min (10 to 20 mm/s) ±25 % when obtaining resistance data. Other rates of penetration may be used between tests.

NOTE 9—The rate of 2 ft/min (10 mm/s) provides the time the operator needs to read properly the resistance values when using the mechanical friction-cone penetrometer. The rate of 4 ft/min (20 mm/s) is suitable for the single resistance reading required when using the mechanical cone penetrometer and provides for the efficient operation of electric penetrometers. The European standard requires 4 ft/min (20 mm/s).

NOTE 10—Rates of penetration either slower or faster than the standard rate may be used for special circumstances, such as pore pressure measurements. This is permissible provided the rate actually used and the reason for the deviation is noted on the test record.

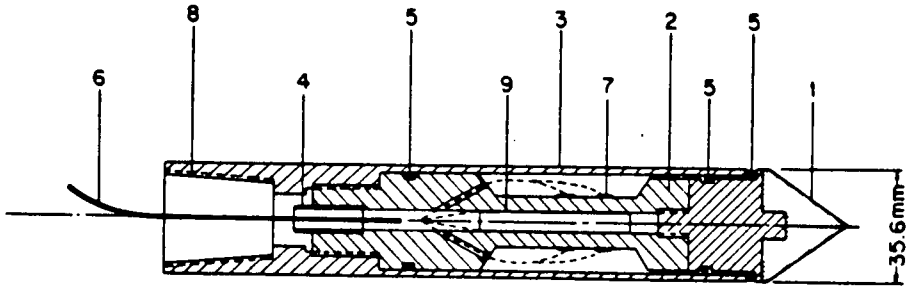

1 Conical point (10 cm²)
2 Load cell
3 Protective mantle
4 Waterproof bushing
5 O-rings
6 Cable
7 Strain gages
8 Connection with rods
9 Inclinometer

FIG. 3 Electric-Cone Penetrometer Tip

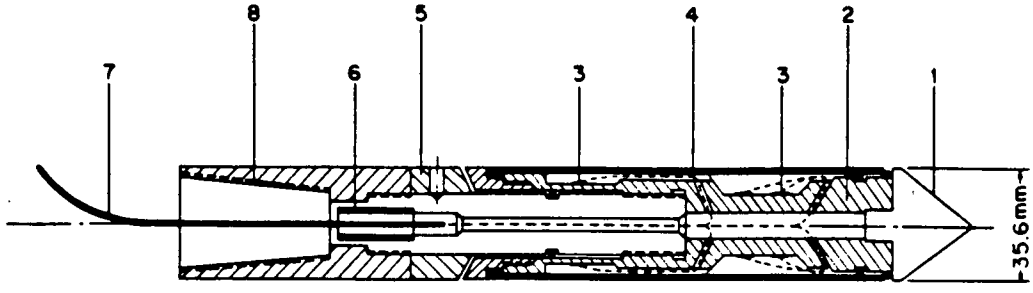

1 Conical point (10 cm²)
2 Load cell
3 Strain gages
4 Friction sleeve (150 cm²)
5 Adjustment ring
6 Waterproof bushing
7 Cable
8 Connection with rods

FIG. 4 Electric Friction-Cone Penetrometer Tip

NOTE 11—Pore pressures generated ahead of and around the penetrating cone or friction cone penetrometer tip can have an important effect on the q_c and f_s values measured. Piezocone tips with simultaneous pore pressure measurement capability have proven useful to help evaluate such effects and to provide additional data about the stratigraphy and engineering properties of the soils penetrated.

5.2 *Mechanical Penetrometers:*

5.2.1 *Cone Penetrometer*—*(1)* Advance penetrometer tip to the required test depth by applying sufficient thrust on the push rods; and *(2)* Apply sufficient thrust on the inner rods to extend the penetrometer tip (see Fig. 1). Obtain the cone resistance at a specific point (see 5.2.3) during the downward movement of the inner rods relative to the stationary push rods. Repeat step *(1)*. Apply sufficient thrust on the push rods to collapse the extended tip and advance it to a new test depth. By continually repeating this two-step cycle, obtain cone resistance data at increments of depth. This increment shall not ordinarily exceed 8 in. (203 mm).

5.2.2 *Friction-Cone Penetrometer*—Use this penetrometer as described in 5.2.1 but obtain two resistances during the step *(2)* extension of the tip (see Figs. 2 and 5). First obtain the cone resistance during the initial phase of the extension. When the lower part of the tip engages and pulls down the friction sleeve, obtain a second measurement of the total resistance of the cone plus the sleeve. Subtraction gives the sleeve resistance.

NOTE 12—Because of soil layering, the cone resistance may change during the additional downward movement of the tip required to obtain the friction measurement.

NOTE 13—The soil friction along the sleeve puts an additional overburden load on the soil above the cone and may increase cone resistance above that measured during the initial phase of the tip extension by an unknown, but probably small amount. Ignore this effect.

5.2.3 *Recording Data*—To obtain reproducible cone-resistance test data, or cone and friction-resistance test data when using a friction-cone tip, record only those thrust readings that occur at a well-defined point during the downward movement of the top of the inner rods in relation to the top of the push rods. Because of the elastic compression of inner rods (see Note 4), this point ordinarily should be at not less than 1.0 in. (25 mm) apparent relative movement of the inner rods. When using the friction-cone penetrometer, this point shall be just before the cone engages the friction sleeve.

NOTE 14—Figure 5 shows one example of how the thrust in the hydraulic load cell can vary during the extension of the friction-cone tip. Note the jump in gage pressure when the cone engages the sleeve.

5.2.3.1 Obtain the cone plus friction-resistance reading as soon as possible after the jump so as to minimize the error described in Fig. 5. Unless using continuous recording as in Fig. 5, the operator should not record a cone plus friction resistance if he suspects the cone resistance is changing abruptly or erratically.

5.3 *Electric Penetrometers:*

5.3.1 If using continuous electric cable, prethread it through the push rods.

5.3.2 Record the initial reading(s) with the penetrometer tip hanging freely in air or in water, out of direct sunlight, and after an initial, short penetration, test hole so that the tip temperature is at soil temperature.

5.3.3 Record the cone resistance, or cone resistance and friction resistance, continuously with depth or note them at intervals of depth not exceeding 8 in. (203 mm).

5.3.4 At the end of a sounding, obtain a final set of readings as in 5.3.2 and check them against the initial set. Discard the sounding, and repair or replace the tip if this check is not satisfactory for the accuracy desired for the resistance component(s).

6. Special Techniques and Precautions

6.1 *Reduction of Friction Along Push Rods*—The purpose of this friction reduction is to increase the penetrometer depth capability, and not to reduce any differences between resistance components determined by mechanical and electric tips as noted in 1.3. To accomplish the friction reduction, introduce a special rod with an enlarged diameter or special projections, called a "friction reducer," into the string of push rods or between the push rods and the tip. Another allowable method to reduce friction is to use push rods with a diameter less than that of the tip. In accordance with 4.1.4, any such projections or changes in diameter must begin no closer than 1.0 ft (0.3 m) from the base of the cone or the top

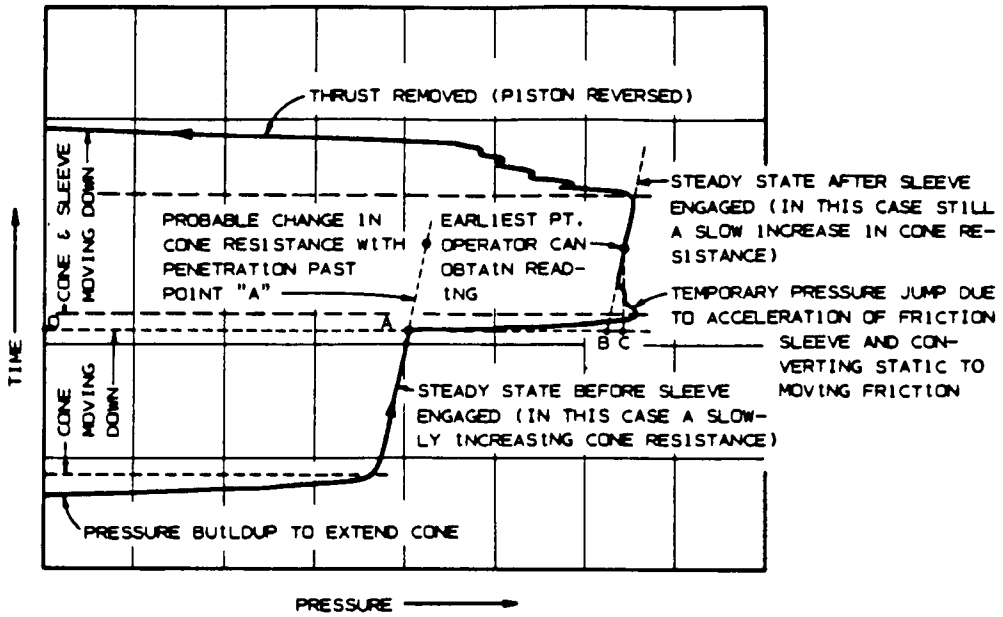

NOTE—"o-a" represents the correct cone resistance reading just before the pressure jump associated with engaging the friction sleeve during the continuing downward extension of the tip. "a-b" is the correct friction resistance if the friction sleeve could be engaged instantaneously and the cone plus friction resistance read instantaneously. However, the operator cannot read a pressure gage dial until it steadies, such as at point "c." By this forced wait, the operator has introduced a friction resistance error of "b-c." The operator must read the gage as soon as possible after the jump to minimize this error. Erratic or abrupt changes in cone resistance may make this error unacceptable.

FIG. 5 Annotated Chart Record of the Pressure Changes in the Hydraulic Load Cell Measuring Thrust on Top of the Inner Rods During an Example Extension of the Mechanical Friction-Cone Penetrometer Tip

of the friction sleeve when using cones with the standard 4.1.1 diameter. For other cones (see Note 2) use no closer than 8 diameters.

NOTE 15—Non-mechanical techniques to reduce friction, such as the use of drilling mud above the tip, are also allowable.

6.2 *Prevention of Rod Bending Above Surface*—Use a tubular rod guide, at the base of the thrust machine, of sufficient length to prevent significant bending of the push rods between the machine and the ground surface.

NOTE 16—Special situations, such as when working through water, will require a special system of casing support to restrict adequately the buckling of the push rods.

6.3 *Drift of Tip*—For penetration depths exceeding about 40 ft (12 m), the tip will probably drift away from a vertical alignment. Occasionally, serious drifting occurs, even at less depth. Reduce drifting by using push rods that are initially straight and by making sure that the initial cone penetration into soil does not involve unwanted, initial lateral thrust. Passing through or alongside an obstruction such as boulders, soil concretions, thin rock layers, or inclined dense layers may deflect the tip and induce drifting. Note any indications of encountering such obstructions and be alert for possible subsequent improper tip operation as a sign of serious drifting.

NOTE 17—Electric penetrometer tips may also incorporate an inclinometer to monitor drift and provide a warning when it becomes excessive.

6.4 *Wear of Tip*—Penetration into abrasive soils eventually wears down or scours the penetrometer tip. Discard tips, or parts thereof, whose wear changes their geometry or surface roughness so they no longer meet the requirements of 4.1. Permit minor scratches.

6.5 *Distance Between Cone and Friction Sleeve*—The friction resistance of the sleeve applies to the soil at some distance above the soil in which the cone resistance was obtained at the same time. When comparing these resistances for the soil at a specified depth, for example when computing friction ratios or when plotting these data on graphs, take proper account of the vertical distance between the base of the cone and the midheight of the friction sleeve.

6.6 *Interruptions*—The engineer may have to interrupt the normal advance of a static penetration test for purposes such as removing the penetrometer and drilling through layers or obstructions too strong to penetrate statically. If the penetrometer is designed to be driven dynamically without damage to its subsequent static performance (those illustrated herein in Figs. 1 to 4 are not so designed), the engineer may drive past such layers or obstructions. Delays of over 10 min due to personnel or equipment problems shall be considered an interruption. Continuing the static penetration test after an interruption is permitted provided this additional testing remains in conformance with this standard. Obtain further resistance component data only after the tip passes through the engineer's estimate of the disturbed zone resulting from the nature and depth of the interruption. As an alternative, readings may be continued without first making the additional tip penetration and the disturbed zone evaluated from these data. Then disregard data within the disturbed zone.

NOTE 18—Interruption of the piezocone sounding after a push allows the engineer to examine the dissipation of positive or negative excess pore water pressure.

6.7 *Below or Adjacent to Borings*—A cone or friction-cone sounding shall not be performed any closer than 25 boring diameters from an existing, unbackfilled, uncased boring hole. When performed at the bottom of a boring, the engineer should estimate the depth below the boring of the disturbed zone and disregard penetration test data in this zone. The depth may vary from one to five diameters. Where the engineer does not have sufficient experience with this variable a depth of at least three boring diameters should be used.

6.8 *Mechanical Penetrometers:*

6.8.1 *Inner Rod Friction*—Soil particles and corrosion can increase the friction between inner rods and push rods, possibly resulting in significant errors in the measurement of the resistance component(s). Clean and lubricate the inner rods.

6.8.2 *Weight of Inner Rods*—For improved accuracy at low values of cone resistance, correct the thrust data to include the accumulated weight of the inner rods from the tip to the topmost rod.

6.8.3 *Jamming*—Soil particles between sliding surfaces or bending of the tip may jam the mechanism during the many extensions and collapses of the telescoping mechanical tip. Stop the sounding as soon as uncorrectable jamming occurs.

6.9 *Electric Penetrometers:*

6.9.1 *Water Seal*—Provide adequate waterproofing for the electric transducer. Make periodic checks to assure that no water has passed the seals.

NOTE 19—Some electric tip sleeve designs are not compensated for hydrostatic end area effects and require a calibration correction. Determining the net end area of the cone under hydrostatic pressure also requires a hydrostatic calibration measurement. The tip manufacturer can usually supply these calibration correction constants. Their importance increases as the soil being tested becomes weaker.

7. Report

7.1 *Graph of Cone Resistance, q_c*—Every report of a cone or friction-cone sounding shall include a graph of the variation of cone resistance (in units of tons or kPa) with depth (in feet or metres). Successive cone-resistance test values from the mechanical cone and friction-cone penetrometers, usually determined at equal increments of depth and plotted at the depth corresponding to the depth of the measurement, may be connected with straight lines as an approximation for a continuous graph.

7.2 *Friction-Cone Penetrometer:*

7.2.1 *Graph of Friction Resistance, f_s*—In addition to the graph of cone resistance (7.1) the report may include an adjacent or superposed graph of friction resistance or friction ratio, or both, with depth. Use the same depth scale as in 7.1 (see 6.5).

7.2.2 *Graph of Friction Ratio, R_f*—If the report includes soil descriptions estimated from the friction-cone penetrometer data, include a graph of the variation of friction ratio with depth. Place this graph adjacent to the graph for cone resistance, using the same depth scale (see 6.5).

7.3 *Piezocone Penetrometer*—In addition to the 7.1 and 7.2 report requirements, a piezocone sounding shall include a parallel graph, to the same depth scale, of measured pore water pressure during the penetration versus depth. Excess pore water pressure versus time plots may also be constructed at those depths where the piezocone sounding is interrupted (see Note 1).

7.4 *General*—The operator shall record his name, the name and location of the job, date of sounding, sounding number, location coordinates, and soil and water surface elevations (if available). The report shall also include a note as to the type of penetrometer tip used, the type of thrust machine, tip and thrust calibration information, or both, any zero-drift noted, the method used to provide the reaction force, if a friction reducer was used, the method of tip advancement, the method of recording, the condition of the rods and tip after withdrawal, and any special difficulties or other observations concerning the performance of the equipment.

7.5 *Deviations from Standard*—The report shall state that the test procedures were in accordance with this Test Method D 3441. Describe completely any deviations from this test method.

8. Precision and Bias

8.1 Because of the many variables involved and the lack of a superior standard, engineers have no direct data to determine the bias of this method. Judging from its observed reproducibility in approximately uniform soil deposits, plus the q_c and f_s measurement effects of special equipment and operator care, persons familiar with this method estimate its precision as follows:

8.1.1 *Mechanical Tips*—Standard deviation of 10 % in q_c and 20 % in f_s.

8.1.2 *Electric Tips*—Standard deviation of 5 % in q_c and 10 % in f_s.

NOTE 20—These data may not match similar data from mechanical tips (see 1.3).

SOIL CLASSIFICATION USING THE CPT

P.K. Robertson

Professor of Civil Engineering
University of Alberta
Edmonton, Alberta T6G 2G&
Tel: (403) 492 - 5106

March 1989

Abstract

Several charts exist for evaluating soil type from cone penetration test (CPT) data. A new system is proposed based on normalized CPT data. The new charts are based on extensive data available from published and unpublished experience worldwide. The new charts are evaluated using data from a 300 m deep borehole with wireline CPT. Good agreement was obtained between samples and the CPT data using the new normalized charts.

Recommendations are provided concerning the location to measure pore pressures during cone penetration.

Keywords: Soil classification, cone penetration test, in-situ

INTRODUCTION

One of the primary applications of the Cone Penetration Test (CPT) is for stratigraphic profiling. Considerable experience exists concerning the identification and classification of soil types from CPT data. Several soil classification charts exist for CPT and cone penetration testing with pore pressure measurements (CPTU).

In this paper the limitations of existing CPT and CPTU classification charts are discussed and a new system proposed based on normalized measurements. A discussion is also presented regarding the recommended position to measure pore pressures during cone penetration.

SOIL CLASSIFICATION

Some of the most comprehensive recent work on soil classification using electric cone penetrometer data was presented by Douglas and Olsen (1981). One important distinction made by Douglas and Olsen (1981) was that CPT classification charts cannot be expected to provide accurate predictions of soil type based on grain size distribution but provide a guide to soil behaviour type. The CPT data provide a repeatable index of the aggregate behaviour of the in-situ soil in the immediate area of the probe.

In recent years soil classification charts have been adapted and improved based on an expanded data base (Robertson 1986, Olsen and Farr 1986). An example of such a soil classification chart for electric CPT data is shown in Figure 1. The chart in Figure 1 is based on data obtained predominantly at depths less than 30 m and is global in nature. Therefore, some overlap in zones should be expected.

Most classification charts, such as the one shown in Fig. 1, use the cone penetration resistance, q_c, and friction ratio, R_f, where;

$$R_f = \frac{f_s}{q_c} \times 100\% \qquad [1]$$

and f_s = sleeve friction.

Recent research has illustrated the importance of cone design and the effect that water pressures have on the measured penetration resistance and sleeve friction due to unequal end areas (Campanella et al., 1982; Baligh et al., 1981). Thus cones of slightly different designs, but conforming to the International Standard (ISSMFE-1977) and Reference Test Procedure (ISOPT-1988), will give slightly different values of q_c and f_s, especially in soft clays and silts.

For electric cones (Figure 2) that record pore pressures, corrections can be made to account for unequal end area effects. Baligh et al. (1981) and Campanella et al. (1982) proposed that the cone resistance, q_c could be corrected to a total cone resistance, q_t using the following expression;

$$q_t = q_c + (1-a)u \qquad [2]$$

where u = pore pressure measured between the cone tip and the friction sleeve

a = net area ratio.

It is often assumed that the net area ratio is given by

$$a = \frac{d^2}{D^2} \qquad [3]$$

where d = diameter of load cell support

D = diameter of cone.

However, this provides only an approximation of the net area ratio since additional friction forces are developed due to distortion of the water seal O-ring. Therefore, it is recommended that the net area ratio should always be determined in a small calibration vessel (Battaglio and Maniscalco, 1983; Campanella and Robertson 1988).

A similar correction can also be applied to the sleeve friction (Lunne et al 1986, Konrad 1987). Konrad (1987) suggested the following expression to determine the total stress sleeve friction, f_t;

$$f_t = f_s - (1 - \beta b)cu \qquad [4]$$

where:

$$b = \frac{A_{st}}{A_{sb}}$$

$$c = \frac{A_{sb}}{A_s}$$

$$\beta = \frac{u_s}{u}$$

A_{st} = end area of friction sleeve at top

A_{sb} = end area of friction sleeve at bottom

A_s = outside surface area of friction sleeve

u_s = pore pressure at top of friction sleeve

However, to apply this correction, pore pressure data are required at both ends of the friction sleeve. Konrad (1987) showed that this correction could be more than 30% of the measured f_s for some cones. However, the correction can be significantly reduced for cones with an equal end area

friction sleeve (i.e. b = 1.0).

The corrections in [2] and [4] are only important in soft clays and silts where high pore pressures and low cone resistance occur. The corrections are negligible in cohesionless soils where penetration is generally drained and cone resistance is generally large. The author believes that the correction to the sleeve friction is generally unnecessary provided the cone has an equal end area friction sleeve.

Recent studies have shown that even with careful procedures and corrections for pore pressure effects the measurement of sleeve friction is often less accurate and reliable than the tip resistance (Lunne et al. 1986). Cones of different designs will often produce variable friction sleeve measurements. This can be caused by small variations in mechanical and electrical design features, as well as small variations in tolerances.

To overcome problems associated with sleeve friction measurements, several classification charts have been proposed based on q_t and pore pressures (Jones and Rust, 1982; Baligh et al., 1980; Senneset and Janbu, 1984).

The chart by Senneset and Janbu (1984) uses the pore pressure parameter ratio, B_q, defines as;

$$B_q = \frac{u - u_o}{q_t - \sigma_{vo}} \qquad [5]$$

where u = pore pressure measured between the cone tip and the friction sleeve

u_o = equilibrium pore pressure

σ_{vo} = total overburden stress

The original chart by Senneset and Janbu (1984) uses q_c. However, it is

generally agreed that the chart and B_q should use the corrected total cone resistance, q_t.

Experience has shown that, although the sleeve friction measurements are not as accurate as q_t and u, generally more reliable soil classification can be made using all three pieces of data (i.e., q_t, f_s, u). A first attempt at defining a system that uses all three pieces of data was proposed by Robertson et al. (1986) and used q_t, B_q and R_f.

Normalized CPT Data

A problem that has been recognized for some time with soil classification charts that use q_t and R_f is that soils can change in their apparent classification as cone penetration resistance increases with increasing depth. This is due to the fact that q_t, f_s and u all tend to increase with increasing overburden stress. For example, in a thick deposit of normally consolidated clay the cone resistance (q_c) will increase linearly with depth resulting in an apparent change in CPT classification for large changes in depth. Existing classification charts are based predominantly on data obtained from CPT profiles extending to a depth of less than 30 m. Therefore, for CPT data obtained at significantly greater depths some error can be expected using existing CPT classification charts that are based on q_t (or q_c) and R_f.

Attempts have been made to account for the influence of overburden stress by normalizing the cone data (Olsen, 1984; Douglas et al., 1985; Olsen and Farr, 1986). These existing approaches require different normalization methods for different soil types, which produces a somewhat complex iterative interpretation procedure that requires a computer program.

Conceptually, any normalization to account for increasing stress should

also account for changes in horizontal stresses; since penetration resistance is influenced in a major way by the horizontal effective stresses (Jamiolkowski and Robertson, 1988). However, at present, this has little practical benefit without a prior detailed knowledge of the in-situ horizontal stresses. Even normalization using only vertical effective stress requires some input of soil unit weights and ground water conditions.

Wroth (1984) and Houlsby (1988) suggested that CPT data should be normalized using the following parameters;

Normalized cone resistance, $$Q_t = \frac{q_t - \sigma_{vo}}{\sigma_{vo}'} \quad [6]$$

Normalized friction ratio, $$F_R = \frac{f_s}{q_t - \sigma_{vo}} \times 100\ (\%) \quad [7]$$

Normalized pore pressure, $$B_q = \frac{u - u_o}{q_t - \sigma_{vo}} = \frac{\Delta u}{q_t - \sigma_{vo}} \quad [8]$$

Based on these normalized parameters and using the extensive CPTU data base now available in published and unpublished sources, modified soil behaviour type classification charts have been developed and are shown in Figure 3.

The two charts shown in Figure 3 represent a three-dimensional classification system that incorporates all three pieces of CPTU data. For basic CPT data where only q_c and f_s are available the lefthand chart (Fig. 3) can be used. T error in using uncorrected q_c data will generally only influence the data in the lower part of the chart where normalized cone resistance is less than about 10. This part of the chart is for soft, fine grained soils where q_c can be small and penetration pore pressures (u) can be large.

Included on the normalized soil behaviour type classification charts is a zone that represents approximately normally consolidated soil behaviour. A guide is also provided to indicate the variation of normalized CPT and CPTU data for changes in; overconsolidation ratio (OCR), age and sensitivity (S_t) for fined grained soils, where cone penetration is generally undrained, and OCR, age, cementation and friction angle (ϕ') for cohesionless soils, where cone penetration is generally drained.

Generally, soils that fall in zones 6 and 7 represent approximately drained penetration, whereas, soils in zones 1, 2, 3 and 4 represent approximately undrained penetration. Soils in zones 5, 8 and 9 may represent partially drained penetration. An advantage of pore pressure measurements during cone penetration is the ability to evaluate drainage conditions more directly.

The charts in Figure 3 are still global in nature and should be used as a guide to define soil behaviour type based on CPT and CPTU data. Factors such as changes in, stress history, in-situ stresses, sensitivity, stiffness, macrofabric and void ratio will also influence the classification.

Occasionally soils will fall within different zones on each chart, in these cases judgement is required to correctly classify the soil behaviour type. Often the rate and manner in which the excess pore pressures dissipate during a pause in the cone penetration will significantly aid in the classification. For example, a soil may have the following CPTU parameters; q_t = 0.9 MPa, f_s = 40 kPa and Δu = 72 kPa at a depth where σ_{vo} = 180 kPa and σ_{vo}' = 90 kPa. Hence, the normalized CPTU parameters are;

$$\frac{q_t - \sigma_{vo}}{\sigma_{vo}'} = 8$$

$$\frac{f_s}{q_t - \sigma_{vo}} \times 100 = 5.6\%$$

$$B_q = \frac{\Delta u}{q_t - \sigma_{vo}} = 0.1$$

Using these normalized parameters the soil would classify as a slightly overconsolidated clay (clay to silty clay) on the normalized friction ratio chart and as a silt mixture (clayey silt to silty clay) on the normalized pore pressure ratio chart. However, if the rate of pore pressure dissipation during a pause in penetration were very slow this would add confidence to the classification as a clay. If the dissipation were more rapid, say 50% dissipation in 2 to 4 minutes (2 mins < t_{50} < 4 mins), the soil is more likely to be a clayey silt.

The manner in which the dissipation occurs can also be important. In stiff, overconsolidated clay soils, the pore pressure behind the tip can be very low and sometimes negative of the equilibrium pore pressure u_o, whereas, the pore pressure on the face of the cone can be very large due to the large increase in normal stresses created by the cone penetration. When penetration is stopped in overconsolidated clays, pore pressures recorded behind the tip may initially increase before decreasing to the equilibrium pore pressure. The rise can be caused by local equilization of the high pore pressure gradient around the cone tip (Campanella et al., 1986).

CASE HISTORY

To illustrate the advantage of using normalized data a case history involving a deep borehole with wireline CPT will be briefly presented. The deep borehole was performed as part of a research program to study the land subsidence of Bologna in Italy (Belfiore et al. 1989). The borehole was 300 m

deep using a hydraulic drill rig equipped with a wire-line system for sampling and cone penetration testing. During the boring 30 undisturbed samples were taken and 27 static penetration tests were performed, using both electric CPT and CPTU. At suitable elevations dissipation tests were carried out with the CPTU in order to measure equilbrium pore pressures and the rate of dissipation of the excess pore pressures. Geophysical data were also obtrained including electrical, seismic and radioactivity logs. Full details of the test program are given by (Belfiore et al. 1989).

A summary of the soil profile and CPTU data are presented in Figure 4. Based on all the results from the boring, a total of 14 well defined compressible layers were identified and are marked by a C in Figure 4. The compressible layers consist of approximately normally consolidated clayey silt and silty clay, of medium to high plasticity. A total of 13 cohesionless drainage layers were also identified and marked by a D in Figure 4.

It can be seen from Figure 4 that the points of minimum q_t represent the compressible layers and lie approximately on a striaght line corresponding to a normalized cone resistance of about 2.8. The corrected cone resistance values (q_t) range from 3.7 MPa (37 bars) to 15 MPa (150 bars) at depths of about 65 m to 280 m. The calculated friction ratio values (R_f) vary from 3.3% to 1.3%. Hence, the predicted soil behaviour type using the classification chart in Figure 1 would change with increasing depth from a clayey silt to a sand. However, using normalized cone data and the proposed normalized charts the compressible layers (C) are more correctly classified as a clay soil behaviour type throughout the depth range investigated. A summary of the CPT and CPTU data from the deep borehole plotted on the normalized charts is shown in Figure 5.

It is interesting to note that the excess pore pressures during cone

penetration ($\Delta_u = u - u_o$) have high positive values in the clay layers, negative values in silty layers and values close to zero (i.e. equilibrium pore pressures) in coarse grained layers.

The proposed charts in Figure 3 were developed before the data from Bologna were available. Belfiore et al. (1989) found that the proposed classification chart (Fig. 3) based on normalized CPTU data showed good agreement with the samples and other field data.

The Bologna data represents a somewhat extreme example of a deep CPT sounding. Generally, most on-shore CPT's are performed to a depth of less than 30 m and existing charts using non-normalized data, such as the one shown in Figure 1, often provide reasonable good evaluations of soil behaviour type.

A disadvantage of the charts shown in Figure 3 is that an estimate is required of the soil unit weights and equilibrium pore pressures to calculate σ_{vo} and σ_{vo}'. However, charts using normalized CPT data are conceptually more correct than the previous chart in Figure 1.

It is likely that the simplified chart in Figure 1 will continue to be used because of its simplicity and because the basic field data can be applied without complex normalization. However, with the increasing use of field computers normalized charts such as that presented in Figure 3 should become more frequently used.

Pore Pressure Element Location for CPTU

The pore pressure ratio shown in Figure 3 is based on pore pressures measured immediately behind the cone tip and in front of the friction sleeve. Much has been published in recent years concerning the locations for recording cone penetration pore pressures (Roy et al. 1982, Smits, 1982, Campanella et al. 1982, Battaglio et al. 1986). Recommendations concerning

the location of the piezometer element have generally been based on considerations of either equipment and procedures or interpretation methods. Based on a review of existing experience the following comments can be made about pore pressure measurements during cone penetration.

In terms of equipment design and test procedures there has been a trend towards placing the pore pressure element behind the cone tip, usually in front of the friction sleeve. This location has the advantages of good protection from damage due to abrasion and smearing and generally easier saturation procedures. The location behind the tip is also the correct location to adjust the measured penetration resistance (q_c) to total resistance (q_t) due to unequal areas. Filter elements located on the face of the cone tip need very careful design to avoid filter element compression and load transfer as well as high resistance to abrasion and smearing.

In terms of interpretation it is generally agreed that pore pressures measured on the face of the cone tip produce the maximum values and provide excellent stratigraphic detail, provided problems with filter compression and load transfer have been removed. For a more detailed understanding of interpretation it is helpful to distinguish between drained and undrained penetration. For cone penetration in coarse grained soils, such as clean sands, any pore pressures generated due to penetration dissipate almost as rapidly and penetration is essentially drained. However, for cone penetration in fine grained soils significant excess pore pressures can be generated and penetration is essentially undrained. There is a class of soils that may exhibit a partially drained penetration at the standard penetration rate of 20 mm/sec. Partially drained penetration can occur in soils such as, fine sands and silty sands, for which quantitative interpretation is difficult. Hence, interpretation of cone penetration pore pressures is generally limited

to fine grained soils in which penetration is essentially undrained.

For undrained cone penetration interpretation is generally directed towards the evaluation of undrained shear strength (s_u) and stress history (OCR, σ_p'). To evaluate the preferred measurement parameter (q_c or u) to be used for interpretation it is necessary to distinguish between soft, uncemented fine grained soils and stiff, fine grained soils with high OCR. Figure 6 presents a summary of the main differences in measurement parameters between soft, low OCR and stiff, high OCR soils.

For cone penetration in soft, uncemented fine grained soils the measured cone penetration resistance (q_c) is generally small whereas, the pore pressures on the face or behind the tip (on the shaft) are both large. Generally, for cone penetration in soft soils, the pore pressure on the shaft just behind the tip is approximately 80 percent of the face pore pressure. However, both pore pressure locations (on the face or behind the tip) provide large pore pressures and good stratigraphic detail. The pore pressures further up the shaft away from the tip tend to be somewhat smaller and provide a less detailed response to changes in stratigraphy. Because q_c is generally small and the pore pressures are large the correction to q_t is generally significant. Hence, it is generally important to record the pore pressure on the shaft just behind the tip so that the correct pore pressure can be applied to obtain q_t using equation [2]. Because of a generally decreased accuracy in recording the small q_c values and the need to make significant corrections due to unequal area effects, the preferred measurement for use in interpretation in soft soils is the penetration pore pressure (u). Because of equipment and procedural considerations (saturation), the preferred location for the pore pressure measurement is just behind the cone tip.

For cone penetration in stiff, high OCR, fine grained soils the measured

cone penetration resistance is generally large. The pore pressure on the face of the cone is also generally large but problems with filter compression are frequently encountered and pore pressures may be unreliable (Battaglio et al., 1986). However, the pore pressure measured just behind the tip is often small and can sometimes be negative of the equilibrium pore pressure. An exception to this can occur in cemented and/or sensitive stiff clays where large pore pressures can be recorded behind the tip due to the collapse of the soil structure. Because the q_c values are generally large and the pore pressures just behind the tip are generally small, the correction to q_t is often small and negligible. Hence, the penetration resistance (q_c) is often a more reliable measurement than the penetration pore pressure and is preferred for interpretation when penetrating stiff, high OCR, fine grained soils.

During a stop in the penetration any excess pore pressures start to dissipate and the rate of dissipation can be interpreted to evaluate consolidation characteristics of the surrounding soil (Tortensson, 1977). In soft, low OCR soils the pore pressure dissipation data are generally good for pore pressure element locations both on the face and behind the tip. However, in stiff, high OCR soils the dissipation data behind the tip can suffer from local equilization with the much higher pore pressured on the face of the tip and interpretation can be difficult.

Based on the above observations it is clear that there is no single location for pore pressure measurements that meet all requirements for all soil types. Hence, the preference is to record pore pressures at two or more locations simultaneously. Cones presently exist that can record pore pressures at two or more locations but saturation procedures are often complex. To avoid increased complexities with equipment and saturation procedures it is recommended to have flexibility in cone design so that pore

pressures can be measured either on the face of the cone tip or just behind the tip. Many cone designs already exist that enable the filter location to be easily changed in the field.

For general piezocone testing it is therefore recommended to measure the pore pressure just behind the tip for the following reasons:

1. good protection from damage
2. easy saturation
3. generally good stratigraphic detail
4. generally good dissipation data
5. right location to correct q_c

However, if a stiff, high OCR, clay deposit is encountered and measured pore pressure behind the tip become very small, it is recommended to change the location (in the field) to record pore pressures on the face of the tip. For quantitative interpretation of the pore pressures measured on the face of the tip during penetration in stiff soils it is important to avoid, or be aware of, potential errors due to filter compression.

SUMMARY

A new soil behaviour type classification system has been presented using normalized cone penetration test parameters. The new charts represent a three-dimensional classification system incorporating all three pieces of data from a CPTU. The charts are global in nature and can be used to define soil behaviour type. Factors such as changes in, stress history, in-situ stresses, sensitivity, stiffness, macrofabric and void ratio will also influence the classification. A guide to the influence some of these variables have on the classification have been included on the charts.

Occasionally soil will fall within different zones on each chart, in these cases the rate and manner in which the excess pore pressures dissipate duirng a pause in the penetration can significantly aid in the classification. A case history involving wireline CPTU data from a 300 m deep borehole has been presented to illustrate the usefulness of applying normalized data for soil classification.

A discussion has also been presented regarding the recommended position to measure pore pressures during cone penetration. No single location for pore pressure measurements meet all requirements for all soils. Hence, the ideal situation is to record pore pressures at two or more locations simultaneously. However, to avoid increased complexities with equipment and saturation procedures it is recommended to have flexibility in cone design so that pore pressures can be measured either on the face of the cone tip or just behind the tip. For penetration into granular soils and soft cohesive soils it is recommended to measure the pore pressures just behind the cone tip. For penetration into stiff, high OCR clay or silt deposts it is recommended to change the location (in the field) to record pore pressures on the face of the cone tip. However, for quantitative interpretation of pore pressures measured on the face of the tip during penetration in stiff soils it is important to avoid, or be aware of, potential errors due to filter element compression.

ACKNOWLEDGEMENTS

The assistance of Prof. R.G. Campanella, the technical staff and past graduate students of the Civil Engineering Department, University of British Columbia is much appreciated. The support and assistance of Prof. M. Jamiolkowski during the authors stay in Italy is also much appreciated.

The support of the Natural Sciences and Engineering Research Council during the authors stay at the University of British Columbia is also acknowledged.

REFERENCES

Baligh, M.M., Vivatrat, V. and Ladd, C.C. 1980. Cone Penetration in Soil Profiling, ASCE Journal of Geotecnical Engineering Division, Vol. 106, GT4, April, pp. 447-461.

Baligh, M.M., Azzouz, A.S., Wissa, A.Z.E., Martin, R.T. and Morrison, M.H. 1981. The Piezocone Penetrometer, ASCE Geotechnical Division, Symposium on Cone Penetration Testing and Experience, St. Louis, pp. 247-263.

Battaglio, M. and Maniscalco, R. 1983. Il Peizocone Esecuzione ed Interprtatzione, Scienza della Construzioni Politecnico di Torino, No. 607.

Battaglio, M., Bruzzi, D., Jamiolkowski, M. and Lancellotta, R. 1986. Interpretation of CPT's and CPTU's - Undrained Penetration of Saturated Clays, Proceedings 4th International Geotechnical Seminar, Singapore.

Belfiore, F., Colombo, P.F., Pezzelli, G. and Villani, B. 1989. A Contribution to the study of the Subsidence of Bologna, XII International Conference on Soil Mechanics and Foundation Engineering, Rio de Janeiro, Brazil.

Campanella, R.G., Gillespie, D. and Robertson, P.K. 1982. Pore Pressures during Cone Penetration Testing, Proceedings 2nd European Symposium on Penetration Testing, ESOPT-11, pp. 507-512.

Campanella, R.G. and Robertson, P.K. 1988. Current Status of the Piezocone Test, Proceedings 1st International Symposium on Penetration Testing, ISOPT-1, Vol. 1, pp. 93-116.

Douglas, B.J. and Olsen, R.S. 1981. Soil Classification Using Electric Cone Penetrometer. Symposium on Cone Penetration Testing and Experience, Geotechnical Engineering Division, ASCE, St. Louis, pp. 209-227.

Douglas, B.J., Strutynsky, A.I., Mahar, L.J. and Weaver, J. 1985. Soil Strength Determinations from the Cone Penetration Test, Proceedings of Civil Engineering in the Arctic Offshore, San Francisco.

Houlsby, G. 1988. Discussion Session Contribution, Penetration Testing in the U.K., Birmingham.

ISSMFE, 1977. International Society for Soil Mechanics and Foundation Engineering. Report of the Subcommittee on Standardization of Penetration Tsting in Europe. Proceedings 9th International Conference on Soil Mechanics and Foundation Engineering, Tokyo, Vol. 3, Appendix 5, pp. 95-152.

ISOPT, 1988. International Symposium on Penetration Tsting. Report of the ISSMFE Technical Committee on Penetration Testing, CPT Working Party. Vol. 1, pp. 27-51.

Jamiolkowski, M. and Robertson, P.K. 1988. Future trends for Penetration Testing, Closing Address, Proceedings Penetration Testing in the U.K., Birmingham, England.

Jones, G.A. and Rust, E.A. 1982. Piezometer Penetration Testing CUPT. Proceedings of the 2nd European Symposium on Penetration Testing, ESOPT II, Amsterdam, Vol. 2, pp. 607-613.

Konrad, J-M. 1987. Piezo-Friction-Cone Penetrometer Testing in Soft Clays. Canadian Geotechnical Journal, Vol. 24, No. 4, November, pp. 645-652.

Lunne, T., Eidsmoen, T., Gillespie, D. and Howland, J.D. 1986. Laboratory and Field Evaluation of Cone Penetrometers, Proceedings of InSitu 86, Specialty Conference, ASCE, Blacksburg, Virginia.

Olsen, R.S. 1984. Liquefaction Analysis Using the Cone Penetration Test. Proceedings of the 8th World Conf. on Earthquake Engineering, San Francisco.

Olsen, R.S. and Farr, J.V. 1986. Site Characterization Using the Cone Penetration Test, Proceedings of In-situ '86, ASCE Specialty Conference, Blacksburg, Virginia.

Robertson, P.K. 1986. In-Situ Testing and Its Application to Foundation Engineering, 1985 Canadian Geot. Colloquium, Canadian Geot. Journal, Vol. 23, No. 23, No. 4, pp. 573-594.

Robertson, P.K., Campanella, R.G., Gillespie, D. and Grieg, J. 1986. Use of Piezometer Cone Data, Proceedings of InSitu 86, ASCE Specialty Conference, Blacksburg, Viriginia.

Roy, M., Tremblay, M., Tavenas, F. and LaRochelle, P. 1982. Development of pore pressures in quasi-static penetration tests in sensitive clay. Canadian Geotechnical Journal, 19: pp. 124-138.

Senneset, K. and Janbu, N. 1984. Shear Strength Parameters Obtained from Static Cone Penetration Tests, ASTM STP 883, Symposium, San Diego.

Smits, F.P. 1982. Penetration Pore Pressure Measured with Piezometer Cones, Proceedings Second European Symposium on Penetration Testing, ESOPT II, Amsterdam, Vol. 2, pp. 871-876.

Tortensson, B.A., 1975. Pore Pressure Sounding Instrument, Proceedings, ASCE Specialty Conference on In-situ Measurement of Soil Properties, Raliegh, N.C., Vol. 11, pp. 48-54.

Wroth, C.P. 1984. Interpretation of In Situ Soil Test, 24th Rankine Lecture, Geotechnique, 34, pp. 449-489.

List of Figures

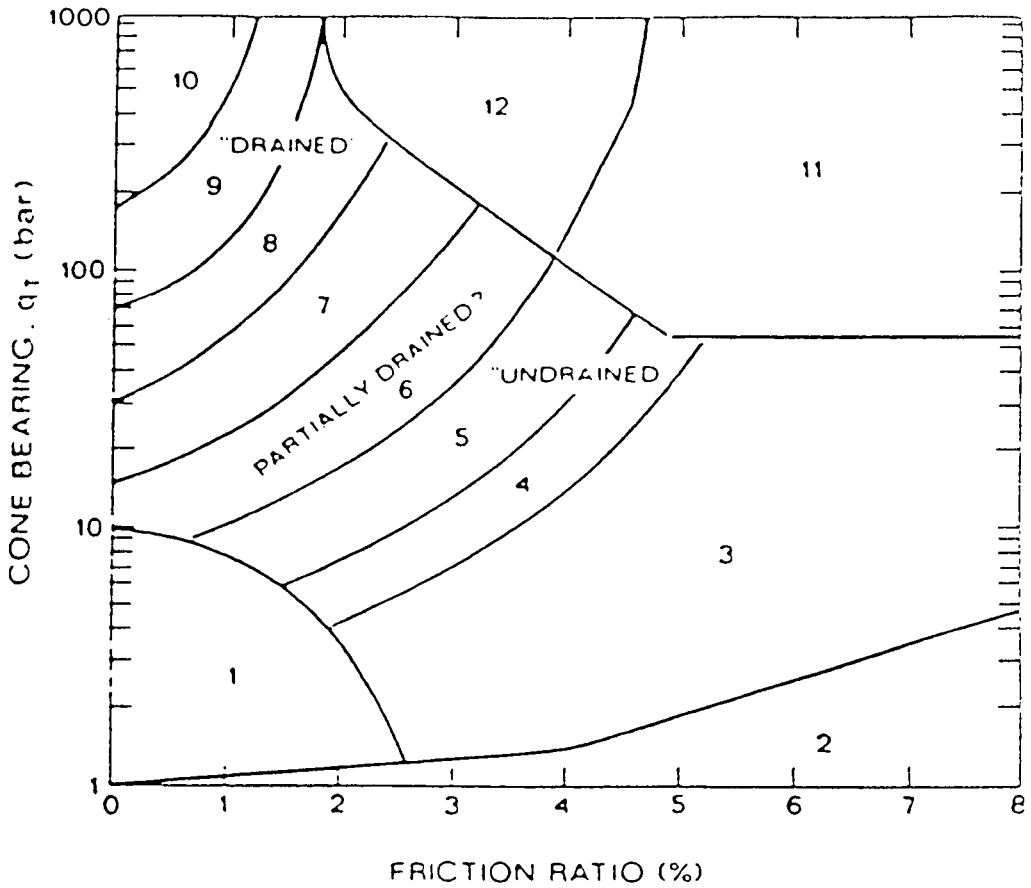

Zone	Qc/N	Soil Behaviour Type
1)	2	sensitive fine grained
2)	1	organic material
3)	1	clay
4)	1.5	silty clay to clay
5)	2	clayey silt to silty clay
6)	2.5	sandy silt to clayey silt
7)	3	silty sand to sandy silt
8)	4	sand to silty sand
9)	5	sand
10)	6	gravelly sand to sand
11)	1	very stiff fine grained (*)
12)	2	sand to clayey sand (*)

(*) overconsolidated or cemented

Figure 1. Simplified soil behaviour type classification for standard electric friction cone (Robertson 1986).

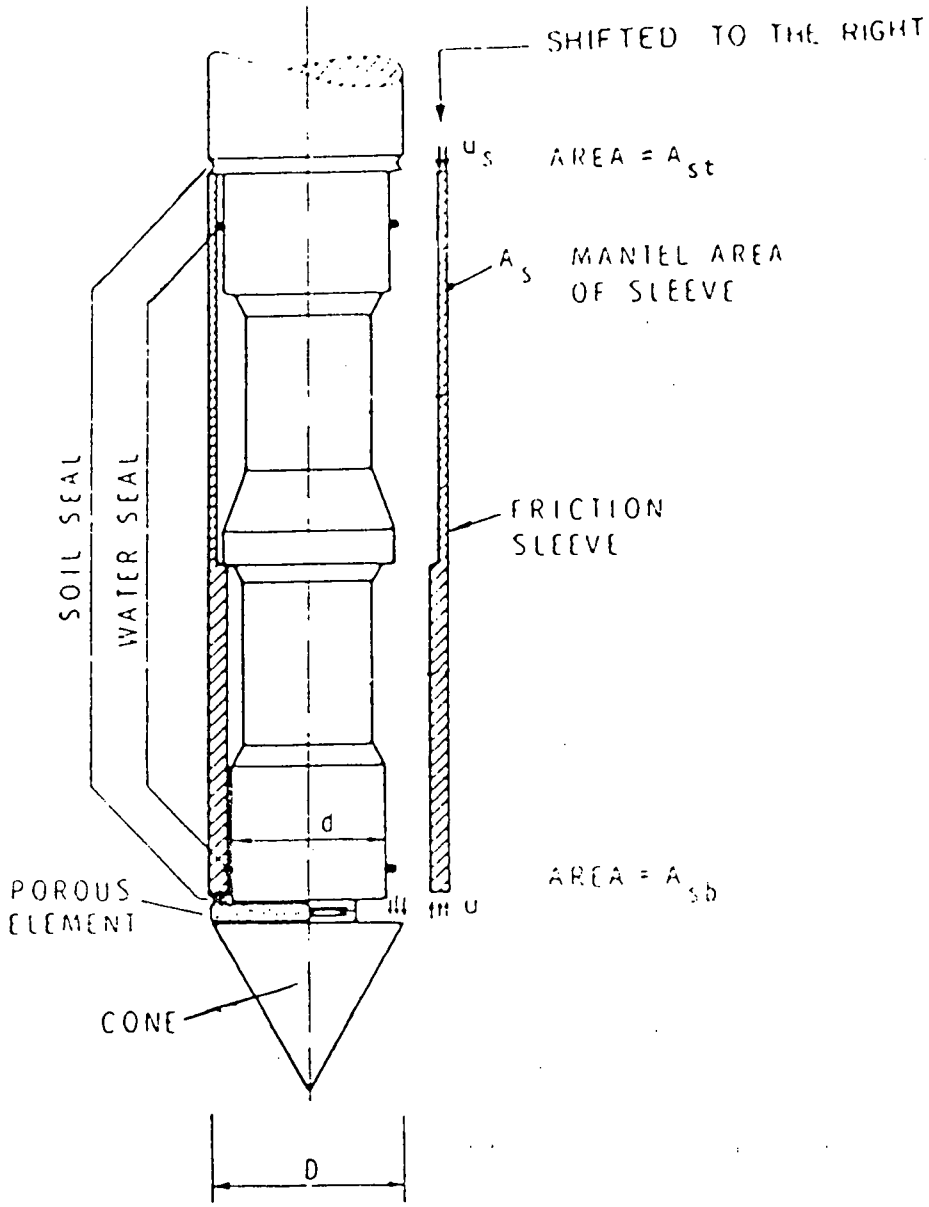

Figure 2. Schematic representation of piezo-friction-cone penetrometer (Adapted from Konrad, 1987).

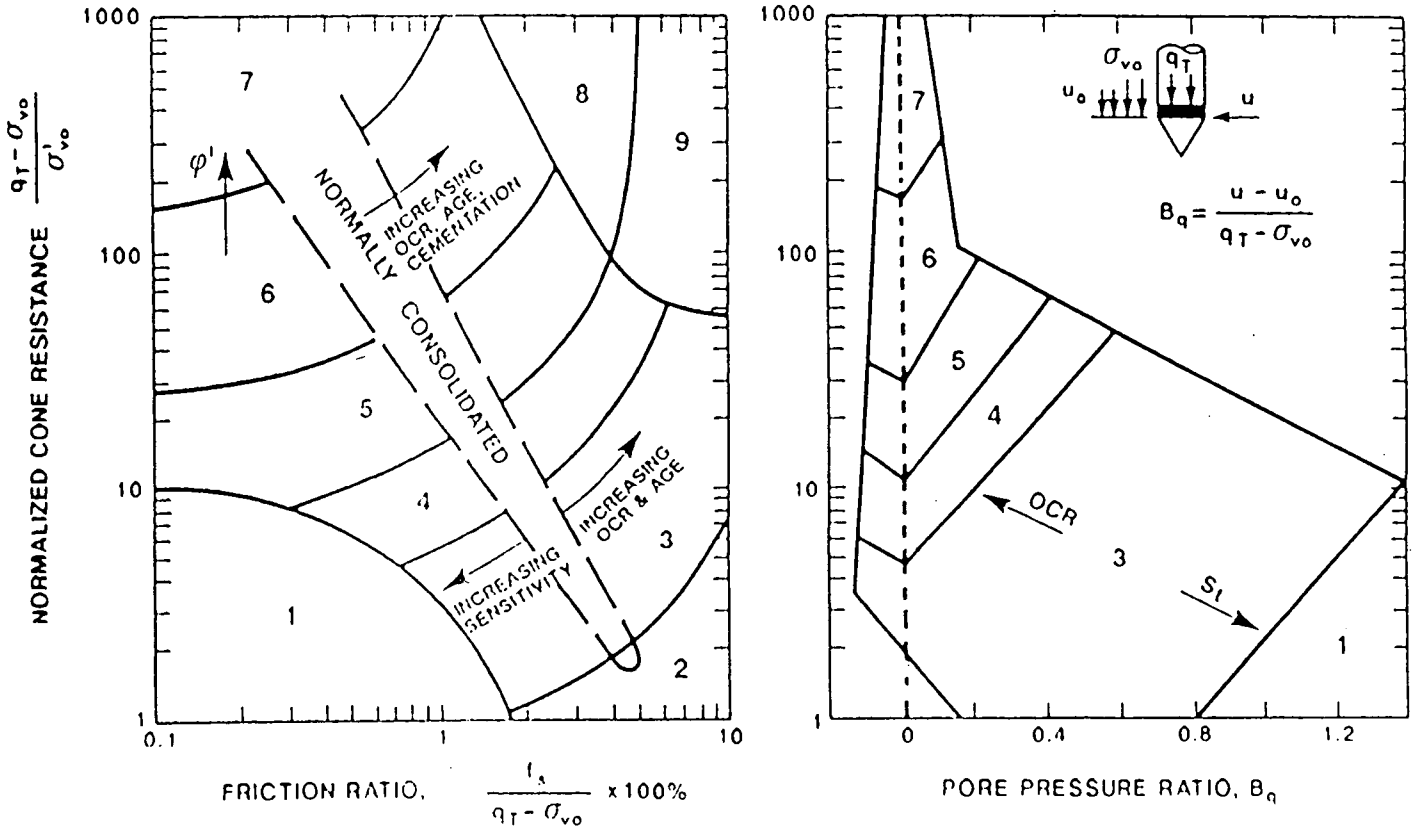

1. SENSITIVE FINE GRAINED
2. ORGANIC SOILS - PEATS
3. CLAYS - CLAY TO SILTY CLAY
4. SILT MIXTURES - CLAYEY SILT TO SILTY CLAY
5. SAND MIXTURES - SILTY SAND TO SANDY SILT
6. SANDS - CLEAN SAND TO SILTY SAND
7. GRAVELLY SAND TO SAND
8. VERY STIFF SAND TO CLAYEY* SAND
9. VERY STIFF FINE GRAINED*

(*) HEAVILY OVERCONSOLIDATED OR CEMENTED

Figure 3. Proposed soil behaviour type classification chart based on normalized CPT and CPTU data.

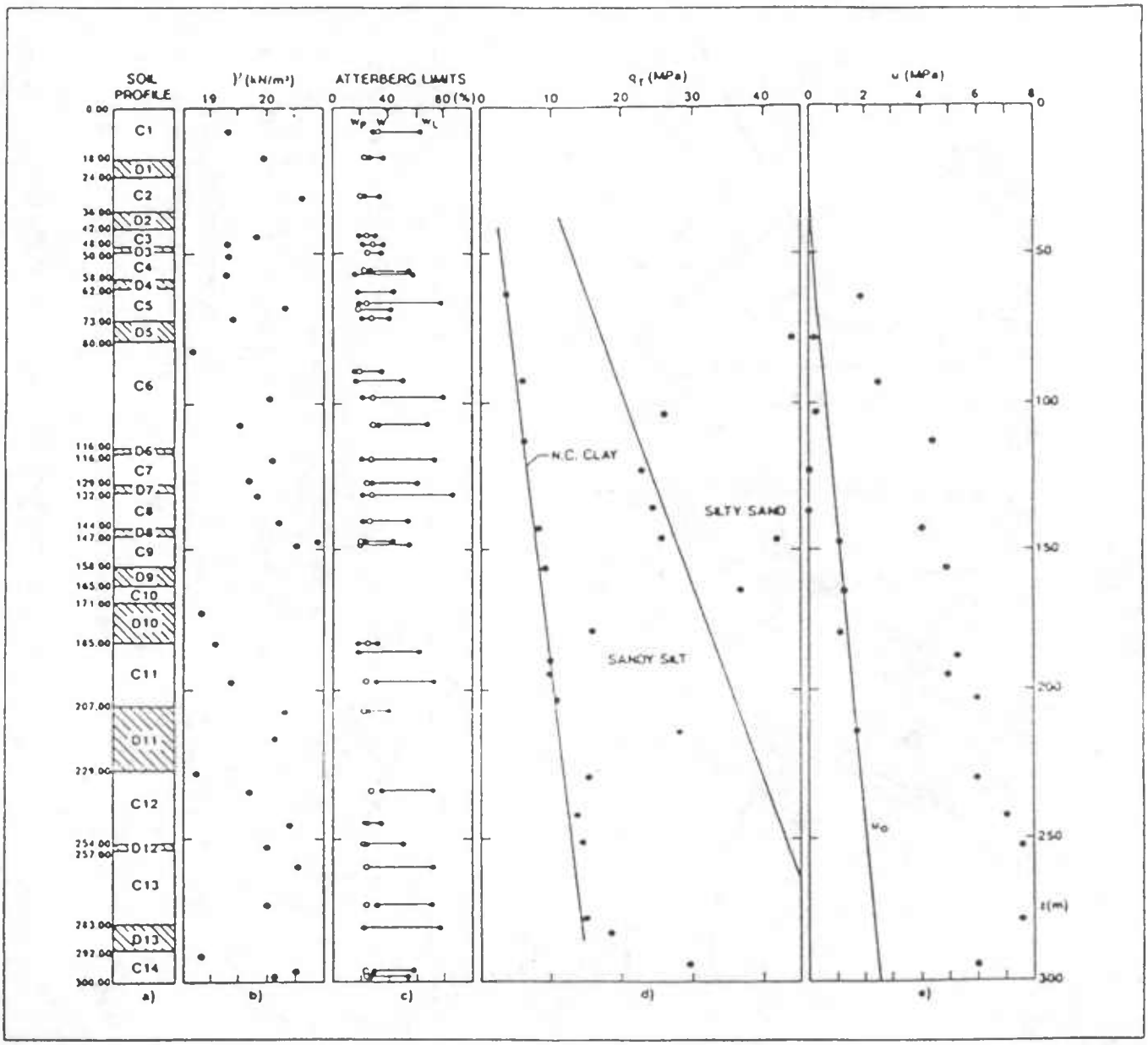

Figure 4. Summary of soil profile and geotechnical characteristics from 300 m deep borehole (After Belfiore et al. 1989).

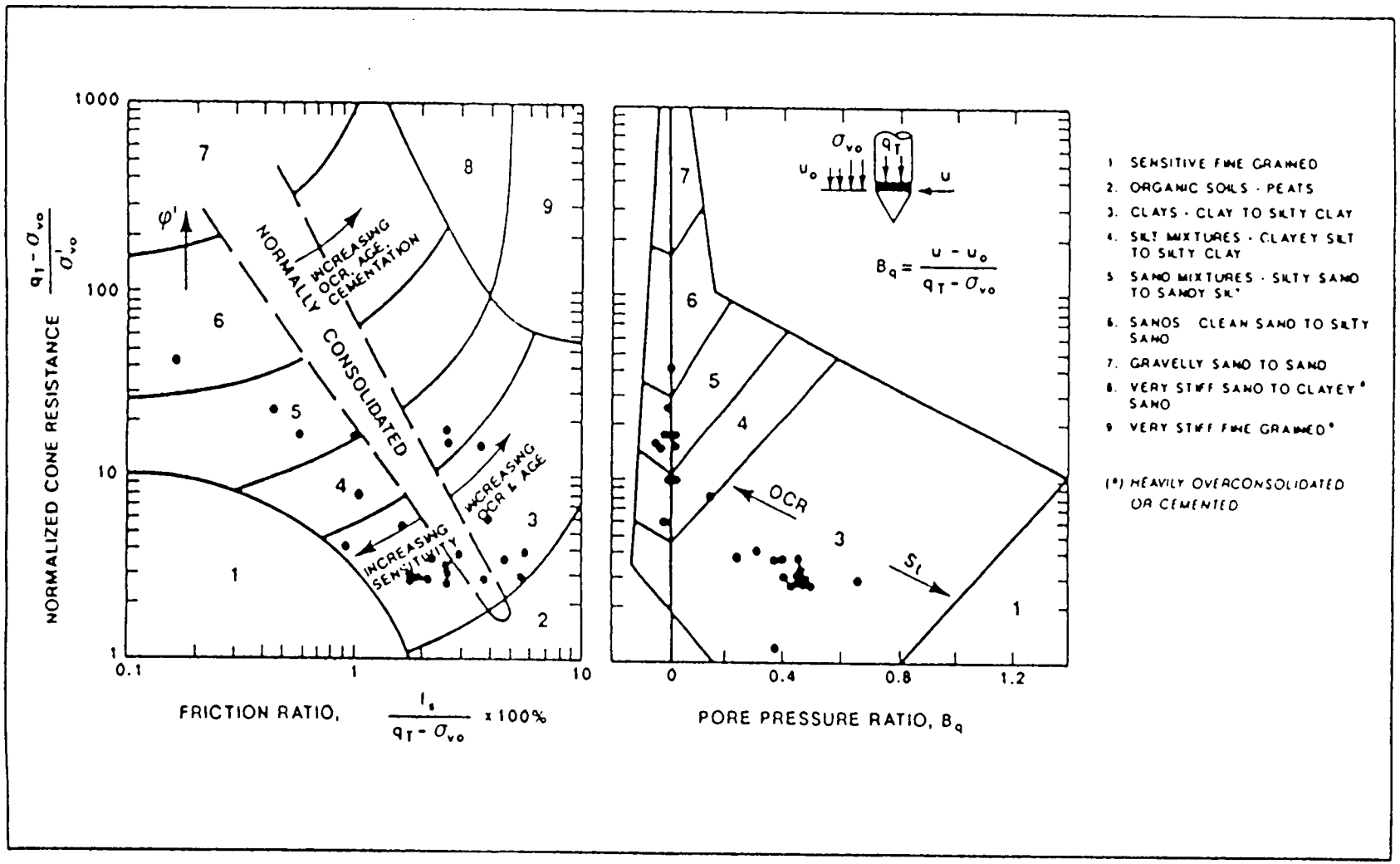

Figure 5. CPT and CPTU data from the deep borehole plotted on the proposed normalized soil behaviour type classification charts.

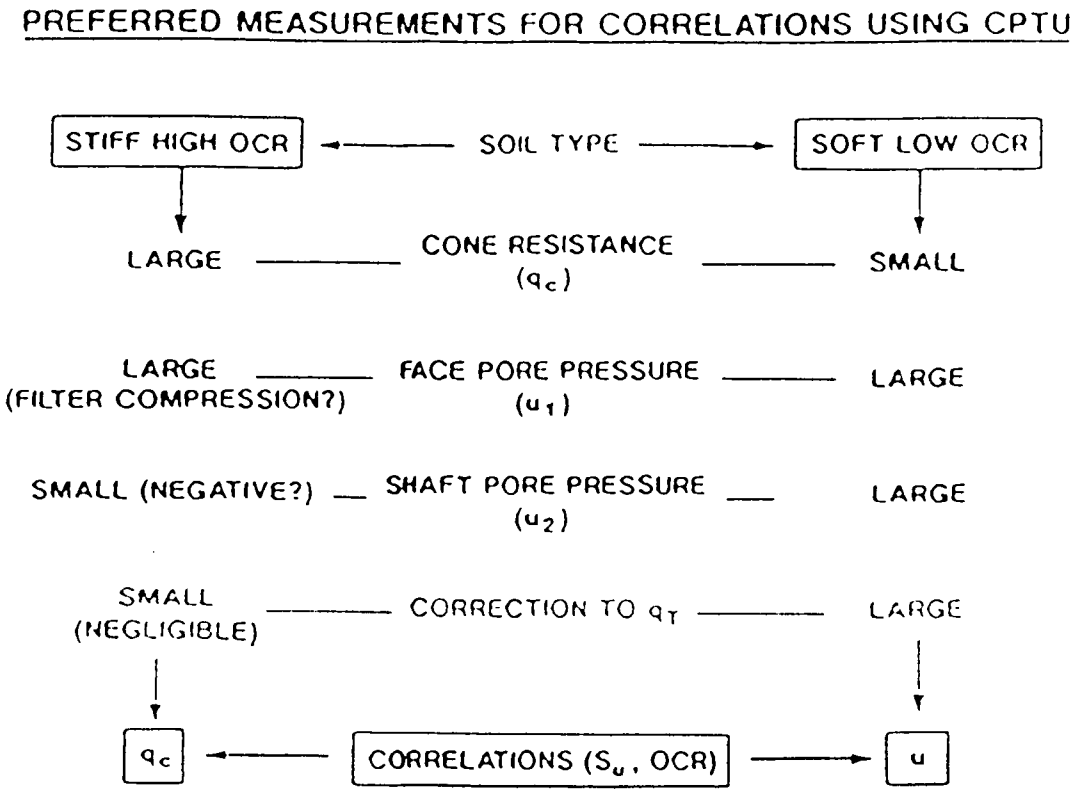

Figure 6. Preferred measurements for correlations using CPTU.

PRESENTED BY: